Molecular regulation of apoptosis and cell cycle by Bcl-2 and FKBP38

Feng, Lin

2007

Feng, L. (2007). Molecular Regulation of Apoptosis and Cell Cycle by Bcl-2 and FKBP38. Doctoral thesis, Nanyang Technological University, Singapore.

https://hdl.handle.net/10356/6579

https://doi.org/10.32657/10356/6579

NANYANG TECHNOLOGICAL UNIVERSITY

MOLECULAR REGULATION OF APOPTOSIS AND CELL CYCLE BY BCL-2 AND FKBP38

FENG LIN

SCHOOL OF BIOLOGICAL SCIENCES

2007

Molecular Regulation of Apoptosis and Cell Cycle by Bcl-2 and FKBP38

Feng Lin

School of Biological Sciences

A thesis submitted to the Nanyang Technological University
in fulfilment of the requirement for the degree of
Doctor of Philosophy

2007

To my parents

Acknowledgements

I would like to express a highly special appreciation to my supervisor Prof. Yoon Ho Sup for his valuable guidance, encouragement and inspiration on my PhD study.

I deeply thank Prof. Liu Ding Xiang, Prof. Valerie Lin, Prof. Kenneth Yu, who provided many valuable suggestions and helps on my molecular and cellular experiments.

I greatly thank Prof. James Tam, Chair of SBS, Prof. Alex Law, Associate Chair of SBS, Prof. Lars Nordenskiöld, Head of Division, for their kind care and support during my PhD study.

I am very grateful to Prof. Sail Bose for his kind suggestions in writing my thesis.

I also want to thank all members in our laboratory and all colleagues in SBS, for their cooperation in my research.

I would like to present this thesis as a gift to my dear parents.

Summary

The anti-apoptotic protein Bcl-2 is a central player in apoptosis. It is mainly localized at the mitochondrial outer membrane and keeps the mitochondria intact. In addition, the biological function of Bcl-2 has been shown to delay the cell cycle progression, especially by retarding $G_1 \rightarrow S$ transition. Bcl-2 also acts as an antioxidant to reduce the generation of reactive oxygen species (ROS) inside cells. Taken together, the known functions of Bcl-2 make the anti-apoptotic protein an essential player in apoptosis and important molecular target for development of anti-cancer drugs.

In this study, by using siRNA-mediated RNA interference, we studied the molecular regulation of Bcl-2. The silencing of Bcl-2 led to the increase of the expression of pro-apoptotic protein such as Bax and the activation of caspase-3, which acted as the executor in apoptosis. Also an increase of the mitochondrial outer membrane permeabilization was detected. In addition, we examined the role of Bcl-2 in the cell cycle transition. We demonstrated that the down-regulation of Bcl-2 initiated the cell cycle progression with cells arrested in the early S-phase accompanying with an increase of ROS.

FKBP38 is a novel molecular chaperon, which has been shown to bind Bcl-2 and help Bcl-2 localizing at the mitochondrial outer membrane. Currently, molecular mechanism how these two proteins communicate to each other remains unclear. In this study, to define the molecular interaction between Bcl-2 and FKBP38, several plasmids with Bcl-2 loop deletion mutants were constructed and co-transfected with

the plasmids expressing FKBP38 into Hela cells. We demonstrated that the region of P65-V89 in the long flexible loop was mainly responsible for the molecular interaction with FKBP38. Deleting this region weakened the binding with FKBP38 significantly, and resulted in the misdistribution and degradation of Bcl-2 inside cells.

In addition, the silencing of FKBP38 by RNA interference also resulted in the initiation of cell cycle progression and apoptosis. However, compared to Bcl-2, the silencing of FKBP38 resulted in a greater number of cells arrested in S- or G_2/M-phase with a significant increase of cyclin A and activation of CDK2. The antioxidant protected the mitochondrial membrane from damage and inhibited the apoptotic cell death initiated by FKBP38 suppression, while the antioxidant didn't inhibit Bcl-2-suppression-induced mitochondrial damage and apoptosis. Thus, besides its chaperone function anchoring Bcl-2 to the mitochondria, FKBP38 acts as a novel link between apoptosis and cell cycle through the ROS-mediated damage on the mitochondria, independent of Bcl-2.

Key words: Bcl-2, FKBP38, Apoptosis, Cell cycle

Table of Contents

List of abbreviations

2',5'-AS (2',5'-oligoadenylate synthetase)

AIF (apoptosis-inducing factor)

ANT (adenine nucleotide transporter)

Apaf-1 (apoptotic protease-activating factor-1)

Ape 1 (apurinic endonuclease-1)

ASON (antisense oligonucleotides)

Bcl-2 (B Cell Leukemia/Lymphoma-2)

BH (Bcl-2 homology)

CAD (caspase-activated DNase)

CAT (catalases)

CDK (cyclin-dependent kinase)

CHOP/GADD153 (C/EBP homologous protein)

CTL (cytotoxic T lymphocyte)

CyP-40 (cyclophilin 40)

DcR (Decoy receptor)

DD (death domain)

DED (death effecter domain)

DISC (death-inducing signaling complex)

DMEM (dulbecco's modified eagle medium)

EDAR (ectodysplasin A receptor)

eIF (eukaryotic initiation factor)

Endo-G (Endonuclease G)

ER (endoplasmic reticulum)

FADD (Fas-associated death domain protein)

FADD (Fas-associated death domain)

FasL (Fas ligand)

FKBP38 (FK506 binding protein 38)

FLIP (FLICE-inhibitory protein)

GPX (glutathione peroxide)

GSH (glutathione)

GSSG (oxidized glutathione)

GzmA (granzyme A)

H_2O_2 (hydrogen peroxide)

IAPs (inhibitors of apoptosis)

ICAD (inhibitor of CAD)

JNK (c-Jun NH_2-terminal kinase)

miRNA (microRNA)

MMR (mismatch repair)

MOMP (mitochondrial outer membrane permeabilization)

mTOR (mammalian Target of Rapamycin)

NGFR (nerve growth factor receptor)

PARP (poly (ADP ribose) polymerase)

PBS (phosphate buffer solution)

PCD (Programmed Cell Death)

PERK (PKR-like ER kinase)

PP5 (protein phosphatase 5)

PPIase (peptidylprolyl isomerase)

PS-1 (Presenilin-1)

PT (permeability transition)

PTGS (posttranscriptional gene-specific silencing)

rasiRNAs (repeat-associated short interfering RNAs)

Rb (retinoblastoma protein)

RdRP (RNA-dependent RNA polymerase)

RISC (RNA-induced silencing complex)

RNAi (RNA interference)

ROS (reactive oxygen species)

RT-PCR (reverse transcription polymerase chain reaction)

SDS-PAGE (sodium dodecyl sulfate polyacrylamide gel electrophoresis)

siRNA (small interfering RNA)

SOD (superoxide dismutase)

tBid (truncated Bid)

TBS (Tris-buffered saline)

TMD (transmembrane domain)

TNF (tumour necrosis factor)

TNFR1 (tumor necrosis factor receptor 1)

TPR (tetratricopeptide repeats)

TRAIL (TNF-related apoptosis-inducing ligand)

TSC (tuberous sclerosis complex)

TTBS (Tween-20 Tris-buffered saline)

UPR (unfolded protein response)

VDAC (voltage-dependent anion channel)

List of Figures and Tables

Chapter 1 Literature Review

1.1 Overview of Bcl-2

1.1.1 Bcl-2 and tumorigenesis

Bcl-2 (B Cell Leukemia/Lymphoma-2) gene is a proto-oncogene located on the human chromosome 18. The overexpression of Bcl-2 gene was first discovered as the translocated locus of t(14;18)(q32.3;q21) in a B-cell leukemia (Tsujimoto Y et al., 1984). This translocation places the Bcl-2 gene close to the heavy chain gene enhancer which makes the Bcl-2 expression high in these transformed B cells (Aisenberg AC et al., 1988). In addition to the translocation of Bcl-2 gene in some of the hematologic cancers, up-regulation of Bcl-2 expression without any apparent gene rearrangement has also been found in other tumors (Ilmonen S et al., 2005; Linjawi A et al., 2004; Meterissian SH et al., 2001).

So far, the high-level expression of Bcl-2 has been found in a wide variety of human cancers, including breast cancers, prostate cancers, colorectal cancers, gastric cancers, small-cell lung carcinomas, non-small-cell lung cancers, neuroblastomas, and B cell lymphomacrase, suggesting an important role of the Bcl-2 gene in tumorigenesis (Reed JC, 1997; Sartorius UA et al., 2002). Overexpression of Bcl-2 also correlates with a resistance to chemo- and radio-therapies and a poor prognosis in cancer (Reed JC, 1995). Down-regulation of Bcl-2 can enhance the chemosensitivities to various anti-cancer drugs (Webb A et al., 1997; Bettaieb A et al., 2003). Thus, modulating the activity of Bcl-2 will provide a good therapeutic opportunity in designing novel anticancer drugs.

Bcl-2 contributes to cell survival by inhibiting apoptosis, rather than by stimulating cell division (Mcdonnell TJ et al., 1989). It enables cells to survive in certain stress-induced conditions, such as growth-factor withdrawal, hypoxia, nutrient deprivation, DNA damage and presence of toxins.

1.1.2 Bcl-2 in normal cells

Bcl-2 is also found expressed in normal cells and plays a role in the normal physiological activities. For example, Bcl-2 was found to be expressed in normal human B- and T-lymphocytes after stimulation with appropriate mitogens, suggesting that the proto-oncogene may be involved in the control of normal cellular growth (Reed JC et al., 1987). Bcl-2 also regulates hormone-dependent growth of endometrium (Gompel A et al., 1994).

1.1.3 Bcl-2 family proteins

All Bcl-2 family members share at least one conserved Bcl-2 homology (BH) domain (Fig. 1.1). According to the homology and function of each protein, Bcl-2 family is classified into three subfamilies, Bcl-2 subfamily, Bax subfamily and BH3-only subfamily (Gross A et al., 1999).

Bcl-2 subfamily includes Bcl-2, Bcl-x_L, Bcl-w, Mcl-1, Al/Bfl-1 and Boo/Diva/Bcl-B. The members of the Bcl-2 subfamily proteins are composed of BH1, BH2, BH3, BH4 and a transmembrane domain (TM) at the C-terminus. Bcl-2 subfamily proteins are predominantly localized in the cytoplasmic faces of intracellular membranes, including the mitochondrial outer membrane, the endoplasmic reticulum membrane and the nuclear envelope (Krajewski S et al., 1993).

Bax subfamily includes Bax, Bak, Bok/Mtd and Bcl-x_S. The members of the Bax subfamily proteins comprise BH1, BH2, BH3 and TM at the C-terminus (not the case of Bcl-x_S). Bax subfamily proteins are found predominantly in the cytosol. When activated, the Bax subfamily proteins translocate to the mitochondrial outer membrane to initiate pro-apoptotic activity (Hsu YT et al., 1997).

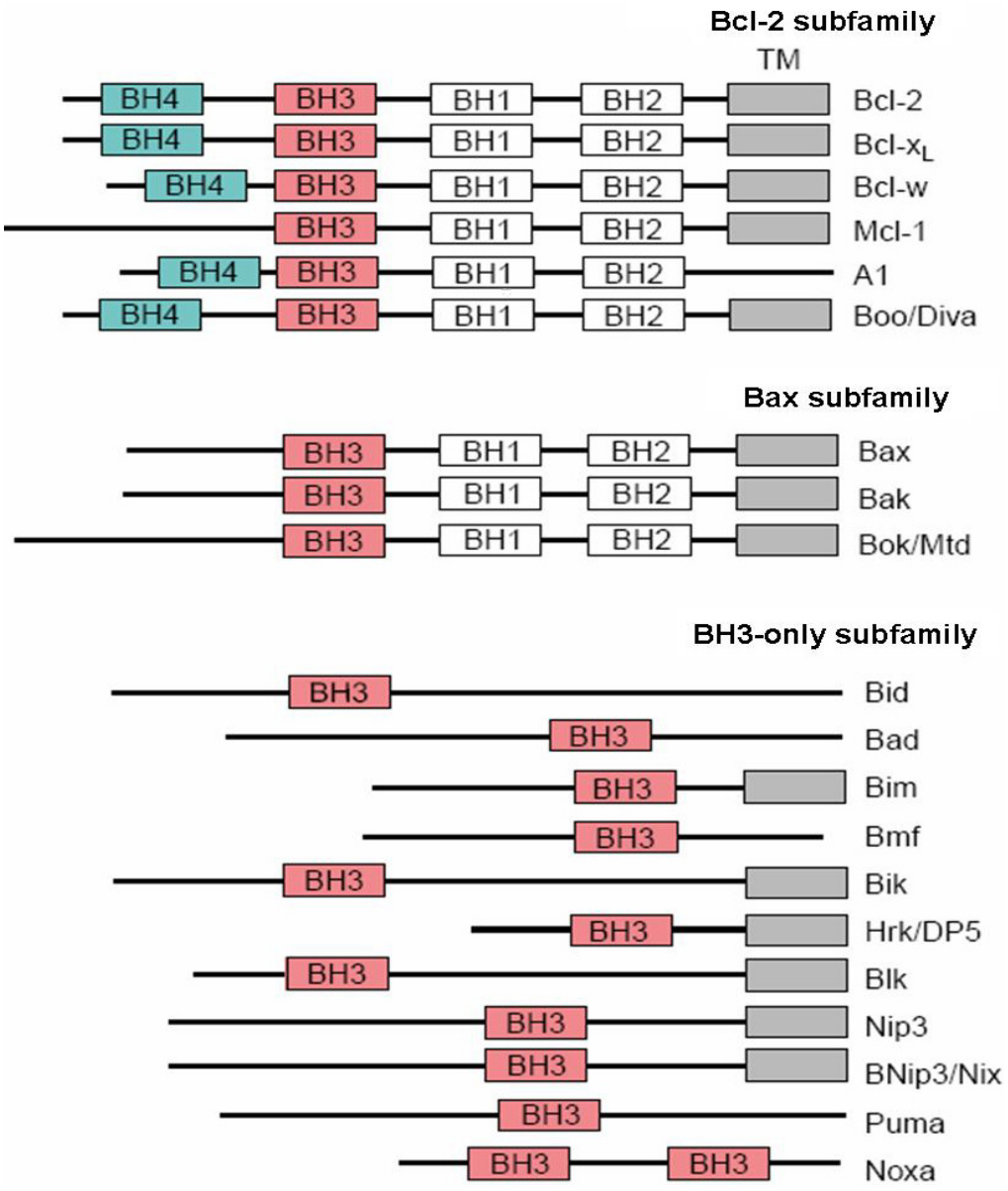

Adapted from Gross A, et.al (1999). **BCL-2 family members and the mitochondria in apoptosis**. *Genes Dev.*

Fig. 1.1 Schematic representation of Bcl-2 family proteins, including Bcl-2 subfamily proteins, Bax subfamily proteins and BH3-only subfamily proteins (Gross A et al., 1999). The BH domains, BH1, BH2, BH3 and BH4 and the transmembrane domain (TMD) are indicated. Through dimerizations, heterodimerization or homodimerization, Bcl-2 family proteins regulate apoptosis.

BH3-only subfamily includes Bid, Bad, Bik/NBK, Blk, Hrk, Bim/Bod, NIP3, NIX/BNIP3, Puma and Noxa. BH3-only members are so named because they have only the conserved BH3 domain without BH domains 1, 2 and 4 (Wang K et al., 1996). Most BH3-only proteins also contain a TM close to the COOH-terminus. BH3-only family proteins usually stay inactive. Once stimulated by pro-apoptotic signals, this family proteins gain pro-apoptotic potential by transcriptional up-regulation and/or posttranslational modification. BH3-only family proteins have been recognized as essential initiators of apoptosis (Yang E et al., 1995).

Although Bcl-2, Bcl-x_L and Bax contain a hydrophobic segment at their C-terminal ends, which is believed to serve as a membrane anchor, these proteins actually exist in various forms and localize at different sites inside cells. Bcl-2 is found exclusively membrane-bound, whereas Bax is present predominantly in the cytosol with the C-terminal tail-anchor sequence sequestered in a hydrophobic binding pocket (Suzuki M et al., 2000), and Bcl-x_L is present in both soluble and membrane-bound forms (Hsu YT et al., 1997).

After the apoptotic pathway is initiated, Bax is activated by a transient interaction with a BH3-only member such as tBid, which is truncated Bid cleaved by caspase-8 (Korsmeyer SJ et al., 2000; Wei MC et al., 2000). tBid can induce a conformational change in Bax that is presumed to expose the C-terminal tail-anchor sequence, and this C-terminal tail-anchor sequence is required for specifically targeting Bax to the mitochondrial membrane (Wolter KG et al., 1997; Nechushtan A et al., 1999; Roucou X et al., 2002). Bax migrates from the cytosol to the mitochondrial membrane to cause damage of the mitochondrial membrane and to induce the release of cytochrome c from mitochondria to cytosol (Heimlich G et al.,

2004; Annis MG et al., 2005). Other pro-apoptotic proteins, such as Bak appears to be inserted into mitochondrial membrane in an inactive conformation. Upon induction of apoptosis, it undergoes conformational changes to become active and consequently dimerizes with other Bcl-2 family proteins to induce the release of cytochrome *c* from mitochondria to cytosol (Sattler M et al., 1997; Griffiths GJ et al., 1999). And tBid was found to regulate the activation of Bak. As critical regulators in apoptosis, these features of apoptosis-dependent conformational changes of Bcl-2 family proteins and the ability of shifting localizations between cytosol and intracellular compartments in response to apoptotic stimuli suggest that apoptosis is a tightly regulated biological process.

The formation of homodimers or heterodimers is one of the striking features among Bcl-2 family proteins in regulating apoptosis (Yin XM et al., 1994). The NMR spectroscopy of Bcl-2 revealed that there are six α-helices in the domain BH1, BH2 and BH3, which can form a stable hydrophobic groove on the surface of this protein. This groove is further stabilized by another α-helix in the domain BH4 mediated by shielding of hydrophobic residues in the interior of the molecule from exposure to the aqueous environment. During apoptosis, the hydrophobic groove can bind the BH3 amphipathic α-helix of a pro-apoptotic Bcl-2 family protein (Bax subfamily proteins or BH3-only family proteins) through hydrophobic and electrostatic forces (Petros AM et al., 2001). This BH3 cleft coupling, similar to the ligand-receptor engagement, accounts for all dimerizations within the Bcl-2 family proteins. Further studies showed that BH4 was required for anti-apoptotic activity (Hunter JJ et al., 1996) while BH3 was essential for pro-apoptotic activity (Bouillet P et al., 2002).

The heterodimerization of Bcl-2 family proteins initiates apoptosis and is essential for BH3-only subfamily members to perform their pro-apoptotic activity

(Bouillet P et al., 2002; Zha J et al., 1997). Through heterodimerization and homodimerization, Bcl-2 family proteins form pores on the outer mitochondrial membrane or modify existing pores to increase the mitochondrial permeability, which results in the release of several apoptotic factors including cytochrome *c* and Smac/Diablo from mitochondria to cytosol to initiate the irreversible apoptosis (Antonsson B et al., 2000; Kuwana T et al., 2002).

Three-dimensional structure of Bcl-x_L is similar to the pore-forming sturctures of diphtheria toxin and the bacterial colicins. In addition, Bcl-x_L, Bcl-2 and Bax have also shown the ability to form ion channels in synthetic membranes or in apoptotic cells (Antonsson B et al., 1997; Minn AJ et al., 1997; Schendel SL et al., 1997; Schlesinger PH et al., 1997).

1.2 Bcl-2 and Apoptosis

1.2.1 Apoptosis

Apoptosis or programmed cell death (PCD) is a highly regulated cell death process which involves a systematic disassembly of an unwanted cell without causing damage or stress to neighboring cells in a multicellular organism (Kerr JF et al., 1972). Apoptosis is characterized with cell shrinkage, cell membrane blebbling, chromatin condensation, DNA degradation, apoptotic body formation (Rudel T et al., 1997).

Apoptosis is involved in many biological processes. Apoptosis occurs naturally as a part of biological development and aging of animals and is important in embryonic development and in tissue homeostasis maintenance (Meier P et al., 2000; Milligan CE et al., 1997). During animal development, numerous structures with

over-production of excess cells are formed that are later removed by apoptosis. This enables greater flexibility for ensuring normal tissue development as primordial structures can be adapted for different functions at various stages of life. Also, apoptosis plays a critical role in maintaining health by eliminating aging, unnecessary, and unhealthy cells (Bright J et al., 1994). Too little or too much apoptosis may result in many diseases (Carson DA et al., 1993). If there is dysfunctional apoptosis, cells that should have been removed may persist to become immortal, which could cause cancer, autoimmune diseases and some inflammatory diseases, such as bronchial asthma and pulmonary inflammation (Watson AJ, 1995; Newcomb EW, 1995; Masunage A et al., 1994; Woolley KL et al., 1996; Grigg JM et al., 1991). On the other hand, cells that should live may be dying in too large numbers that may result in grave tissue damage, which can cause immunodeficiency, AIDS, neurodegeneration, such as Alzheimer's disease and Pakinson's disease (Ameisen JC et al., 1992; Gschwind M et al., 1995). Therefore, the understanding of the molecular and biochemical mechanism of apoptosis will not only contribute to our insight into the pathogenesis of various diseases, but also will facilitate the development of therapeutic interventions targeting different apoptotic pathways which could potentially alter the course of the disease (Thompson CB, 1995).

1.2.2 Apoptotic pathways

The two classic apoptotic pathways involved in apoptosis are the death-receptor pathway or extrinsic pathway and the mitochondrial pathway or intrinsic pathway (Hengartner MO, 2000) (Fig. 1.2). Recently, an additional possible pathway which involves the endoplasmic reticulum (ER) initiated by stresses was discovered, but the detail molecular mechanisms are still not well established (Lam M et al., 1994;

Hacki J et al., 2000). All of these above pathways are through the activation of caspase cascade to initiate apoptosis. Another pathway, caspase-independent pathway could be initiated by granzyme A (GzmA) (Fan Z et al., 2003. Martinvalet D et al., 2005).

1.2.2.1 Death-receptor pathway

The death-receptor pathway is triggered by members of the death-receptor superfamily. The death-receptor superfamily belongs to the tumor necrosis factor receptor superfamily, which is defined by similar, cysteine-rich extracellular domains (Macfarlane M et al., 2004; Bhardwaj A et al., 2003). Eight members of the death receptor superfamily have been characterized so far, including tumor necrosis factor receptor 1 (TNFR1, also known as DR1/CD120a/p55/p60), CD95 (also known as DR2/APO-1/Fas), DR3 (also known as APO-3/LARD/TRAMP/WSL1), TNF-related apoptosis-inducing ligand receptor 1 (TRAILR1, also known as DR4/APO-2), TRAILR2 (as known as DR5/KILLER/ TRICK2), DR6, ectodysplasin A receptor (EDAR), and nerve growth factor receptor (NGFR) (Ashkenazi A et al., 1998). All death-receptor superfamily members are type I membrane proteins that contain two to four cysteine-rich extracellular domains and a ~80-aa cytoplasmic motif termed as the death domain (DD) (Ashkenazi A et al., 1998).

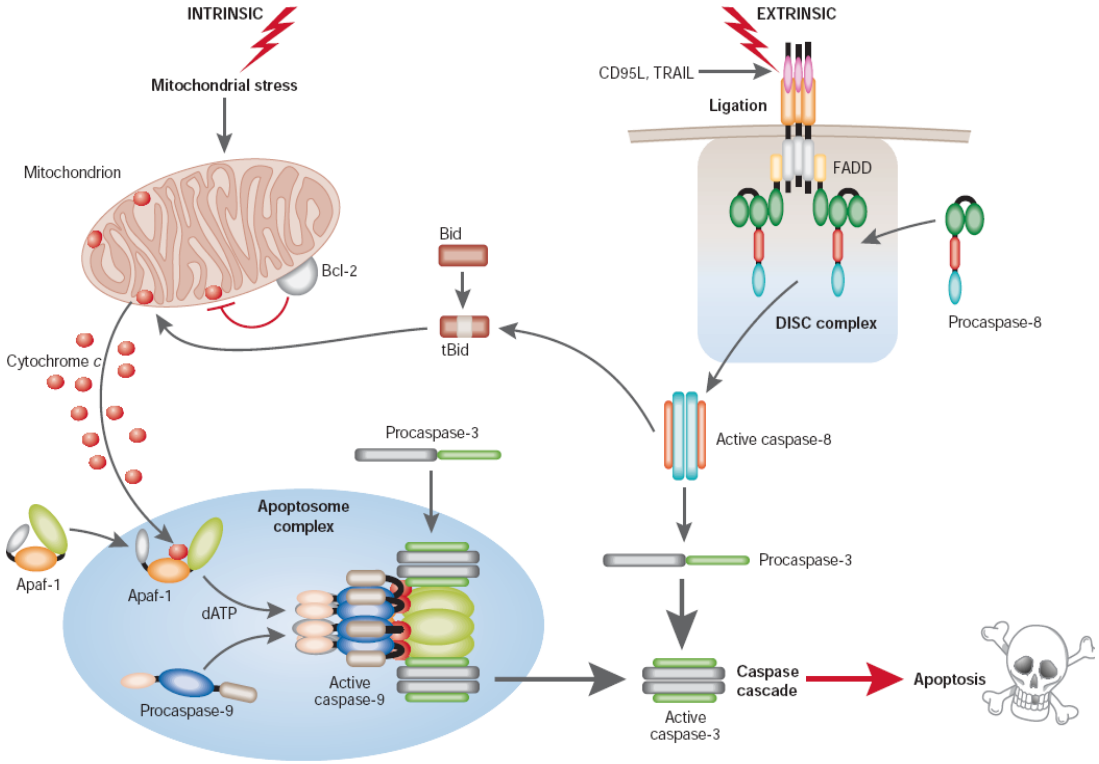

Adapted from MacFarlane M, et.al (2004). **Apoptosis and disease: a life or death decision**. *EMBO Rep*.

Fig. 1.2 Two major apoptotic pathways. The death-receptor pathway or extrinsic pathway is triggered by tumour necrosis factor (TNF) receptor superfamily, such as CD95 and TNF-related apoptosis-inducing ligand (TRAIL). Binding of CD95L to CD95 induces receptor trimerization and formation of a death-inducing signaling complex (DISC) through the homophilic DED-DED interaction between the adaptor molecule Fas-associated death domain protein (FADD) and procaspase-8, resulting in caspase-8 activation by automatic proteolysis. Active caspase-8 subsequently activates the effector capase-3 to induce apoptosis. The mitochondrial pathway or intrinsic pathway is initiated by the damage on the mitochondrial membrane by various stimuli or stresses. Several apoptogenic proteins are then released, such as cytochrome c, once released, it binds to apoptotic protease-activating factor (Apaf1) and procaspase-9 to form apoptosome complex, resulting in caspase-9 activation by automatic proteolysis. Active caspase-9 subsequently activates the effector caspase-3 to induce apoptosis. Crosstalk between these two pathways is provided by Bid. After activated by caspase-8, truncated Bid (tBid) translocalizes to mitochondria to induce the release of cytochrome c (Hengartner MO, 2000; French LE et al., 2003).

A variety of death signals can trigger the binding of death ligands with the members of the death-receptor family, initiating the signal transduction of apoptosis. The best-studied DR signaling pathway to date is the mechanism triggered by the binding of Fas ligand (FasL) to Fas. The binding of FasL to its receptor induces the trimerization of the FasL receptor. An adapter protein called Fas-associated death domain (FADD), which is composed of a death domain (DD) in its carboxyl-terminal part and a death effecter domain (DED) in its amino-terminal part, then binds through its own DD to the clustered death receptor DD in the cytoplasmic region via DD-DD interaction (Chinnaiyan AM et al., 1995). Also, FADD recruits the zymogen form of caspase-8, procaspase-8 (also known as FLICE/MACH) by binding to an analogous DED domain repeated in tandem within procaspase-8 processed via DED-DED interaction (Boldin MP et al., 1996) to form the death-inducing signaling complex (DISC). Immediately after recruitment, the single polypeptide procaspase-8 is processed by automatic proteolysis to the active dimeric species composed of large and small catalytic subunits that amplify the apoptotic signal by activating other downstream caspases (Muzio M et al., 1997; Srinivasula SM et al., 1996; Medema JP et al., 1997). The activation of the caspase cascade eventually leads to apoptosis. Active caspase-8 can directly cleave caspase-3, an effector caspase which acts as an executor to induce apoptosis (Enari M et al., 1998). In another pathway, active caspase-8 cleaves Bid, a BH3-only subfamily protein, and the cleaved or truncated Bid (tBid) translocates to the mitochondrial membrane to induce apoptosis (Korsmeyer SJ et al., 2000; Gu Q et al., 2005). Subsequently, the mitochondrial release of cytochrome c induced by the later pathway plays a major role in caspase-8-induced apoptosis (Kuwana T et al., 1998).

Death-receptor apoptotic pathway plays an important role mainly in three types of physiological apoptosis (Nagata S, 1997), including peripheral deletion of activated mature T-cells at the end of an immune response, killing of targets such as virus-infected cells or cancer cells by cytotoxic T-cells or natural killer cells, and killing of inflammatory cells at "immune-privileged sites" such as the eyes and testis with constitutive expression of FasL. Death-receptor apoptotic pathway can be modulated on several levels. Decoy receptors (DcRs) do not possess DDs and so cannot form signal complex. FLICE-inhibitory protein (FLIP) can block procaspase-8 activation at the DISC (Peter ME et al., 2003). And the further downstream inhibitors of apoptosis (IAPs) can inhibit effector caspase activation (Bhardwaj A et al., 2003; Lavrik I et al., 2005).

1.2.2.2 Mitochondrial pathway

Mitochondrion is a subcellular organelle that conducts cellular aerobic respiration (oxidative phosphorylation) and produces most of the ATP in eukaryotic cells. The mitochondrial pathway or intrinsic pathway is defined by the mitochondrial outer membrane permeabilization (MOMP), which can be initiated by various extracellular signal-transducing molecules and intracellular stresses or pathological stimuli, including hypoxia, cytotoxin and DNA damage (Hengartner MO, 2000).

Mitochondrion is a double membrane organelle having an external membrane and an inner membrane with numerous folds called cristae. In general, two different types of mechanisms have been described in MOMP involving the inner mitochondrial membrane or the outer mitochondrial membrane. In the first mechanism, many pore-dependent models have been proposed, including permeability transition (PT) pore, adenine nucleotide transporter (ANT) in the inner

membrane and the voltage-dependent anion channel (VDAC) in the outer membrane. Opening of the pores can be triggered by multiple stimuli which allow water and molecules up to ~1.5 kD to pass through, leading to the mitochondrial membrane potential ($\Delta \Psi m$) loss and the swelling of the matrix (Halestrap AP, 1999; Crompton M, 1999). The sufficient swelling of the matrix finally results in breaking the outer membrane to induce MOMP. In the second mechanism, MOMP is mediated by Bcl-2 family members, which act directly on the outer mitochondrial membrane. Biochemical studies identified that several apoptogenic proteins reside in the intermembrane space of mitochondria. In response to a variety of apoptotic stimuli, these proteins are released to the cytosol and/or to the nucleus through the pores formed by Bcl-2 family proteins in the mitochondrial outer membrane. These released apoptogenic proteins promote apoptosis either by activating caspases and nucleases or by neutralizing cytosolic inhibitors of apoptosis (Wang X, 2001).

Cytochrome c is a component of the mitochondrial electron transfer chain, and the release of cytochrome c from the mitochondria to the cytosol is a major event of the intrinsic apoptotic pathway to initiate caspase cascade activation (Liu X et al., 1996). After released into the cytosol, cytochrome c binds to apoptosis protease activating factor-1 (Apaf-1), which is a cytosolic protein containing a caspase-recruitment domain (CARD), a nucleotide-binding domain, and multiple WD-40 repeats. Normally, Apaf-1 exists as an inactive monomer in the cytosol. The binding of cytochrome c induces a conformational change in Apaf-1, enhancing its binding capability with the nucleotide dATP or ATP. This dATP/ATP-Apaf-1-cytochrome c complex triggers its oligomerization, forming a structure called the apoptosome. The CARD domain of Apaf-1 then becomes exposed, and procaspase-9 binds to the apoptosome and is subsequently autoactivated through self-cleavage (Zou H et al.,

1997; Zou H et al., 1999). The activated caspase-9 then activates the downstream executioner caspase-3, caspase-6 and caspase-7. These effector caspases are responsible for cleaving many important intracellular substrates, leading to characteristic morphological changes, such as chromatin condensation, nucleosomal DNA fragmentation, nuclear membrane breakdown, externalization of phosphatidylserine, and formation of apoptotic bodies (Adams JM, 2003; Danial NN et al., 2004).

In addition to cytochrome c, several other apoptogenic molecules are also released from the mitochondria. Smac/Diablo, a 25-kD mitochondrial protein, after released into the cytosol during apoptosis, binds to the inhibitors of apoptosis proteins (IAPs) in the cytosol. Through this binding activity, Smac/Diablo neutralizes IAPs' anti-apoptotic activity to insure that they do not stop the pro-apoptotic programme by inhibiting caspases (Du C et al., 2000). Apoptosis-inducing factor (AIF) is a 57-kD flavoprotein residing in the mitochondrial intermembrane space. Upon apoptosis activation, AIF translocates from the mitochondrion to the nucleus and causes chromatin condensation and large-scale DNA fragmentation (Susin SA et al., 1999). Endonuclease G (Endo-G) is a 30-kD nuclease in the mitochondria. Once released from mitochondria, Endo-G is able to induce nucleosomal DNA fragmentation independent on caspase activity (Susin SA et al., 1999; Li LY et al., 2001).

Thus, both the death-receptor and mitochondrial apoptotic pathways lead to the activation of an initiator caspase, caspase-8 in death-receptor pathway or caspase-9 in mitochondrial pathway, which leads to a proteolytic cascade, ultimately resulting in apoptosis. The cross-talk between the death-receptor pathway and the mitochondrial pathway is provided by Bid.

The activation of caspase-3 is the converging point for both of these two pathways. Like other caspase family proteins, the activated caspase-3 is a tetramer composed of two large and two small subunits. Active caspase-3 subsequently cleaves various down-stream cellular proteins or cell-death substrates. Poly (ADP-ribose) polymerase (PARP) is a nuclear enzyme involved in DNA repair, and the cleavage of PARP by caspase was found at the early stage of apoptosis (Kaufmann SH et al., 1993). Such cleavage inactivates the enzyme by destroying its binding ability to DNA strand breaks, finally resulting in the internucleosomal DNA fragmentation (Boulares AH et al., 1999; Oliver FJ et al., 1999). This degradation of chromosomal DNA into nucleosome-sized fragments is one of the characteristics of apoptotic cell death, and caspase-activated DNase (CAD) was also found to facilitate this chromosomal DNA degradation (Mcilroy D et al., 1999). Activated caspase-3 cleaves the inhibitor of CAD (ICAD) to release CAD, which then enters the nucleus to degrade DNA (Sakahira H et al., 1998). Other caspase family proteins, such as caspase-6, -7 and -9 can also be activated by caspase-3 (Schwartz SM, 1998), suggesting a positive feedback existing among caspase family proteins, which should amplify apoptotic signals and enhance the enzymatic activity of caspases. In addition, caspase-3 cleaves Bcl-2 which converts it into a pro-apoptotic protein. The cleaved Bcl-2 promotes the release of cytochrome c from mitochondria to cytosol (Cheng EH et al., 1997; Kirsch DG et al., 1999). The sum of these proteolysis results in the ordered dismantling and removal of the cell.

1.2.2.3 Endoplasmic Reticulum (ER) pathway

Recently, another cell-death pathway, referred to as the endoplasmic reticulum (ER) stress-mediated apoptotic pathway was found (Lam M et al., 1994; Hacki J et al.,

2000). ER is an important organelle in charge of synthesis, folding, post-translational modification, assembly and trafficking of the secretory and cell-surface proteins. In addition, ER is a major intracellular calcium storage compartment for maintaining cellular calcium homeostasis and Ca^{2+}-mediated cell signaling (Kaufman RJ, 2002). Various conditions can disrupt ER functions, including glucose deprivation, perturbation of calcium homeostasis and expression of misfolded proteins. The dysfunction and proteotoxicity in ER induced by the various stimuli are termed "ER stress" (Schroder M et al., 2005). Disruption of these physiological functions by ER stress has been implicated in a wide variety of human diseases, including Alzheimer's disease, Parkinson's disease and diabetes mellitus.

Various ER stresses result in misfolded protein accumulation, which triggers a signaling network called the unfolded protein response (UPR) (Schroder M et al., 2005). For survival, cells upregulate the expression of ER chaperone proteins and foldases so as to alleviate protein aggregation. In addition, cells decrease the biosynthetic burden of the secretory pathway by downregulating expression of genes encoding secreted proteins. Furthermore, the ubiqutin-proteasome system can be activated to perform the degradation of misfolded proteins. However, if ER stress is too severe and prolonged, UPR can activate other pathways that lead to cell death through apoptosis (Ferri KF et al., 2001).

So far, several pathways have been implicated in ER stress-induced apoptosis. One of these pathways involves the C/EBP homologous protein, (CHOP)/GADD153, which is a transcriptional factor. ER stress induces CHOP/GADD153 expression at the transcriptional level. Elevated CHOP/GADD153 sensitizes cells to ER stress through promoting protein synthesis, down-regulating the expression of the antiapoptotic protein Bcl-2 and drastically depleting the cells of glutathione, which is

the primary intracellular scavenger of reactive oxygen species (ROS) (Marciniak SJ et al., 2004; McCullough KD et al., 2004). ER stress also activates the ER transmembrane protein kinase/ribonuclease (IRE1) and PKR-like ER kinase (PERK), which have been implicated in the activation of the pro-apoptotic protein c-Jun NH_2-terminal kinase (JNK) (Harding HP et al., 1999; Urana F et al., 2000). Activation of JNK by endogenous signals can initiate apoptosis through a pathway similar to that initiated by cell surface death receptors in response to extracellular signals, and promoting Bax translocation to mitochondria to induce cytochrome c release and apoptosis (Tsuruta F et al., 2000). Furthermore, ER stress leads to proteolytic cleavage of caspase-12 to iniatiate apoptosis (Yoneda T et al., 2001; Nakagawa T et al., 2000). However, the details of the mechanisms involved in ER stress-mediated apoptosis are still not fully established.

1.2.2.4 Caspase-independent pathway

The caspase-independent apoptotic pathway is induced by granzyme A (GzmA), which is an abundant serine protease released by cytotoxic T lymphocyte (CTL) and natural killer (NK) cell granules (Beresford PJ et al., 1999; Fan Z et al., 2003).Once in a cell, GzmA targets a special 270-420 kDa endoplasmic reticulum (ER)-associated complex, termed the SET complex, which contains the GzmA-activated DNase NM23-H1, the protein phosphatase PP2A inhibitor pp32, the nucleosome assembly protein SET, the base excision repair enzyme Ape1, and the DNA bending protein HMG-2 (Beresford PJ et al., 2001). The activation of NM23-H1 occurs indirectly, through the cleavage of proteins that inhibit NM23-H1 in the SET complex. And the activated NM23-H1 leads to a distinctive form of DNA damage, which is single-stranded DNA nicking (Fan Z et al., 2003a). The targets of

GzmA in the SET complex also have other important functions. Apurinic endonuclease-1 (Ape1) repairs oxidative DNA damage and its cleavage by GzmA contribute to DNA degradation and apoptosis (Fan Z et al., 2003b). Other targets of GzmA include HMG-2 and nuclear lamins responsible for maintaining nuclear structure and histones. And the inactivation of the complex may block the maintenance of DNA and chromatin structural integrity and consequently promote apoptosis (Fan Z et al., 2002).

Mitochondria are the critical organelles for cell survival. The damage of mitochondrial function is essential to initiate the caspase-dependent apoptotic pathway (Green DR et al., 2004). Although GzmA was not found to cleave or disrupt the mitochondrial outer membrane (MOM), it directly caused a rapid increase in ROS and the loss of mitochondrial membrane potential (MMP) (Martinvalet D et al., 2005). Thus, there may be a crosslink between caspase-dependent and caspase-independent pathways through influencing the mitochondrial function.

In conclusion, the caspase-independent GzmA-activated apoptotic pathway not only plays a role in immune surveillance to prevent cancer develoment, but also provide a failsafe way to eliminate viruses and tumors that can evade caspase-dependent apoptosis.

1.2.3 Bcl-2 family proteins in apoptosis

Bcl-2 family proteins regulate apoptosis mainly through controlling the mitochondrial outer membrane permeability and the release of apoptogenic protease activators, including cytochrome c, Smac/DIABLO and apoptosis-inducing factor (AIF) from mitochondria to cytosol. Pro-apoptotic members of Bcl-2 family can

induce the release of the apoptogenic protease activators and anti-apoptotic proteins can inhibit their release (Heimlich G et al., 2004; Shimizu S et al., 1998).

The regulation of mitochondrial outer membrane permeability (MOMP) by the Bcl-2 family proteins is a complex three-way interaction between pro- and anti-apoptotic Bcl-2 members. Bax subfamily proteins, such as Bax and Bak, which upon activated will migrate from the cytosol to the mitochondria to form protein-conducting channels in the mitochondrial outer membrane. Bcl-2 subfamily proteins, such as Bcl-2 and Bcl-x_L, however, when in excess, prevent pore formation by binding and sequestering activated pro-apoptotic proteins. BH3-only subfamily proteins, such as Bid and Bad, once activated by cell death stimuli, appear to directly activate Bax and Bak and/or inhibit Bcl-2. Thus, the ratio of pro-apoptotic and anti-apoptotic proteins is important as it determines the fate of the cell, to survive or die.

Besides their direct regulatory functions on mitochondrial outer membrane permeabilization, Bcl-2 family proteins are also involved in other apoptotic pathways and act as linkers among different cell death pathways. For example, the BH3-only subfamily protein Bid can be activated by caspase-8 and consequently translocate to the mitochondrial outer membrane to induce cytochrome c release, thereby, making a link between death-receptor pathway and mitochondrial pathway. In addition, Bcl-2 family proteins can act as molecular links in the ER stress-initiated mitochondrial apoptotic pathway. It has been demonstrated that Bax/Bak could also localize in the ER membrane. They are activated in response to ER stress, leading to calcium depletion, MOMP increase and apoptosis (Scorrano L et al., 2003). Bcl-2 was also shown to localize in the ER membrane, thereby playing a role in stabilizing ER membrane integrity (Hacki J et al., 2000) by preventing apoptosis.

The characteristics of regulating apoptosis by Bcl-2 family proteins are also modified by various factors. Posttranslational modifications such as phosphorylation on Bcl-2 family proteins can determine their active or inactive conformations. For example, phosphorylation of Bad results in its sequestration in the cytosol; whereas dephosphorylated Bad interacts with Bcl-2 or Bcl-x_L in mitochondria, triggering apoptosis. Further, the interactions between Bcl-2 and other non-Bcl-2-family proteins can modulate the function of Bcl-2 in regulating apoptosis, either facilitating its antiapoptotic function, such as by binding with FKBP38 (Shirane M et al., 2003), or abolishing its prosurvival ability, such as by binding with an orphan nuclear receptor Nur77/TR3 (Lin B et al., 2004).

1.3 Bcl-2 and cell cycle

1.3.1 Cell cycle

Like apoptosis, cell cycle is another fundamental biological process. Cell cycle includes an orderly sequence of events through which a cell duplicates its contents and then divides into two daughter cells. The cell cycle events must be coordinated precisely to allow mitosis to be completed correctly. Cell cycle is under a strict control system, which behaves like an autonomous biochemical timer that is precisely programmed to initiate cell cycle events in the correct order at specific intervals, such that each event is allowed just enough time to complete before the next event is triggered (Fig. 1.3).

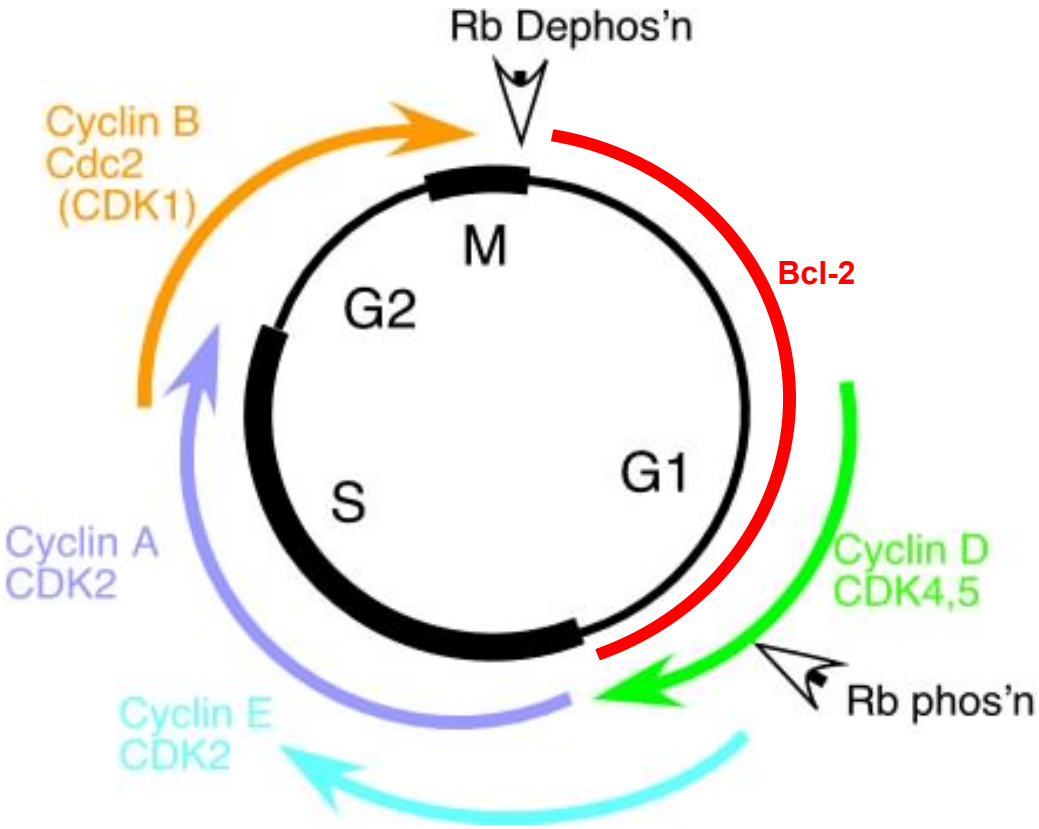

Adapted from Mazel S, et.al (1996). **Regulation of cell division cycle progression by bcl-2 expression: a potential mechanism for inhibition of programmed cell death.** ***J Exp Med.***

Fig. 1.3 Cell cycle. According to the chromosomal events, cell cycle is defined as different stages. S phase is the cell-cycle phase of DNA replication and chromosome duplication. M phase is the cell-cycle phase during which the duplicated chromosomes are segregated and packaged into two daughter nuclei and distributed into two daughter cells. G_1 and G_2 phases are the two gap phases between S and M phases providing additional time for cell growth and cell cycle regulatory checkpoints. Each phase is accompanied with specific regulatory proteins, cyclins and cyclin-dependent kinase (CDK). Expression of Bcl-2 is found to retard G_1/S transition (Mazel S et al., 1996; Deng X et al., 2003).

Most of a cell's components, such as the cytoplasmic organelles, plasma and intracellular membranes, structural proteins and RNAs are replicated continuously throughout the cell cycle, which results in the gradual doubling of cell size by the end of the cell cycle. However, the chromosomes are duplicated only once per cell cycle.

The stage during which a cell synthesizes hereditary materials and duplicates its chromosomes are called the synthetic or S phase. The distribution of duplicated components into individual daughter cells occurs in a brief stage called the mitotic or M phase. There are still additional phases between S and M phases known as gap phases. Gap phases provide additional time for cell growth and the preparation to duplicate and segregate the chromosomes. Gap phases also serve as important regulatory checkpoints for cell cycle phase transitions, during which progression to the next cell-cycle stage can be controlled by a variety of intracellular and extracellular signals. G_1 phase is the cell-cycle gap phase between M and S phase. G_2 phase is the cell-cycle gap phase between S and M phase. In the presence of unfavorable growth conditions or inhibitory signals, cells may pause for extended periods in G_1 phase or enter a prolonged nondividing state called G_0 phase.

Tissue homeostasis requires a balance between cell proliferation and cell death. Control of cell number is determined by an intricate balance of cell death and cell proliferation. Accumulation of cells through suppression of cell death can contribute to cancer, while excessive cell death may result in impaired development and in degenerative diseases (Rubin LL et al., 1993; Collins K et al., 1997; King KL et al., 1998). Thus, there appears to be links between cell cycle and apoptosis control mechanisms. Elucidating these mechanisms will enable further understanding of tumor progression and designing new models of effective anti-tumor therapy.

1.3.2 Bcl-2 in cell cycle

In addition to its well-established function in regulating apoptosis, Bcl-2 family has also been found to regulate cell survival and growth by influencing the cell cycle progression (Mazel S et al., 1996; Gao G et al., 2000). Further studies showed

that the expression of the bcl-2 gene resulted in an inhibition of cell cycle progression. The transition of quiescent cells into the S phase could be inhibited by Bcl-2 and Bcl-x_L, as well as adenovirus Bcl-2 homolog E1B19KD. This Bcl-2-mediated cell survival and growth inhibition could be antagonized by the pro-apoptotic protein, Bax. For example, G_1 phase is found to be shortened in lymphocyte without the expression of Bcl-2 or with the expression of Bax. Conversely, the expression of bcl-2 gene results in a substantial increase in the length of G_1 phases. The relationship between the antiapoptotic function of Bcl-2 and the inhibitory influence on cell cycle entry is not very clear. Further experiments have shown that these two functions can be separated. The critical amino acid residue is a tyrosine residue Y28, which is within the conserved N-terminal BH4 region of Bcl-2. A mutant with alanine replacing Y28 cannot retard cell cycle entry of fibroblasts without affecting the antiapoptotic function of Bcl-2 (Huang DC et al., 1997)

1.4 Bcl-2 and antioxidation

1.4.1 Reactive Oxygen Species (ROS)

Reactive oxygen species (ROS) are produced during the process of metabolism with oxygen. Normally, 98%-99% of O_2 is consumed by the electron transport throughout the mitochondrial respiratory chain, and some of them can be converted into ROS as a byproduct of cellular energy production. If the metabolic activation increases, the consumption of oxygen goes up, and an increased amount of ROS is generated. Thus, the mitochondria are major sites of ROS production (Boveris A et al., 1973; Zamzami N et al., 1995). Meantime, mitochondria are also the targets of ROS. Although it was not entirely understood, ROS may oxidize the pores in the

mitochondrial outer membrane, which results in the disruption of the mitochondrial membrane potential and causes cytochrome c release leading to apoptosis (Zamzami N et al., 1995; Kannan K et al., 2000; Simon HU et al., 2000). Yet, ROS shows a dual function. At very low concentration, it may act as a second messenger in receptor-mediated signaling pathway (Suzuki YJ et al., 1997).

ROS includes oxygen ions, free radicals and peroxides both in inorganic and organic. They are generally very small molecules and are highly reactive due to the presence of unpaired valence shell electrons. Superoxide radical, $O_2^{\cdot -}$ is formed when O_2 takes up one electron. The principal loss of electrons that convert O_2 to $O_2^{\cdot -}$ involves co-enzyme Q, ubiquinone and its complexes (Boveris A, 1977). As the primary product of e^- attack on O_2, $O_2^{\cdot -}$ itself does not result in lipid peroxidation because of the poor reactivity with lipid, and it can be reduced by superoxide dismutase (SOD) to form hydrogen peroxide (H_2O_2). In the presence of Fe^{2+} or Cu^+, H_2O_2 produces the most reactive species, hydroxyl radical ($OH^{\cdot}$). ROS, $O_2^{\cdot -}$, H_2O_2 and $OH^{\cdot}$ may consequently damage a wide variety of cellular components through mechanisms such as lipid peroxidation, protein oxidation and genetic damage through oxidation of DNA.

1.4.2 General regulations on ROS

Normally, cells defend against ROS damage through the use of enzymes such as superoxide dismutases (SOD), glutathione peroxide (GPX) and catalases (CAT). There are three SOD isomers: cytosolic copper-zinc superoxide dismutase (Cu-Zn-SOD/SOD1), mitochondrial manganese dismutase (Mn-SOD/SOD2) and extracellular copper-zinc superoxide dismutase (Cu-Zn-SOD/SOD3). All SODs can convert superoxide, $O_2^{\cdot -}$, to H_2O_2. Mn-SOD expression is regulated, and this protein has been

shown to protect against tumor necrosis factor, radiation, and chemotherapeutic agent cytotoxicity (Wong GH et al., 1988). H_2O_2 can also be removed by CAT and GPX. CAT reacts with H_2O_2 to form water and molecular oxygen. GPX detoxifies H_2O_2 by interacting with reduced glutathione (GSH) to produce water and oxidized glutathione (GSSG). GSSG is then recycled to GSH by glutathione reductase (GR). CAT mainly exits in the peroxisome fraction and GPX is found in the cytoplasm and the matrix of mitochondria (DelMaestro R et al., 1989).

1.4.3 Bcl-2 and the intracellular ROS

Bcl-2 was found to act as an antioxidant to prevent the lipid peroxidation and the cellular damage such as base modifications or single-strand DNA breaks (Jang JH et al., 2003) caused by the ROS without affecting the generation of $O_2^{\cdot -}$. Bcl-2-deficient mice develop two potentially redox-related pathologies, polycystic kidney disease and hypopigmentation (Veis DJ et al., 1993), possibly due to the over-production of ROS. The antioxidant defense mechanism by Bcl-2 is not very clear. However, it was found that Bcl-2 could promote the expressions of anti-oxidant enzymes and GSH (Papadopoulos MC et al., 1998). Also, Bcl-2 can alter GSH localization. It was found that over-expression of Bcl-2 led to a relocalization of GSH from cytosol to nucleus, which may change the nuclear redox potential, creating a highly reducing environment (Voehringer DW et al., 1998) to inhibit or retard apoptosis.

Combined with the cell survival and growth inhibitory function through retarding cell cycle progression from G_1 to S phase, the efficient antioxidant activity of Bcl-2 could serve as a key mechanism in rapidly dividing cells by slowing cell

growth and increasing cell survival in order to provide the cells more time to monitor and repair cellular damage provoked by increased ROS levels which could be generated by the higher mitochondrial electron respiratory chain activity.

On the other hand, the overexpression of Bcl-2 could also increase the chance of mutagenesis through its antioxidant function by further rendering cancer cells less vulnerable to oxidative stress-induced apoptosis, which could result in the resistance to anti-cancer drugs. This cell survival and growth inhibitory function could also prolong cancer cell survival time by reducing oxygen consumption and metabolism especially in hypoxic conditions.

1.5 Bcl-2 and mismatch repair activity

DNA repair is a major defense against environmental damage to cells. DNA repair is involved in processes that minimize cell killing, mutations, replication errors, persistence of DNA damage and genomic instability.

There are three major DNA repairing mechanisms, base excision, nucleotide excision and mismatch repair. Abnormalities in any of these three repairing mechanisms have been implicated in cancer and aging (Peterson CL et al., 2004).

Beside its antiapoptotic function, Bcl-2 may mediate oncogenesis through suppressing mismatch repair activity to enhance mutagenesis (Youn CK et al., 2005). One of the most significant finding was that Bcl-2 can inhibit the transcription factor E2F transcriptional activity. Bcl-2 expression triggered the increased expression of cyclin-dependent kinase 2 (Cdk2) inhibitors, such as $p27^{Kip1}$. Correspondingly, the tumor-suppressor retinoblastoma protein (Rb) could not be phosphorylated. Hypophosphorylated Rb binds to E2F; and the Rb-E2F complex further prevented

E2F from binding DNA, which downregulated the transcription of the human MSH2 gene (hMSH2), which correlates with a disease in MMR activity and increase in mutagenesis.

1.6 Post-translational modifications on Bcl-2

1.6.1 The role of Bcl-2 loop in its post-translational modification

Besides its expression level in cells, the post-translational modifications of Bcl-2 such as phosphorylation and proteolytic cleavage play important roles in its functions including anti-apoptosis, antioxidant and cell cycle progression inhibition (Yin XM et al., 1994; Deng X et al., 2003; Furukawa Y et al., 2000; Ruvolo PP et al., 2001; Ito T et al., 2001; Thomas A et al., 2000). The post-translational modification can affect Bcl-2's capacity for dimerization or interaction with other proteins as well as its stability (Dimmeler S et al., 1999; Breitschopf K et al., 2000). And the long non-conserved flexible loop region between BH4 and BH3 domains in Bcl-2 was found to be responsible for its post-translational modifications (Srivastava RK et al., 1999; Kang CB et al., 2005).

Several amino acid residues in this loop region, including threonine 56 (T56), serine 70 (S70), threonine 74 (T74) and serine 87 (S87) have been found to be important for the phosphorylation modification on Bcl-2. However, the different residues may play different roles to different stimuli. For example, phosphorylation of Bcl-2 on T56 or S87 appeared to be critical for its inhibition on glucocorticoid-induced apoptosis, whereas phosphorylation of S70 appeared to be irrelevant for its anti-apoptotic function under this stimulus (Huang ST et al., 2002). However,

phosphorylation of Bcl-2 on S70 was essential for its inhibitory action on etoposide-induced apoptosis. The loss of being phosphorylated on S70 through mutation of serine to alanine completely abolished the anti-apoptotic function when etoposide was treated (Ito T et al., 1997). On the other hand, phosphorylation on the residues within the unstructured loop of Bcl-2 by Jun N-terminal protein kinase (JNK) may promote apoptosis induced by the microtubule-damaging agents, and the Ser70Ala restored resistance to apoptosis. Thus, the type of stimulus, the regulatory pathways involved, and the phosphorylation at specific Bcl-2 residues produce different outcomes on apoptosis regulation.

In addition to affecting Bcl-2 anti-apoptotic activity, phosphorylation modification on Bcl-2 also influences its stability. It has been found that tumor necrosis factor alpha (TNF-α) could induce dephosphorylation and subsequent ubiquitin-proteasome-dependent degradation of Bcl-2 (Dimmeler S et al., 1999). The dephosphorylation of S87 appeared to play a major role in Bcl-2 degradation (Breitschopf K et al., 2000) in response to this stimulus. In addition to phosphorylation, the loop domain of Bcl-2 was found to be necessary for Bcl-2 proteolytic cleavage. *In vitro* experiments showed that Bcl-2 could be cleaved by caspase-3 at Asp34, a site in the loop region (Cheng EH et al., 1997). The carboxyl-terminal Bcl-2 cleavage product could further triggered apoptosis and accelerated Sindbis virus-induced apoptosis. Moreover, the inhibition of ubiquitin-proteasome pathway also induced Bcl-2 cleavage by a caspase-3-like protease. This cleavage of Bcl-2 promoted cell death through the apoptotic pathway (Zhang XM et al., 1999).

1.6.2 Interactions of Bcl-2 with other non-Bcl-2 family proteins

It is well known that Bcl-2 family proteins can interact with each other through homodimerization and/or heterodimerization to protect or damage the integrity of the mitochondrial outer membrane, and further determine the cell fate. In addition, the features of Bcl-2 family proteins to interact with non-Bcl-2 family proteins have also been found to play important roles in regulating Bcl-2 activity through different mechanisms. And Bcl-2 flexible loop has been shown responsible for these interactions.

1.6.2.1 Interaction between Bcl-2 and Presenilins

Presenilins are integral membrane proteins with six to nine membrane-spanning domains and a large hydrophilic loop facing the cytosol (Doan A et al., 1996; Laudon H et al., 2005). Presenilins are mainly localized in the endoplasmic reticulum (ER) and function as regulators in intracellular trafficking and in calcium homeostasis (Levitan D et al., 1995; Leem JY et al., 2002; Buxbaum JD et al., 1998). Presenilin-1 (PS-1) was found to practically co-localize with Bcl-2 and interact directly with Bcl-2 (Alberici A et al., 1999). Recently, it was found that PS-1 could reduce the distribution of Bcl-2 in mitochondria by competitively binding with another Bcl-2-interacting protein FKBP38, and consequently apoptosis was induced. Thus, the mechanisms in regulating apoptosis through the interaction of Bcl-2 with PS-1 maybe related to the regulation of calcium homeostatsis in ER as well as the maintenance of the integrity of the mitochondrial membrane (Keller JN et al., 1998; Wang HQ et al., 2005).

1.6.2.2 Interaction between Bcl-2 and Nur77/TR3

Nur77 / TR3 is a member of the orphan steroid receptor family (Mangelsdorf DJ et al., 1995). During apoptosis, Nur77/TR3 expression is rapidly up-regulated and it translocates from the nucleus to the mitochondria to induce the release of cytochrome *c* (Li H et al., 2000). Recently, it has been found that Nur77/TR3 could bind to Bcl-2 after translocating to the mitochondria. This interaction is through Bcl-2 loop region, triggering a conformational change in the Bcl-2 molecule, which exposed the pro-apoptotic BH3 domain, thereby converting Bcl-2 from an anti-apoptotic protein to a pro-apoptotic protein.

1.6.2.3 Interaction between Bcl-2 and p53

The nuclear transcription factor, p53, is a tumor suppressor gene, which induces apoptosis by up-regulating the transcription of pro-apoptotic genes and by down-regulating anti-apoptotic genes (Yonish-Rouach E et al., 1991; Shaw P et al., 1992). In addition, p53 has a transcription-independent direct apoptogenic role through its rapid translocation to the mitochondrial membrane after the induction of DNA damage (Marchenko ND et al., 2000). In the mitochondria, p53 interacts directly with members of the Bcl-2 family to regulate mitochondrial outer membrane permeability (MOMP).

Interaction between Bcl-2 and p53 also occurs through the loop region. Interestingly, the flexible loop of Bcl-2 was found to have both positive and negative regulatory functions on its anti-apoptotic function and the binding with p53 (Deng X et al., 2006). The part of Q32-R68 enhanced their binding activity and negatively regulates the anti-apoptotic function of Bcl-2. The part of T69-S87 abrogated Bcl-2 binding capacity with p53 and positively regulates the anti-apoptotic function of Bcl-2.

The direct interaction between p53 and the pro-apoptotic proteins led to the oligomerization of Bax and/or Bak, which consequently results in the MOMP and apoptosis (Chipuk JE et al., 2004; Leu JI et al., 2004).

1.6.2.4 Interaction between Bcl-2 and FKBP38

1.6.2.3.1 FKBP38 background

FK506 binding protein 38 (FKBP38) is another protein which has been recently shown to bind to Bcl-2 at the mitochondria and regulate apoptosis. However, the difference from the other Bcl-2-interacting proteins is that FKBP38 acts as an anti-apoptotic protein by binding to Bcl-2.

FKBP38 belongs to the immunophilin families, which are highly conserved intracellular receptors for the immunosuppressants including cyclosporine A, FK506 and rapamycin (Schreiber SL, 1991; Standaert RF et al., 1990; Siekierka JJ et al., 1989; Jin YJ et al., 1991; Jin YJ et al., 1992). The immunophilins are ubiquitous and conserved proteins, which include FKBPs, cyclophilin 40 (CyP-40) and protein phosphatase 5 (PP5) (Silverstein AM et al., 1997; Pedersen KM et al., 1999). All members of the immunophilins have peptidylprolyl *cis/trans* isomerase (PPIase) activity (Galat A, 1993), which are folding helper enzymes with the capability to catalyze the *cis/trans* isomerization of proly bonds of a target protein. The lower molecular weight immunophilins, such as FKBP12 and CyP-18, are thought to be the cellular components responsible for the immunosuppression. The higher molecular weight immunophilins, such as FKBP52 and CyP-40 are components of steroid receptor heterocomplexes, function as chaperones and participate in the regulation of

steroid receptors such as the folding and trafficking of a glucocorticoid receptor complex between the cytoplasm and nucleus (Freeman BC et al., 1996; Schiene-Fischer C et al., 2001; Pratt WB, 1993). In addition to the PPIase domains possessed by the low molecular weight immunophilins, these high molecular weight immunophilins also contain three tetratricopeptide repeats (TPR) and a calmodulin-binding domain in their C-terminal part (Smith DF et al., 1993; Ratajczak T et al., 1993). TPR domains consist of a variable number of degenerate tandem 34-amino acid repeats, which have a variety of functions, including being as targeting domains, mediating specific protein-protein interactions (Lamb JR et al., 1995; Radanyi C et al., 1994). Calmodulin-binding domains are responsible for the interaction with calmodulin (CaM), which are subdivided into calcium-dependent and calcium-independent modes. Ca^{2+}-CaM can bind to target proteins to alter their function, acting as a part of a calcium signal transduction pathway. Ca^{2+}-free CaM can bind to other target proteins, including neuron proteins, receptors, second messenger signaling proteins, cytoskeletal and muscle proteins, responding to neurotransmitter production, nerve growth, synaptic development, intracellular movement and smooth muscle relaxation.

As immunophilins, FKBPs are responsible for the binding to the immunosuppressant FK506. FKBPs are found in diverse spectrum of species in both prokaryotic and eukaryotic cells with the molecular masses ranging among 12-63 kD (Siekierka JJ et al., 1989; Jin YJ et al., 1991; Jin YJ et al., 1992). In all of the FKBP members, there is a conserved FKBP domain which is involved in both their FK506-binding activity and their PPIase activity. The FKBP family proteins were found localized in the cytosol, the mitochondrial membrane and the nucleus (Ruff VA et al., 1992; Jin YJ et al., 1993; Riviere S et al., 1993). FKBP12 is the first member of the

FKBP family to be found (Harding MW et al., 1989), and also is a well-characterized immunophilin with the binding capabilities to both FK506 and rapamycin. FKBP12-FK506 complex can bind and inhibit the activity of calcineurin, a calcium/calmodulin-dependent serine/threonine phosphatase (Liu J et al., 1991). FKBP12-rapamycin complex inhibits the mammalian Target of Rapamycin (mTOR), which functions as an ATP sensor in controlling ribosome biogenesis and cell growth (Dennis PB et al., 2001). Another FKBP family protein, FKBP52 also showed the similar binding capacity to FK506 through its PPIase domain (Yem AW et al., 1992). Yet, unlike FKBP12, FKBP52-FK506 complex does not inhibit calcineurin activity (Lebeau MC et al., 1994). As a high-molecular weight immuphilin protein, FKBP52 binds to Hsp90 through its TPR domain, and functions as a co-chaperon protein in steroid receptors function and subcellular trafficking (Riggs DL et al., 2003; Davies TH et al., 2005). Furthermore, FKBP52 may also be involved in nerve regeneration (Gold BG, 1999).

FKBP38 is a novel FKBP family member with an N-terminal FKBP domain, which is 33% identical to FKBP12 (Lam E et al., 1995). Similar to other high-molecular weight immuphilins, FKBP38 contains a tripartite TPR domain with 21% similar to FKBP52 and 27% similar to Cyp-40, respectively. Also, FKBP38 contains a putative CaM-binding domain with 29% similar to FKBP52 and 27% similar to Cyp-40, respectively. In addition, FKBP38 has a transmembrane domain at its C-terminus, which is responsible for FKBP38 localizing in cellular membrane (Shirane M et al., 2003). Although FKBP38 has a highly homologous FKBP domain, it does not have the FK506-binding activity and the canonical PPIase activity (Shirane M et al., 2003). By using the co-immunoprecipitation and *in vitro* calcineurin activity assay, it was reported that FKBP38 shows an inhibitory capability on calcineurin in the

absence of FK506, suggesting FKBP38 as a intrinsic inhibitor of calcineurin (Shirane M et al., 2003). In contrast, in SH-SY5Y and Jurkat cells previous studies suggest that FKBP38 failed to interact with calcineurin physically (Weiwad M et al., 2005). Interestingly, FKBP38's interaction with Bcl-2 and PPIase were demonstrated to be regulated by Ca^{2+}-bound CaM (Shibasaki F et al., 1997; Klee CB et al., 1979).

1.6.2.3.2 Molecular interaction of FKBP38 with Bcl-2

Recently, it was found that FKBP38 could bind to the anti-apoptotic proteins Bcl-2 and Bcl-x_L (Shirane M et al., 2003). The *in vitro* experiments showed that the long flexible loop between BH3 and BH4 domains of Bcl-2 is also responsible for their interactions (Kang CB et al., 2005). The interaction between FKBP38 with Bcl-2 or Bcl-x_L targeted them localized at mitochondria for their anti-apoptotic function. After the removal of FKBP38 by using RNA interference, the exogenous Bcl-2 and Bcl-x_L were found misdistributing inside cells. Bcl-2 accumulated around the nuclear membrane and Bcl-x_L diffused throughout the cytosol (Shirane M et al., 2003). Thus, by influencing the distribution of Bcl-2 and Bcl-x_L, FKBP38 may perform its anti-apoptotic function through the Bcl-2-inhibitable mitochondrial apoptotic pathway (Germain M et al., 2003). However, in SH-SY5Y cells, it was found that the interaction between FKBP38 and Bcl-2 was regulated by Ca^{2+}/CaM (Edlich F et al., 2005). Ca^{2+}/CaM activates the PPIase enzymatic activity of FKBP38. The *in vivo* experiments further showed the interaction between FKBP38 and Bcl-2 also influenced the interaction between Bcl-2 and other pro-apoptotic proteins. In contrast to what was observed in HeLa cells, the knocking-down of FKBP38 by RNA interference in SH-SY5Y prevents apoptosis. These contradicting results may come from the different apoptotic pathways activated in different cells used in the studies.

Recently, it was found that FKBP38 interacts with Presenilin 1/2 (PS-1/2) (Wang HQ et al., 2005). FKBP38 targeted Bcl-2 to mitochondria and protected Bcl-2 from degradation. PS1/2 was shown to compete with FKBP38 for the subcellular distribution of Bcl-2 between mitochondria and ER/Golgi and regulate apoptosis.

1.6.2.3.3 FKBP38's other functions

FKBP38 is involved in other cellular functions; gene expression analyses showed that overexpression of the tuberous sclerosis (TSC) genes is accompanied with the up-regulation of FKBP38, which resulted in cell size reduction (Rosner M et al., 2003). And inhibiting FKBP38 with a neurotrophic FKBP38-specific ligand, *N*-(*N'*, *N'*-Dimethylcarboxamidomethyl) cycloheximide caused neuronal protection and neural stem cell proliferation and differentiation (Edlich F et al., 2006).

1.7 RNA interference

Several approaches have been used for down-regulating genes in transcriptional level or post-transcriptional level, including antibiotics against specific region of 30s and 50s ribosomal subunits (Tenson T et al., 2006), ribozymes (Krugere K et al., 1982), antisense oligonucleotides (ASONs) and RNA interference (RNAi) (Hannon GJ, 2002). Recently, it has been demonstrated that synthetically designed small interfering RNAs (siRNA)-mediated RNA interference can be used to knock-down mRNA of interest and consequently suppress protein function in mammalian cells (Fire A et al., 1998). RNAi is an evolutionarily conserved biological process to act as a natural cellular defense against viral infection and genetic disorders in plants and animals (Hannon GJ, 2002). However, in mammalian cells, if the length of

dsRNA is greater than 30 bps, it can trigger interfering response by activating the protein kinase PKR and 2',5'-oligoadenylate synthetase (2',5'-AS) (Manche L et al., 1992; Minks MA et al., 1979). Activated PKR inhibits mRNA translation by phosphorylating the α subunit of protein synthesis eukaryotic initiation factor (eIF-2α). In the meantime, activated 2',5'-AS causes mRNA degradation by 2',5'-oligoadenylate-activated ribonuclease L. These responses finally lead to a global shut-off in protein synthesis as well as non-specific mRNA degradation (Stark GR et al., 1998).

Small interfering RNA (siRNA) is a 21- to 23-nucleotide (nt) double-strand RNA duplex, which can induce sequence-specific RNAi activity to lead the target mRNA degraded in mammalian cells, without causing broad shutdown of protein synthesis by triggering the interfering response (Fire A et al., 1998; Elbashir SM et al., 2001). Thus, siRNA-mediated gene silencing is rapidly emerging as a convenient tool to study gene function in a variety of organisms to produce specific downregulation of protein expression at the posttranscriptional level.

When a long double-stranded RNA is introduced into cells, it could be processed into ~22-nucleotide fragments by a double-stranded RNA specific RNase III endoribonucleases, named Dicer to initiate RNAi (Filippov V et al., 2000). Dicer has a signature motif composed of 1-2 copies of a 9-residue consensus sequence and conserved in all known prokaryotes and eukaryotes. The long double-stranded RNA can be cleaved by Dicer into precisely ~22-nt size fragments or siRNAs (Blaszczyk J et al., 2001). Then the siRNAs are instantaneously incorporated into a high-molecular-weight (~360 kDa) nuclease complex named RNA-induced silencing complex (RISC). RISC is a protein-RNA effector nuclease complex that recognizes and destroys target mRNAs. RISC is activated by the unwinding of the RNA duplexes

by consuming ATP. Under the guide of the anti-sense strand (guide strand) of the siRNA, RISC recognizes the sequence-specific target mRNA and cleaves it at the middle site of the siRNA (Hannon GJ, 2002; Nykanen A et al., 2001; Meister G et al., 2004). After the double-stranded siRNA is loaded on RISC, helicase may be involved in separating the RNA strands on ATP-dependent manner (Meister G et al., 2004). And Argonaute 2 (Ago 2), an endonuclease with RISC, is in charge of the degradation of the sense strand (anti-guide strand) of the siRNA, as well as in charge of the cleavage of the target mRNA by using the anti-sense strand (guide strand) (Rand TA et al., 2005). The cleaved mRNA is consequently degraded by endo- and exonucleases. In addition, in plants and worms, it is also found that the siRNA can serve as a primer for an RNA-dependent RNA polymerase (RdRP), using mRNA as the template, creating many more siRNAs, which could explain the catalytic mechanism of RNAi, only a few dsRNA molecules are required to degrade a much larger population of mRNAs. Yet, this elongation of siRNA also increases the possibility of non-specific interference by sequences homologous to other genes, which is known as transitive RNAi, and only found in plants and worms (Voinnet O et al., 1998; Dillin A, 2003) (Fig. 1.4). These above features also contribute to the inheritable capacity of RNAi, which make RNAi a long-lasting biological activity.

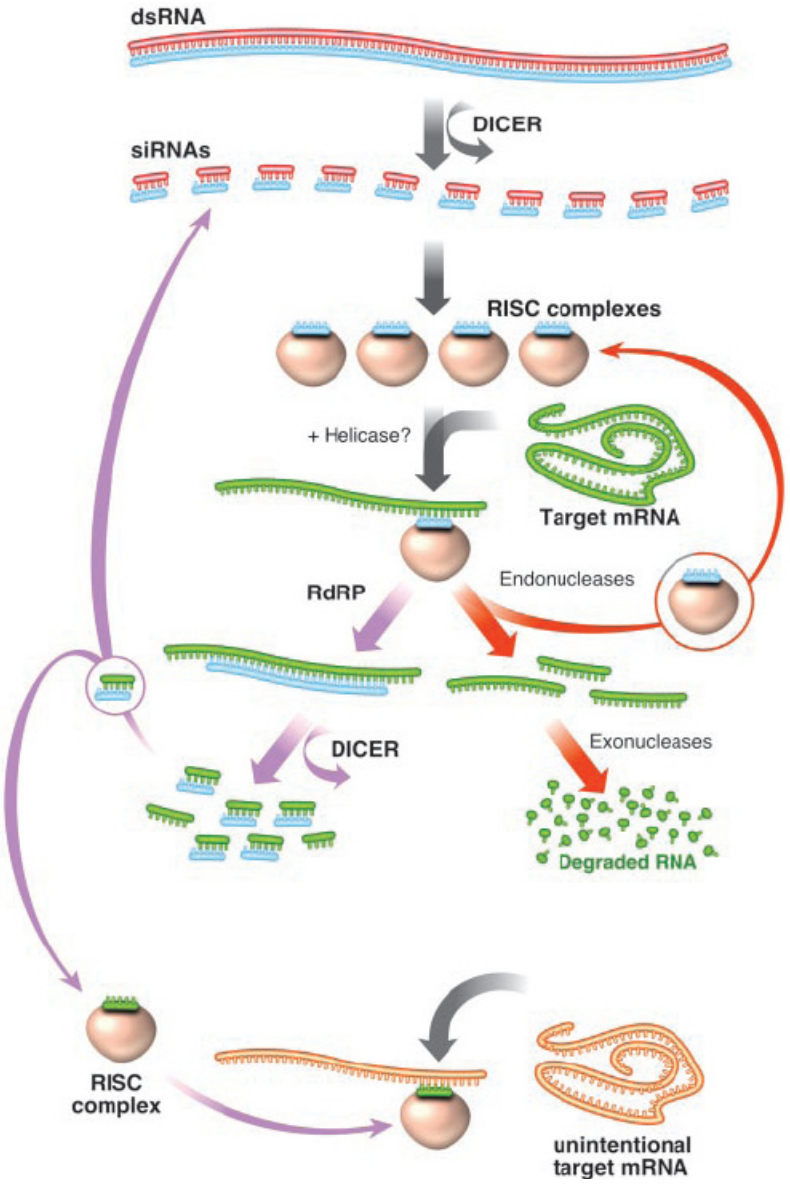

Adapted from Dillin A (2003). **The specifics of small interfering RNA specificity**. *Proc Natl Acad Sci U S A.*

Fig. 1.4 RNA interference (RNAi). Once entering into the cell, long double-stranded RNA (dsRNA) is cleaved by Dicer into ~22-nt small interfering RNAs (siRNAs). siRNAs are incoporated into a large RNA-protein complex, called RNA-inducing silencing complex (RISC). Under ATP-dependent, RISC unwinds siRNAs and targets the specific mRNA under the guide of antisense RNA to cleave the target mRNA at the middle site. The cleaved mRNA is rapidly degraded by endo and exonucleases. siRNA can also serve as a template for RNA-dependent RNA polymerase (RdRP) to synthesize new siRNAs and amplify siRNAs amount. Elongation of the siRNA lead to produce more siRNA as well as increase the chance to degrade the other homologous genes (Dillin A, 2003).

RNAi is ATP-dependent (Nykanen A et al., 2001). And the long dsRNA processing by Dicer and the unwinding of siRNA duplex by RISC are ATP-dependent. The incorporation of siRNAs with the inactive RISC and the recognition and cleavage of the target mRNA are ATP-independent. Besides the small interfering RNAs (siRNAs), there are still two additional small RNAs naturally occurring in mammalian cells, repeat-associated short interfering RNAs (rasiRNAs) and microRNAs (miRNAs) (Aravin AA et al., 2003). rasiRNAs are found abundantly in early embryo and may participate in defining chromatin structure. miRNAs can also function as guide molecules in posttranscriptional gene silencing by base pairing with target mRNAs, which leads to mRNA cleavage or transcriptional repression. Yet different from siRNAs, miRNAs are single-stranded RNAs of 19-25 nucleotides in length that are generated from endogenous hairpin-shaped transcripts. Also siRISC and miRISC are distinct complexes that regulate mRNA stability and translation (Kim VN, 2005; Tang G, 2005).

ASONs and siRNA-mediated gene silencing methods are similar in that both use oligonucleotide sequences complementary to a target gene and cleave it with the recruitment of cellular enzymes; RNase H in the case of ASONs-mediated gene silencing and RISC enzyme complex in the case of RNAi. However, compared to ASONs, RNAi is a catalytic process with less amounts of siRNAs and acts longer. In some systems siRNA-induced RNAi effects persist for as long as 3 weeks (Omi K et al., 2004). Thus, as a catalytic and recyclable process, siRNA-mediated RNAi is a much more simplified and tractable to specifically silence target genes in living cells compared to other existing silencing techniques.

1.8 Objective of this project

The *bcl-2* is a proto-oncogene overexpressed in a variety of cancers and it is well-known for its anti-apoptotic function to enhance cell survival by inhibiting cell death through the protection of the integrity of the mitochondrial outer membrane. In addition, Bcl-2 has also been found to have an antioxidant effect by reducing the generation of reactive oxygen species (ROS) inside cells. ROS is mainly generated in mitochondria as a by-product from the respiratory chain. Excess ROS could damage cellular organelles and finally lead to cell death. Thus, the antioxidant characteristic of Bcl-2 enhances its pro-survival ability through reduction of the cytotoxity of ROS, especially for those rapidly proliferating cells.

Also, Bcl-2 is a regulator of cell cycle. Overexpression of Bcl-2 indicates a $G_1 \rightarrow S$ transition delay to make cells staying in G_0/G_1 phase. G_1 phase plays a key role in cell cycle checkpoints. The long period of G_1 phase provides more time for checking cell cycle and ensuring normal cell division and proliferation. The multiple functions of Bcl-2 suggest its important roles involved in various cellular processes.

Apoptosis and cell cycle are two fundamental biological processes. The balance between these two biological processes is essential to maintain the normal embryonic development and tissue homeostasis. However, the relationship between apoptosis and cell cycle is still not very clear. In this project, by using RNA interference, we systematically explored the regulatory functions of Bcl-2 in both apoptosis and cell cycle, and try to identify the linkage function of Bcl-2 between these two fundamental cellular biological processes.

Overexpression of Bcl-2 also correlates with a resistance to chemo- and radio-therapies and a poor prognosis in cancer. Down-regulation of Bcl-2 can enhance the chemosensitivities to various anti-cancer drugs. Thus, Bcl-2 can be a major target in anticancer therapy. In this project, we also used siRNA-mediated RNAi as a tool to down-regulate Bcl-2 and investigated the effect in cancer cells which overexpress Bcl-2. The influences on chemo-sensitivities of cancer cells to various anti-cancer drugs after suppressing Bcl-2 were evaluated through molecular and biochemical methods.

FK506 binding protein 38 (FKBP38) is a recently identified chaperon protein which shows molecular interactions with Bcl-2 and Bcl-x_L and anchoring them to the mitochondria membrane. After suppressing FKBP38, the exogenous Bcl-2 and Bcl-x_L could not properly localize at the mitochondrial membrane. Thus, FKBP38 may exert its chaperon-like activity to help Bcl-2/Bcl-x_L localizing at the mitochondria membrane for its anti-apoptotic function. However, the detailed regulatory mechanism remains unclear. Given the chaperon-like activity of FKBP38, what are the physiological changes in the cells when FKBP38 is suppressed? Besides the anti-apoptotic proteins Bcl-2 and Bcl-x_L, are there any alternative downstream targets of FKBP38?

Bcl-2 has multiple regulatory functions involved in apoptosis and cell cycle. Our understanding on the biological role of FKBP38 in these processes in connection with Bcl-2 is still limited. Bcl-2 has a long flexible loop between its BH3 and BH4 domains with several phosphorylation sites. Various experiments indicate that this loop part is responsible for the post-translational modification of Bcl-2 and the interaction of Bcl-2 with other proteins, thus, regulating Bcl-2 functions. The *in vitro* study showed that this loop is also responsible for the interaction between FKBP38

and Bcl-2. In this project, we further explored the *in vivo* interactions between FKBP38 and Bcl-2 and studied the function of the flexible loop and the molecular basis in modulating the function of Bcl-2 in apoptosis.

Chapter 2 Materials and Methods

2.1 Materials

2.1.1 Reagents and antibodies

1. Transfection reagents:

   Two transfection reagents were involved in this thesis, including Oligofectamine^{TM} (Invitrogen) and Lipofactamine 2000 (Invitrogen). All of these tranfection reagents were stored at 4^{o}C.

2. Small interfering RNAs:

   All the small interfering RNAs (siRNAs) used in this thesis are from Dharmacon. The siRNAs were dissolved in a buffer provided (100 mM potassium acetate, 30 mM HEPES-KOH, 2 mM magnesium acetate, pH 7.4) to obtain a 20 μM solution before storing at -80^{o}C. Prior to experimentation, the siRNA solution was heated to 90^{o}C for 1 min, and then incubated at 37^{o}C for 60 min, to disrupt higher aggregates and ensure siRNA silencing efficiency.

3. Anti-cancer drugs:

   Four different anti-cancer drugs were used in this theis. *Cis*-Diammineplatinum (II) dichloride (Cisplatin), S-(+)-Camptothecin (Camptothecin) and Paclitaxel (Sigma-Aldrich Chemical Co.) were solubilized in DMSO to a stock concentration of 2mM, 10mM and 20mM respectively. Betulinic Acid (A.G.

Scientific, Inc.) was solubilized in DMSO at 2mM concentration. All of the drug stock solutions were stored at -20^{o}C.

4. Antibodies:

The antibodies involved in this thesis include anti-cytochrome oxidase subunit IV / Cox-IV (Molecular Probes), anti-GAPDH (Ambion), anti-Flag (Sigma), anti-calnexin (Santa Cruz, Cat sc-6465), anti-Bcl-2 (Santa Cruz, Cat sc-509), anti-Bcl-x_L (Santa Cruz, Cat sc-643), anti-Bax (Santa Cruz, sc-6236), anti-p27 (Santa Cruz, sc-1641), anti-cyclin D1 (Santa Cruz, sc-753), anti-cyclin E (Santa Cruz, sc-), anti-cyclin A (Santa Cruz, sc-239), anti-cyclin B1 (Santa Cruz, sc-7393), anti-CDK2 (Santa Cruz, sc-6248) and GFP (Santa Cruz, sc-9996). Antibody against human FKBP38 was a kind gift from Prof. Keiichi I. Nakayama. The antibodies were stored at -20^{o}C or 4^{o}C according to the instruction.

5. Other chemicals and reagents:

Chloroquine, ammino chloride / NH_4Cl, 4'-6'-diamidino-2-phenylindole (DAPI), N-acetylcysteine, propidium iodide, N-benzoyloxycarbonyl (Z)-Leu-Leu-leucinal/MG132 were purchased from Sigma. Clasto-Lactacystin β-lactone was purchased from A.G.Scientific, Inc.. Z-VAD-FMK and Z-DEVD-FMK were purchased from BD PharMingen. Fetal bovine serum (FBS), penicillin-streptomycin, sodium pyruvate, MEM non-essential amino acid and sodium bicarbonate were purchased from Invitrogen. 2',7'-dichlorodihydrofluorescein diacetate (DCHF-DA) was purchased from Molecular Probe. RNase inhibitor was purchase from Roche.

2.1.2 Media for bacteria culture

The LB medium was made of 1% Bacto-tryptone, 0.5% Bacto-yeast extract and 0.5% NaCl. The LB agar plate was made of 1% Bacto-tryptone, 0.5% Bacto-yeast extract, 0.5% NaCl and 2% Bacto-agar.

2.1.3 Media for mammalian cell culture

The media for mammalian cell culture include DMEM (with GlutaMAX), RPMI Medium 1640 (with 25mM HEPES buffer and L-glutomine), minimun essential medium (MEM) (with Earle's salts and L-glutamine) and Opti-MEMI reduced serum medium. All of these media were purchase from Invitrogen.

2.1.4 Solutions and buffers

The solutions and buffers used in this thesis were made in Table 2.1.

Name	components
PBS	137 mM NaCl, 2.7 mM KCl, 4.3 mM Na_2HPO_4, 1.47 mM KH_2PO_4
lysis buffer	50 mM Tris-Cl pH=7.4, 150 mM NaCl, 1% TritonX-100
transfer buffer	25 mmol/L Tris, 192 mmol/L glycine, pH=8.3
TBS	20 mM Tris-Cl, 500 mM NaCl, pH=7.5
TTBS	TBS, 0.05% Tween-20, pH=7.5
blocking solution	5% nonfat milk powder in 1× TBS
antibody buffer	0.5% nonfat milk powder in 1× TTBS
PBST	0.1% Triton-X 100, 3% BSA, PBS
PI staining buffer	50 μg/ml propidium iodide, 10 μg/ml RNase A, 10 mM NaCl, 0.1% NP-40, 10 mM Tris-HCl, pH=8.0
NP-40 buffer	50 mM Tris-Cl, pH=7.4, 150 mM NaCl, 4 mM EDTA, 0.1 % NP-40, 50 mM NaF, 0.1 mM NaV, 10 μg/ml pepstatin A, 10 μg/ml leupeptin,
SDS-PAGE loading buffer(2×)	100 mM Tris-Cl, 4% SDS, 0.2% bromophenol blue, 20% glycerol, 200 mM DTT, pH=6.8
SDS-PAGE running buffer(5×)	25 mM Tris, 250 mM glycine, 0.1% SDS, pH=8.3
Sorbitol-HEPES incubation buffer	1 M sorbitol, 10 mM HEPES pH=7.4, 1 mM EDTA, pH=8.0

Table 2.1 Solutions and buffers used in this thesis.

The SDS-polyacrylamide gel elecrophoresis (SDS-PAGE) are listed in Table 2.2:

Solution components for resolving gel	Volume (ml)	Solution components for stacking gel	Volume (ml)
ddH_2O	3.3	ddH2O	2.7
30% acrylamide mix	4.0	30% acrylamide mix	0.67
1.5M Tris (pH 8.8)	2.5	1.0 M Tris (pH 6.8)	0.5
10% SDS	0.1	10% SDS	0.04
10% ammonium persulfate	0.1	10% ammonium persulfate	0.04
TEMED	0.004	TEMED	0.004

Table 2.2 Solution component for 10 ml of 12% Tris-glycine SDS-polyacrylamid gel elecrophoresis (SDS-PAGE). Volumes for each component are given as ml.

2. 2 Methods

2.2.1 RT-PCR and semi-quantitative RT-PCR

Cells were harvested by trypsinization and total RNAs were isolated by using the RNeasy® Mini Kit (QIAGEN, Cat 74104). The concentrations of total RNAs were measured by DU® 530 UV/Vis Spectrophotometer (BECKMAN COULTER$_{TM}$) at 260nm. 5 µg of total RNAs were taken and incubated for 10 min at 65^{o}C with 1 µl of 10 µM of the corresponding reverse primer. 0.5 µl of RNase inhibitor (40U/µl) was added into the mixture to prevent the degradation of RNAs. The sterile double distilled H_2O

(ddH_2O) was added to make the total amount of mixture to 10 µl. After reaction, the mixture was chilled on ice immediately. 1 µl of dNTPs mixture (10mM each, Invitrogen) and 1 µl of Reverse Transcriptase (New England BioLabs) were added into the above RNA mixture and incubated at 42°C for 2 hours to synthesize cDNAs. The cDNAs product was put on ice again and was amplified by PCR. The PCR reaction mixtures were set up as Table 2.3. The temperature for the initial DNA denature is 95°C for 5 min. The primer melting temperature (Tm) was estimated using the following equation: $T_m = 4$ (G + C) + 2 (A + T), where G, C, A, T represent number of nucleotides in the primer. Anneal the primers with the DNA template for 30 sec to 1 min at the temperature 5°C lower than T_m. After primer annealing, the product was extended at 72°C with 1 min per 1kb of the DNA fragment. After repeating the PCR for 20-30 cycles, the final extension was performed at 72°C for another 10 min to fill in the ends of reaction products. In order to visualize the PCR products, usually 2µl of PCR products were resolved on 1% agarose with 1 µg/ml of ethidium bromide and ran at 100V for 30 min. Documentation of the ethidium bromide stained gels were performed with UV illumination on Chemi Genius2 (SynGene).

Component for PCR	Volume per 50µl of reaction
Template DNA	1-5 ng (for purified plasmids) 5-10 µl (for cDNA products)
Forward primer (10 µM)	0.5 µl
Reverse primer (10 µM)	0.5 µl
dNTP Mix (10 mM/each)	0.5 µl
Taq DNA polymerase	0.1 µl
ThermoPol buffer (10×)	5 µl
DMSO	0-0.5 µl
ddH_2O (nuclease-free)	Variable

Table 2.3 The components of the PCR reaction mixture.

2.2.2 Plasmids construction

After PCR with the corresponding primers, the PCR products were purified with the QIAquick PCR purification Kit (QIAGEN, Cat 28106). Then, PCR products and the potential vector plasmids were digested with the corresponding restriction enzymes at 37^{o}C for 2 hours. The digested PCR products and plasmids were purified with the PCR purification kit again. And the purified digested insert was ligased with the vector by using T_4 DNA ligase at 4^{o}C overnight.

2.2.3 Making competent cells by CaCl2

To make competent cells, first a colony was picked into a 2ml of LB medium without antibiotics and grew *E. coli* at 37^{o}C overnight. Then, the 2 ml of *E. coli* medium was transferred into 50 ml of fresh LB medium and continue to grow at 37^{o}C with shaking until A_{600} to 0.4-0.6. The culture was transferred to sterile centrifuge bottles and the *E. coli* were spun down at 2600 xg (5500rpm) for 10 min at 4^{o}C. After decanting the supernatant, the *E. coli* were resuspended in 25 ml of ice cold sterile 100 mM of $MgCl_2$ and respun down at 2600 xg (5500rpm) for 10 min at 4^{o}C. After decanting the supernatant, the *E. coli* were resuspended in 5 ml of ice cold sterile 100 mM of $CaCl_2$. In order to make the *E. coli* cells to become transformation competent, the *E. coli* in CaCl2 were kept on ice for 2 hours. The competent *E. coli* cells were kept in 50% glycerol at -80^{o}C.

2.2.4 Plasmid transformation and purification

The DH5α competent cells were used for the transformation and purification of plasmids in this thesis. After thawing the DH5α competent cells on ice, 1μl of plasmids were added into 20 μl of competent cells and incubate on ice for 30 min. Then, the competent cells were heat-shocked for 45 sec at 42°C without shaking. After this shock, the cells were immediately put back on ice with the addition of 100 μl of SOC medium to the tube. The competent cells were incubated for 1 hour at 37°C to make the expression of the antibiotic-resistant gene in the plasmids. After spreading the cells evenly on the LB

agar plate with the correct antibiotic, the plate was kept at 37°C to make the cells continue growing.

In order to amplify the plasmids, one colony was picked and put into 2 ml of LB media with the correct antibiotic and incubated overnight at 37°C with shaking at 220 rpm/min. The cells were pulled down through the centrifuge at 2600 xg (5500 rpm) for 5 min. After discarding the LB media, the plasmids inside the cells were isolated with the QIAprep® Spin Miniprep kit (QIAGEN, Cat 27106).

The concentration of the purified plasmids was measured at 260 nm with the BECKMAN COULTER DU®530 Life Science UV/Vis Spectrophotometer. The concentration of the plasmid was calculated with the spectrographic conversion $1A_{260}$ unit of double-stranded DNA = 50 μg/ml plasmid solution.

2.2.5 Mammalian cell culture

1. Cell lines

Six different cancer cell lines were involved in this project, including HeLa cell line (human cervical adenocarcinoma cell line), MDA-MB-231 (human mammary adenocarcinoma cell line), MCF-7 (human mammary adenocarcinoma cell line), A549 (human lung adenocarcinoma cell line), Jurkat (human T cell lymphoblast-like cell line), PC12 (rat pheochromocytoma cell line) and B104 (rat neuroblastoma cell line). All of these cell lines were from American Type Culture Collection.

2. Cell culture

Hela, MDA-MB-231, MCF-7, A549, PC-12 and B104 cells were cultured in DMEM (GlutaMAX-1 supplemented) with 10% fetal bovine serum, 100 units/ml of

penicillin and 100 μg/ml of streptomycin. Jurkat cells were cultured in RPMI Medium 1640 supplemented with 10% fetal bovine serum, 100 units/ml of penicillin and 100 μg/ml of streptomycin.

2.2.6 Protein concentration measurement

After harvesting cells with cell lysis buffer, centrifuge the cell lysates at 4^{o}C to remove cell debris. The total protein concetrations were measured with the Bio-Rad Protein Assay (Bio-Rad, Cat 500-0006), the absorbance was measured at 595 nm, and the protein concentrations were calculated according to the Beer-Lambert's law: $A = \varepsilon bc$ (A is the absorbance, ε is the molar extinction coefficient (L/mol•cm). The standard protein used for determining protein concentration was bovine serum albumin.

2.2.7 siRNA transfection

The siRNAs were transfected into the mammalian cells by using the transfection reagent Oligofectamine (Invirogen). The day before transfection, the mammalian cells were seeded into a six-well plate (2×10^5 cells/well) or 96-well plate (5×10^3 cells/well) and grow for about 24 hours until 50-70% confluence in complete cell culture media at 37^{o}C under a humid environment with 5% CO_2. Before transfection, the siRNAs and the Oligofectamine were respectively diluted in the Opti-MEM I reduced serum medium as shown in Table 2.4 and 2.5.

	6-well plate	96-well plate
siRNAs (pmoles)	60(3µl of 20µM)	6(0.3µl of 20µM)
Opti-MEMI (µl)	200	20

Table 2.4 Dilute siRNA duplexes with Opti-MEMI.

	6-well plate	96-well plate
Oligofectamine (µl)	2	0.2
Opti-MEMI (µl)	60	6

Table 2.5 Dilute Oligofectamine transfection reagent with Opti-MEMI.

After incubating the diluted mixtures for 5-10 min at room temperature, the mixtures were mixed together gently and incubated for another 20-25 min at room temperature to allow the siRNA:Oligofectamine complex to form. Then another 235 µl (for six-well plate) or 23.5 µl (for 96-well plate) of Opti-MEM I were added into the above siRNA:Oligofectamine complex mixture respectively, to make up to 500 µl (for six-well plate) or 50 µl (for 96-well plate) of mixture. After removing the cell culture media from the plated, the whole siRNA:Oligofectamine complex mixtures were added into the cell. After incubating the cells in the siRNA:Oligofectamine complex mixture for 2 hours at 37^{o}C in a humid environment with 5% CO_2, 1.5 ml (for six-well plate) or 150 µl (for 96-well plate) of fresh DMEM with 10% FBS were added into the well. The cells

were continued to be cultured at the same conditions until they are ready for further analysis.

2.2.8 Plasmid transfection

The plasmids were transfected into the mammalian cells by using the transfection reagent Lipofectamine 2000 (Invirogen). The day before transfection, cells were seeded into a six-well plate (2×10^5 cells/well) or 96-well plate (5×10^3 cells/well) and let cells grow for about 24 hours until about 90-95% confluence in the component-complete cell culture media at 37°C under a humid environment with 5% CO_2 supplement. The plasmids (2 μg/well for a six-well plate; 0.2 μg/well for a 96-well plate) and Lipofectamine 2000 transfection reagent (2 μl/well for a six-well plate; 0.2 μl/well for a 96-well plate) were diluted in Opti-MEM I reduced serum media, respectively. After incubating the diluted mixtures for 5-10 min at room temperature, the two diluted mixtures were mixed together gently and incubated for another 20-25 min at room temperature to allow the plasmids:Lipofectamine 2000 complex to form. After changing the cell culture media with the fresh DMEM with 20% FBS without antibiotics into the wells (1.5ml/well for a six-well plate; 150 μl/well for a 96-well plate), the whole plasmids:Lipofecatamine complex mixtures were added into the wells and incubate at 37°C in a humid environment with 5% CO_2 until further analysis.

2.2.9 Cell proliferation assay and IC50 assay

Cells were seeded in a 96-well plate as 5×10^3 cells/well. 24 hours later, cells were treated with plasmids for 24 hours or siRNAs (30nM) for 48 hours or on time-dependent according to the experimental designs. Cell proliferation was determined using the Promega CellTiter 96® AQueous One solution reagent kit (Madison, WI, USA). First, the kit was taken from -20°C freezer and the MTS solution and the PMS solution were thawed at room temperature. The mixtures of DMEM cell culture media:MTS:PMS were made with the ratio of 100 µl: 20 µl: 1 µl per well. After removing the whole media from the wells, 120 µl of the above mixtures was added into each well. The cells were incubated for 1-4 hours at 37°C in a humidified, 5% CO_2 atmosphere. The absorbance of the colored product was read at 490 nm using the Benchmark plus microplate reader (Bio-Rad, Hercules, CA, USA). Growth inhibition was determined by the ratio of the absorbance in wells containing siRNA-treated cells compared to non-siRNA-treated cells (Opti-MEMI). Statistical analysis was performed using Student's *t* test and *P* values less than 0.05 were considered to be statistically significant.

For IC_{50}s assay, 48 hours after the transfection, cells were treated with various concentrations of anti-cancer drugs, Paclitaxel, Camptothecin, Cisplatin and Betulinic Acid from low to high concentrations, respectively, for another 24 hours. Subsequently, cell proliferations were checked using the Promega CellTiter 96® AQueous One solution reagent kit and IC_{50}s were calculated by using KaleidaGraph software.

2.2.10 Caspase-3 activity assay

1. Background

Activation of caspases occurs as a result of cell death process induced by various stimulations. Active caspases participate in a cascaded cleavage event that disables key homeostatic and repair enzymes and bring about systematic disassembly of dying cells.

2. Experimental procedure

Cells were seeded in a six-well plate and treated with siRNAs for 48 hours as described in siRNA transfection part. Cell lysates were made with 100 µl of ice-cold lysis buffer with protease inhibitors. Protein concentrations were measured with Bio-Rad Protein Assay Dye Reagent as described in Protein concentration measurement. Caspase-3 activity was determined by using the Promega CaspACE^{TM} assay kit. First, the caspase-assay mixture was made as following: 32 µl of Caspase Assay Buffer, 2 µl of DMSO and 10 µl of DTT (100 mM). Second, 100 µg of the total protein from each sample were taken and added with ddH_2O to make the volume of sample up to 54 µl. Then, the caspase-assay mixture was combined with the samples together to make up to 98 µl of caspase-sample-assay mixture. Finally, 2 µl of the DEVD-pNA substrate was added to the 98 µl of caspase-sample-assay mixture to make the total reaction volume up to 100 µl. After incubating the 100 µl of caspase-3-activity-assay mixture at 37^{o}C for 24 hours, the developed color was measured at 405nm by the Bio-Rad microplate reader, which reflected the tensity of the specific caspase activity. For inhibited apoptosis samples, Z-VAD-FMK was added into the wells at a final concentration of 20 µM together with siRNAs.

2.2.11 Western blotting.

Cells were washed with 1× ice-cold PBS for three times and then lysed with ice-cold lysis buffer containing protease inhibitors (complete-mini protease tablets; Roche Applied Science) before being freeze-thawed several times to prepare the cell lysate. The lysate was collected and centrifuged at 4^{o}C and at 14,100 ×g for 10min. The supernatant was collected and the total protein concentration was determined using protein assay dye (Bio-Rad Labs). 100μg of total proteins were separated by 12% sodium dodecyl sulfate (SDS)-polyacrylamide gel with the constant current of 30 mA per gel, until the bromophenol blue running to the bottom. A pre-stained protein standard was used as a marker to run together with the samples. After electrophoresis, the SDS-PAGE gel was equilibrated in 1× transfer buffer for 15-30 min. A piece of PVDF membrane (0.2 μm, Bio-Rad, Cat# 162-0177) was prewet in methanol for 30 min at room temperature. Thnk, the membrane was taken out of methanol and soaked into 1× transfer buffer for another 15-30 min together with the filter papers. The "sandwich" for Bio-Rad's semi-dry transfer cell was assembled following the order of filter paper (two pieces), PVDF membrane, SDS-PAGE gel, filter papers (two pieces) from the bottom to the top cover. It is important to make sure that there are no bubbles between gel, membrane and paper. The transfer was performed under the constant voltage of 15V. The current was set according to the area of the membrane as 5.5 mA/cm^2 to prevent excessive heating produced during the transfer. The transfer time was set according to the size of the interested protein as 15 min for protein less than 100 kD, and 60 min for protein more than 100 kD. After finishing transfer, the membrane was blocked in blocking solution for 60 min at room temperature. The interested protein was probed with the specific primary

antibody diluted in antibody buffer (the dilution ratio 1:1, 000) at 4^{o}C overnight. After washing the membrane with washing buffer for 3 times, 15 min per time, the Alkaline Phosphatase(AP)-conjugated secondary antibody (1:3, 000, Bio-Rad) was added and incubate with the membrane for 2 hours at room temperature. After washing the membrane again with washing buffer for 3 times, 15 min per time, the substrate was added evenly onto the membrane and the reaction was allowed going on for 1 min. The membrane was then exposed to the X-ray film for 1-30 min. The film was developed properly to detect the chemiluminescent signals.

2.2.12 Immunoprecipitation

Cells were seeded in a six-well plate as 2×10^5 cells/well. After cotransfecting the cells with Flag-conjugated FKBP38 and YFP-conjugated Bcl-2 plasmids as 2 μg/well for 24 hours, cell lysates were obtained with NP-40 buffer. The total proteins' concentrations were measured with Bio-Rad Protein Assay kit. 600 μg of total proteins were incubated with 1 μg of primary anti-Flag antibody (Sigma) at 4^{o}C overnight. 20 μl of protein G sepharose beads were added to the protein-antibody mixture and incubated for 2 hours at room temperature. After washed with the NP-40 buffer for five times, the sample was boiled in SDS PAGE loading buffer and the precipitants were checked by Western blotting with the specific antibodies.

2.2.13 Subcellular fractionation

1×10^7 HeLa cells were harvested by trypsinization and were washed with ice-cold 1 × PBS for three times. The pellets were resuspened in 5 ml of sorbitol-HEPES incubation buffer with complicated protease inhibitors. Cells were then incubated on ice for 30 min and homogenize cells by passing through 21 1/2G needle for 30 times. The crude lysate was centrifuged at 1,000 *xg* for 20 min at 4°C to remove nuclei and unbroken cells. The supernatant was collect in a new tube and subject it to a 10,000 *xg* centrifugation for 30 min at 4°C. The pellets mainly consisting of mitochondria were resuspended in 30 µl of sorbitol-HEPES incubation buffer and stored at -20°C for further analysis. The supernatant was collected and ultra-centrifuged at 100,000 *xg* for 4 hours at 2°C. The pellets mainly consisting of endoplasmic reticulum (ER) pellets were resuspended in 30 µl of sorbitol-HEPES incubation buffer and stored at -20°C for further analysis. The supernatant was collected as the cytosolic fraction.

2.2.14 Annexin-V/PI Staining

1. Background

In the normal health cells, phosphatidylserine (PS) is located entirely on the inner monolayer surface of the plasma membrane and other cellular membranes, which involved in the signal transduction and the blood coagulation process. In the early stages of apoptotic cells, PS translocates from the inner part of the plasma membrane to the outer layer. Annexin V is a Ca^{2+}-dependent phospholipids-binding protein with high affinity for PS (Vermes I et al., 1995). In the late stages of apoptotic or necrotic cells, DNA also leaks out of nuclei, which can be bound with PS specifically. Thus, the

combination of Annexin-V-fluorescein and PI stainings can be used to differentiate early apoptotic cells from later apoptotic cells or necrotic cells.

2. Procedure

Cells were seeded in a six-well plate and treated according to the experimental designs. Then, cells were harvested by trypsinization and centrifugation at 0.5 ×g for 3 min. Cells were stained with annexin-V-fluorescein and proidium iodide according to the instructions of the Annexin-V-FLOUS staining kit (Cat# 1 988 549, Roche). First, the annexin-V-fluorescein labeling solution was made as diluting the annexin-V-fluorescein labeling reagent and propidium iodide solution with the incubation buffer (provided in the kit) by the ratio of 2 μl: 2 μl: 100 μl. Then, cell pellet (about 10^6 cells) was resuspended in 100 μl of annexin-V-fluorescein labeling solution and incubated for 15 min at room temperature to stain cells with annexin-v-fluorescein and proidium iodide. Add 0.5ml of incubate buffer to the stained cells. The samples were read in a Becton Dickinson FACS using FL1 channel for fluorescein detection, and FL2 channel for propidium iodide detection. Analyses were performed by the Cell Quest Software.

2.2.15 Cell cycle analysis with PI staining.

1. Background

Propidium iodide (PI) is the most commonly used dye to quantitatively assess DNA contents. It can be used to stain whole cells or isolated nuclei. PI intercalates into the major groove of double-stranded DNA and produced a highly fluorescent adduct that can be excited at 488 nm with an emission centred around 600 nm. Since PI also can bind

to double-stranded RNA, it is necessary to treat the cells with RNase for optimal DNA resolution.

2. Procedure

Cells were seeded in a six-well plate and treated according to the experimental designs. Cells were harvested by trypsinization and centrifugation at 0.5 ×g for 3 min. Cell pellets were resuspended in 0.3 ml of PBS, pipetted, and fixed in 5 ml of 70% pre-cold ethanol overnight at -20^{o}C. After centrifugation, cell pellets were resuspended in 1 ml of propidium iodide staining solution and incubated at 4^{o}C for 30min in dark to stain DNA. The cells were then analyzed with flow cytometry and the results were analyzed with ModFit LT cell cycle analysis software. The cell cycle distribution is shown as the percentage of cells containing G_0/G_1, S and G_2/M DNA judaged by propidium iodide staining. The percentage of pre-G_1 cells is the apoptotic population.

2.2.16 Measurement of intracellular ROS

1. Background

Oxidative burst was quantified by measuring the oxidation of 2',7'-dichlorofluorescein diacetate (DCFH-DA). DCFH-DA is a stable, nonfluorescent, nonpolar compound that can diffuse through cell membranes. Once inside the cell, This probe is hydrolyzed to the polar nonfluorescent 6-carboxy- dichlorodihydrofluorescein (H2-DCF), which is rapidly oxidized to highly fluorescent 2',7'-dichlorofluorescein (DCF) by H_20_2 and other peroxides, thus providing a semiquantitative assessment of the oxidative metabolism (Carter WO et al., 1994).

2. Procedure

Cells were seeded in a six-well plate are treated according to the experimental designs. Cells were incubated with 50μM of DCHF-DA for 2 hours at 37^{o}C in a humidified environment with 5% CO_2 for DCF produce. Then cells are harvested by trypsinization and centrifugation at 500 ×g for 3 min at room temperature. After washing with 1 × PBS for three times, cell pellets are resuspended in 1ml of 1× PBS in dark. The fluorescence intensities of DCF are measured by flow cytometry with the excitation at 488 nm and the emission at around 600 nm (FL 1 channel). Data were analyzed with Cell Quest Software (Becton Dickinson).

2.2.17 Measurement of MMP

1. Background

The mitochondrial membrane potential (MMP) was measured by the fluorescent cationic, lipophilic dye, 5, 5' ,6 ,6' - tetrachloro - 1, 1' ,3 ,3' - tetraethylbenzimidazolylcarbocyanine iodide/chloride (JC-1). The JC-1 is used to signal the loss of MMP. In healthy non-apoptotic cells, the negative charge established by the intact mitochondrial membrane potential make the JC-1 to enter the mitochondrial matrix to accumulate there. The aggregated JC-1 form produces red fluorescence. Whereas, in apoptotic cells, the mitochondrial membrane potential collapses, and the JC-1 cannot accumulate within the mitochondria but remain in the cytoplasm in a monomeric form, which produces green fluorescence. Thus, the measurement of the cell population with red fluorescence or green fluorescence reflects the status of the MMP (Reers M, 1995).

2. Procedure

Cells were seeded in a six-well plate and treated according to the experimental designs. Cells were harvested by trypsinization and centrifugation at 500 ×g for 3 min at room temperature. The cell pellets were resuspended in 500 µl of 1× JC-1 reagent solution (the number of cells is less than 1×10^6) provided in the Mitochondrial Membrane Potential detection kit (Stratagene, La Jolla, CA). The cells were incubated in standard growth conditions (37^oC, 5% CO_2, in a humidified incubator) for 15 min in order to stain the cells with JC-1 dye. After that, the cells were centrifuged at 500 ×g for 3 min at room temperature and discard the supernatant. After washing the cells twice with 1× assay buffer by centrifugation and discard the supernatant, the cell pellets were resuspended in 500 µl of 1× assay buffer and analyzed by flow cytometry immediately. The healthy cells containing red JC-1 aggregates are detected with the FL2 channel and the apoptotic cells containing green JC-1 monomers are detected with the FL1 channel. Data are analyzed with Cell Quest software (Becton Dickinson).

2.2.18 DAPI Staining

1. Background

4',6'-diamidino-2-phenylindole hydrochloride (DAPI) can form complexes with double-stranded DNA to produce a bright blue fluorescence, which can be visualized by fluorescent microscopy at excitation wavelength 350 nm. In the normal healthy cells, the nucei showed bright and homogenous. During apoptotic cells, DNA is cleaved into nucleosome-sized units by DNase (Mcilroy D et al., 1999), which contributed to the chromatin condensation and chromosome fragmentation. DAPI staining can be used to detect these nuclear morphological changes and provide the evidence for apoptosis.

2. Procedure

Cells were seeded in a six-well plate with a 22mm^2 pretreated cover slips inside as 2×10^5 cells/well and treated according to the experimental designs. Cells were first fixed with 3.7% paraformaldehyde for 15 min at 37^{o}C, and wash with 1× PBS for three times. Then cells were stained with 5 µg/ml DAPI in 1× PBS for 15 min at 37^{o}C and covered with a coverslip. The morphology of the nuclei was observed using a fluorescence microscope at excitation wavelength 350 nm viewed with a 100× oil immersion objective.

2.2.19 Immunofluorescence

1. Background

Immunofluorescence is a technique allowing the visualization of a specific protein or antigen in cells or tissue sections by binding a specific antibody chemically conjugated with a fluorescent dye such as fluorescein isothiocyanate (FITC). Two major types of immunofluorescence staining methods are: 1) direct immunofluorescence staining in which the primary antibody is labeled with fluorescent dye, and 2) indirect immunofluorescence staining in which a secondary antibody labeled with fluorochrome is used to recognize a primary antibody.

2. Procedure

Cells were seeded in a six-well plate with a pretreated 22mm^2 cover slip inside as 2×10^5 cells/well and treated according to the experimental designs. Cells were stained with 100 nM of MitoTracker in DMEM at 37^{o}C for 15 min. Cells were fixed with 3.7% paraformaldehyde in 1 × PBS at 37^{o}C for 15 min. After washing cells with 1 × PBS for three times, cells were permeabilized with 0.5 % Triton X-100 in 1× PBS at room

temperature for 5 min. Cells were incubated in 5% BSA in 1× PBS pH 7.5 at room temperature for 1 hour to block unspecific binding of the antibodies. Cells were incubated with primary antibody in 1% BSA in PBST pH 7.5 at 4^{o}C overnight. After washing cells with PBST pH 7.5 for three times with 15 min/time, cells were incubated with FITC-labeled secondary antibody in 1% BSA in PBST pH 7.5 at room temperature for 1 hour. Then, cells were washed with PBST pH 7.5 three times with 15 min/time and mounted with antifade reagent. The slide was observed under a confocal microscope.

2.2.20 Colocalization and FRET assay

1. Background

Fluorescence resonance energy transfer (FRET) measures the energy transfer between two fluorophores, a donor and an acceptor. Only when the emission spectrum of the donor overlaps with the excitation spectrum of the acceptor, and the distance between the fluorophores is less than 80 Å, can FRET take place (Wu P et al., 1994). When two proteins interact, they bring the fluorophores close together, thereby facilitating FRET. Thus, FRET microscopy can be used as a powerful approach to investigate interactions between two fluorescently tagged proteins without disruption their localizations inside cells. CFP/YFP is a popular pair of fluorophores to label proteins for FRET since the emission of spectrum of CFP overlaps with the excitation spectrum of YFP (Fig. 2.2)

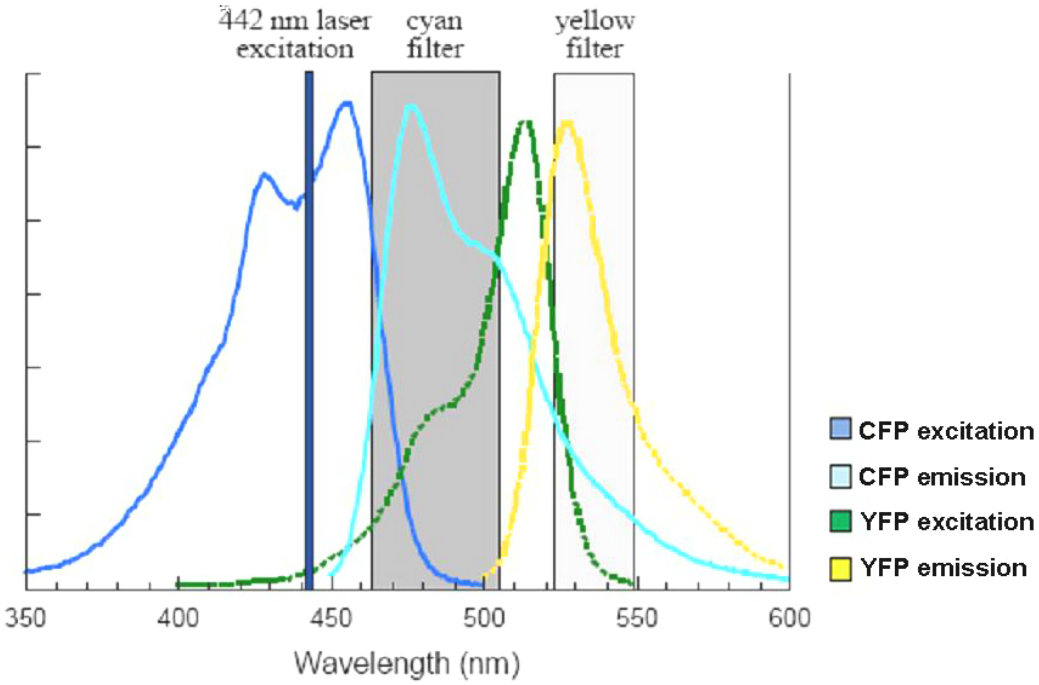

Fig. 2.2 Spectra of CFP and YFP. Excitation wave length of CFP (donor) is 436 ± 10 nm. Excitation wave length of YFP (acceptor) is 500 ± 20 nm. Emission wave length of CFP is 480 ± 20 nm. Emission wave length of YFP is 535 ± 30 nm. Thus, the excitation spectra of donor and acceptor are separated, and the emission spectrum of donor overlaps with excitation spectrum of acceptor.

2. Procedure

In order to study the interaction between two proteins through the FRET, the interested genes were first inserted into pECFPC1 and pEYFPC1 plasmids, respectively. Cells were seeded on a 22mm^2 cover slip within a six-well plate as 2 × 10^5 cells/well. Twenty-four hours after the seeding, cells were cotransfected with CFP- and YFP-conjugated proteins with lipofectamine 2000 as 2 μg plasmids/well for 24 hours. Then, stain the cells with 200 nM of Mito-Tracker® Deep Red 633 or ER-Tracker™ Blue-White DPX for 30min under the standard growth conditions. After washing with 1 × PBS for several times, cells were fixed with 3.7% paraformaldehyde in 1 × PBS at 37°C for

20min. Then cells were washed again with 1 × PBS and the cover slips were mounted with Prolong Antifade reagent and the slides were sealed with nail polish. Slides were kept at 4^{o}C in dark for further analysis.

For the colocaliztion assay, the slides were observed with a 60 × oil immersion lens using the Zeiss LSM 510 META confocal microscope. The excitation wavelengths used are 458nm for CFP, 514nm for YFP, 633nm for Mito-Tracker and 405nm for ER-Tracker. According to the experiment designed, the corresponding wavelengths were used simultaneously to capture images for the colocalization analysis.

For the FRET assay, the slides were selected a region with both the expression of YFP and CFP as the region of interest (ROI). The YFP channel was photobleached by scanning for 10 times. The YFP and CFP images were collected before and after bleach and the fluorescence intensities of YFP and CFP were obtained. The YFP Bleaching efficiency (B_E) was calculated with the formula, $B_E = (I_5 - I_6) \times 100 / I_5$, where I_n was the YFP intensity at the *n*th timepoint. A non-bleached region in same size was always selected as a control. At least 10 events with $B_E > 90\%$ and without bleach in control region were selected to calculate the CFP Increasing or FRET energy transfer efficiency (E_F) by using the formula, $E_F = (I_6 - I_5) \times 100 / I_6$, where I_n was the CFP intensity at the *n*th timepoint (Karpova TS et al., 2003).

Chapter 3 RNA Interference of Bcl-2 induces apoptosis in cancer cells

RNA interference (RNAi) is a highly conserved mechanism found in almost all eukaryotes to serve as a post-transcriptional gene silencing mechanism through the introduction of double-stranded RNA (dsRNA) (Hannon GJ, 2002). However, an interferon response, which is involved in antiviral defense, may also be triggered if the length of dsRNA is more than 30 bps. Small interfering RNA (siRNA) is a 21-nucleotide (nt) long RNA duplex with 19 base pairs and 2 overhanging at 3' ends. The application of siRNA makes the dsRNA-mediated mRNA degradation much potent and specific without triggering the interferon response (Elbashir SM et al., 2001), thus makes RNAi technique applicable in studying gene function in mammalian cells and in exploring gene-specific therapeutics.

The *bcl-2* gene is a proto-oncogene. The overexpression of Bcl-2 protein has been observed to be associated with oncogenesis and resistance to chemotherapies in various cancers. Bcl-2 exerts its influence mainly by enhancing cell survival through the inhibition of apoptosis, rather than through the stimulation of cell division (Tsujimoto Y et al., 1984). This anti-apoptotic feature of Bcl-2 confers the cancer cells stronger survival abilities in the existence of various cell stresses, such as the depletion of growth-factor, hypoxia, nutrient deprivation, DNA damage, and cytotoxin, thus, conferring cancer cells resistance to chemotherapy or radiotherapy (Reed JC, 1995).

In this study, we investigated the silencing effects on Bcl-2 by siRNA-mediated RNA interference in three different cancer cells, HeLa, MCF-7 and MDA-MB-231; all of these cancer cells demonstrated an overexpression of Bcl-2 (Fig. 4.3). Three different siRNAs targeting different sites of Bcl-2 mRNA were designed, named siRNA HYSR1, siRNA HYSR2 and siRNA HYSR3. In addition, a scramble siRNA HYSR4 was always used as a negative control. The down-regulation effects on Bcl-2 were checked by Western blotting on protein level and semi-quantitative RT-PCR on mRNA level. Cell proliferation was checked by MTT assay. Cell death was checked by DAPI staining and quantitatively analyzed by flow cytometry after staining with annexin-V-fluorescein/PI. The siRNA transfection effect and efficiency were assessed by a 5'-fluorescein labeled non-silencing siRNA.

3.1 Results

3.1.1 Small interfering RNAs (siRNAs)

In order to study the function of Bcl-2 in cancer cells by using siRNA-mediated RNA interference method, three siRNAs were designed targeting the different sites of Bcl-2 cDNA. They are the siRNA HYSR1, HYSR2 and HYSR3 (Fig. 3.1). HYSR1 is targeting the sequence of Bcl-2 cDNA from +599 to +619, HYSR2 is targeting the sequence of Bcl-2 cDNA from +49 to +69, HYSR3 is targeting the sequence of Bcl-2 cDNA from +514 to +534.

In addition to the different targeting sites, these three siRNAs was also varied in the GC contents. Among them, the GC content in the siRNA HYSR1 is the highest, about 62%, and the GC content in the siRNA HYSR2 is the lowest GC content, about 33%. The GC content in the siRNA HYSR3 is about 52%.

```
  1 ATGGCGCACG CTGGGAGAAC GGGGTACGAT AACCGGGAGA TAGTGATGAA

 51 GTACATCCAT TATAAGCTGT CGCAGAGGGG CTACGAGTGG GATGCGGGAG
        (HYSR2)
101 ATGTGGGCGC CGCGCCCCCG GGGGCCGCCC CCGCACCGGG CATCTTCTCC

151 TCCCAGCCCG GGCACACGCC CCATCCAGCC GCATCCCGGG ACCCGGTCGC

201 CAGGACCTCG CCGCTGCAGA CCCCGGCTGC CCCCGGCGCC GCCGCGGGGC

251 CTGCGCTCAG CCCGGTGCCA CCTGTGGTCC ACCTGACCCT CCGCCAGGCC

301 GGCGACGACT TCTCCCGCCG CTACCGCCGC GACTTCGCCG AGATGTCCAG

351 CCAGCTGCAC CTGACGCCCT TCACCGCGCG GGGACGCTTT GCCACGGTGG

401 TGGAGGAGCT CTTCAGGGAC GGGGTGAACT GGGGGAGGAT TGTGGCCTTC

451 TTTGAGTTCG GTGGGGTCAT GTGTGTGGAG AGCGTCAACC GGGAGATGTC

501 GCCCCTGGTG GACAACATCG CCCTGTGGAT GACTGAGTAC CTGAACCGGC
                        (HYSR3)
551 ACCTGCACAC CTGGATCCAG GATAACGGAG GCTGGGATGC CTTTGTGGAA

601 CTGTACGGCC CCAGCATGCG GCCTCTGTTT GATTTCTCCT GGCTGTCTCT
       (HYSR1)
651 GAAGACTCTG CTCAGTTTGG CCCTGGTGGG AGCTTGCATC ACCCTGGGTG

701 CCTATCTGGG CCACAAGTGA
```

Fig. 3.1 Bcl-2 cDNA sequence and the siRNA targeting sites. HYSR1 is targeting the sequence of Bcl-2 cDNA from +599 to +619, HYSR2 is targeting the sequence of Bcl-2 cDNA from +49 to +69, HYSR3 is targeting the sequence of Bcl-2 cDNA from +514 to +534.

The different targeting sites together with the different GC contents are supposed to influence the silencing effects on Bcl-2. We want to know which siRNA can get the best silencing effect on Bcl-2.

Besides the specific Bcl-2 siRNAs, there are still two scramble siRNAs, HYSR4 and FITC-siRNA. FITC-siRNA is a double-strand siRNAs labeling with the fluorescein at the 5' of the sense strand. After blasting within the human genome, there are no significant similarities found for both of these two scramble siRNAs.

The five siRNAs used in this study are listed in the Table 3.1.

siRNAs	sequences	locations	GC contents
HYSR1	**Sense strand:** 5'-CUGUACGGCCCCAGCAUGCdTdT-3' **Antisense strand:** 5'-GCAUGCUGGGGCCGUACAdTdT-3'	**599***	**62%**
HYSR2	**Sense strand:** 5'-GUACAUCCAUUAUAAGCUGdTdT-3' **Antisense strand:** 5'-CAGCUUAUAAUGGAUGUACdTdT-3'	**49***	**33%**
HYSR3	**Sense strand:** 5'-CAUCGCCCUGUGGAUGACUdTdT-3' **Antisense strand:** 5'-AGUCAUCCACAGGGCGAUGdTdT-3'	**514***	**52%**
HYSR4	**Sense strand:** 5'-GUCUCCAAGCGGAUCUCGUdTdT-3' **Antisense strand:** 5'-ACGAGAUCCGCUUGGAGACdTdT-3'	**Scramble**	**52%**
FITC-siRNA	**Sense strand:** 5'-fUUCUCCGAACGUGUCACGUdTdT-3' **Antisense strand:** 5'ACGUGACACGUUCGGAGAAdTdT-3'	**Scramble**	**48%**

Table 3.1 Five siRNAs designed for this study, including three siRNAs targeting the different sites of Bcl-2 cDNA, HYSR1 (targeting the sequence of Bcl-2 mRNA from +599 to +619 and with 62% of the GC cotent), HYSR2 (targeting the sequence of Bcl-2 mRNA from +49 to +69 and with 49% of the GC content), HYSR3 (targeting the sequence of Bcl-2 mRNA from +514 to +534 and with 52% of the GC content), two scrambles siRNAs, HYSR4 and 5'-Fluorescein-labelled siRNAs (FITC-siRNAs). *for

bcl-2, the HUMBCL2 sequence was taken from Gene Bank (Asscession Number NM000633) and was confirmed by RT-PCR.

All of these five siRNAs were chemically synthesized and purchased from DHARMACON, USA. They were annealed 21-nt double stranded siRNA with 19 base pairs and 2 nucleotides overhanging at 3' ends. The siRNAs were dissolved in the buffer (100 mM potassium acetate, 30 mM HEPES-KOH, 2 mM magnesium acetate, pH=7.4) to obtain a 20 μM solution and stored at -80^{o}C. Before the first time experiment, the siRNA solution was heated 90^{o}C for 1 min, and incubated at 37^{o}C for 60 min in order to disrupt higher aggregates and ensure siRNA silencing efficiency. FITC-siRNA was the control siRNA labeled with fluorescein at the 5' of the sense strand.

3.1.2 The siRNA transfection effects

In order to observe the distribution of siRNAs inside cells and also to assess the transfection efficiency, 5'-fluorescein-labelled scramble siRNA (FITC-siRNA) was designed and transfected into cells with oligofectamine as described in the Chapter 2. Fig. 3.2 showed the transfection effect in three different cancer cell lines, HeLa, MDA-MB-231 and MCF-7 24 hours after treated with 30 nM FITC-labeled siRNA. The upper were the cell images under the light microscope, and the lower were the corresponding views of the cells under the fluorescent microscope. The green fluorescent dots indicated that the FITC-labeled siRNAs have been transfected into the cells successfully.

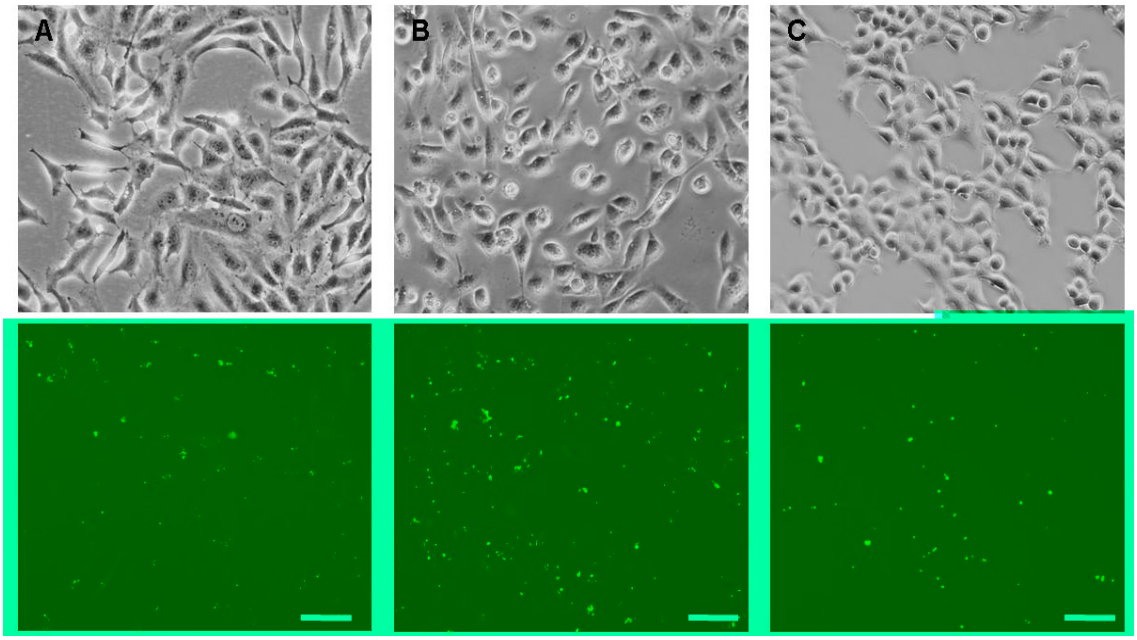

Fig. 3.2 The transfection effects of 5'-fluorescein-labelled siRNAs (FITC-siRNAs) in three cancer cells, HeLa (A), MDA-MB-231 (B), MCF-7 (C). 2×10^5 cells were seeded in a 6-well plate and were transfected with 30 nM of 5'-Fluorescein-labelled siRNA with oligofectamine reagent. Twenty-four hours after transfection, cells were washed with 1× PBS three times and the same cell images were taken under both light microscope and fluorescent microscope. The green fluorescent dots indicated the FITC-siRNAs. Bars are 100 μm.

Transfection is the delivery of the hydrophilic DNA, RNA, proteins and macromolecules into eukaryotic cells through the bilayer cell membrane for the purposes of gene function study, gene regulation and protein expression. The successful transfection depends on cytotoxicity of transfection reagent, transfection efficiency, and transfection reproducibility. Here, by using liposome-mediated transfection with oligofectamine reagent, FITC-siRNAs were observed successfully transfected into the three cell lines employed in this study. There were no abnormal morphological changes in the cells with FITC-siRNAs transfected. And the cell

growth was not disturbed. The bigger green dot inside the cells may be the aggregated siRNAs. It may be caused from the nonfunctional ability of FITC-siRNAs.

3.1.3 The distribution of siRNAs inside the cells

In order to better understand the mechanisms of siRNA-mediated RNAi, the distribution of the exogenous siRNAs inside cells was checked by using confocal microscopy. Fig. 3.3 showed that all of the siRNAs that have been transfected into the cells distributed in the cytoplasm. There was no overlapping between the FITC-siRNAs with the nuclei. This result suggested that the transfected siRNAs only distribute in the cytoplasm, not in the nucleus. Thus, it is provided the evidence that siRNA-mediated RNAi belongs to the post-transcriptional gene silencing (PTGS). And the silencing on Bcl-2 with siRNAs will not affect the transcription of its chromosomal gene, but the mRNA level.

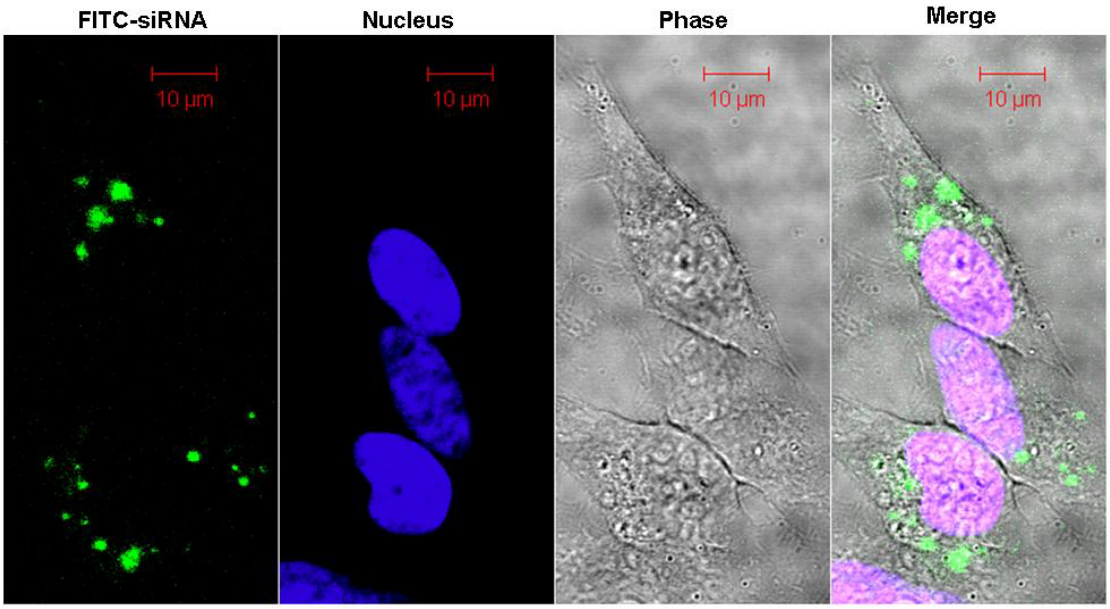

Fig. 3.3 The distribution of siRNAs inside cells. HeLa cells were seeded on a cover slip inside a six-well plate and transfected with 30 nM 5'-fluorescein-labelled siRNAs (FITC-siRNAs) with oligofectamine. Twenty-four hours later, cells were stained with DAPI (100 ng/ml) and observed under the confocal microscope with the excitation wavelengths 488 nm for FITC and 405 nm for DAPI. The phase-contrast cell image was also captured simultaneously.

3.1.4 siRNA transfection efficiency

Transfection efficiency is another important element to ensure the siRNA-induced gene silencing effect, especially in the transient transfection. In order to make sure the accuracy of the results, there must be high transfection efficiency. Thus, the corresponding transfection efficiencies were quantitatively analyzed by flow cytometry after treated with FITC-siRNAs. The results showed that among these three cancer cell lines, HeLa, MDA-MB-231 and MCF-7, the transcient transfection efficiencies varied around 70% (Fig. 3.4). And in HeLa cells, the transfection efficiency got to about 80% (Fig. 3.4A). These high transfection efficiencies mean that the majority of the cells have been successfully transfected with the siRNAs. And these high transfection efficiencies made this siRNA technique applicable in studying the specific gene's functions.

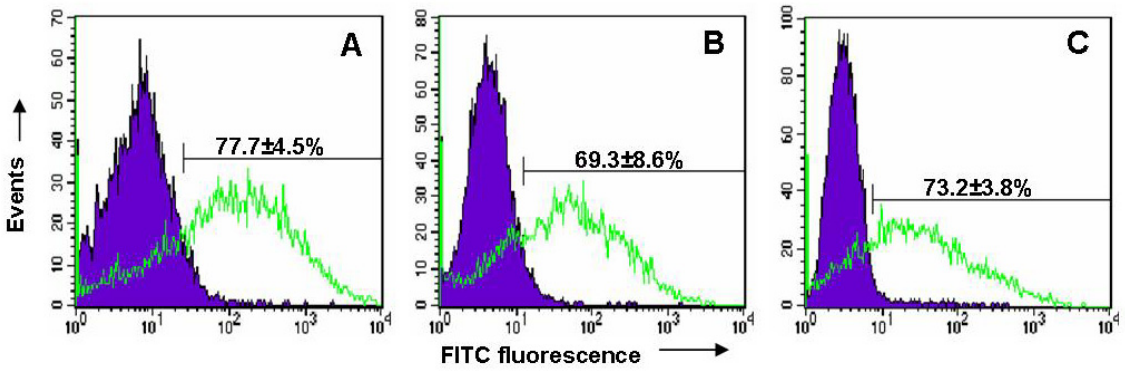

Fig. 3.4 The assessment of siRNA transfection efficiencies in three cancer cells, HeLa (A), MDA-MB-231 (B), MCF-7 (C). 2×10^5 cells were seeded in a six-well plate and were transfected with 30 nM of 5'-fluorescein-labelled siRNA (FITC-siRNA) using Oligofectamine reagent. Twenty-four hours after transfection, cells were washed with 1× PBS three times and collected by trypsinization. After centrifuged at 0.5 *xg* for three min at room temperature, cell pellets were resuspended in 1 × PBS. The transfection efficiencies were analyzed immediately by flow cytometry using FL-1 channel. Experiments were repeated three times and the data were analyzed with the Cell Quest Software (Becton Dickinson).

3.1.5 Comparison of the silencing effects on Bcl-2 by three siRNAs targeting different sites of Bcl-2 mRNA.

In order to check the abilities to specifically down-regulate the expression of the anti-apoptotic protein Bcl-2 by siRNA-mediated RNA interference, the three specific siRNAs, HYSR1, HYSR2 and HYSR3 were transfected into three different cancer cells, HeLa, MDA-MB-231 and MCF-7. A scramble siRNA, HYSR4, which shows no significant homology to the target sequences, was used as a negative control (Table 3.1). Western blotting results showed HYSR2 having the best silencing effect

on the expression of Bcl-2 in all of the three cancer cells used. After treated with 30 nM of siRNA HYSR2, Bcl-2 expression decreased to about 25% in Hela cells, about 23% in MDA-MB-231 cells, and about 21% in MCF-7 cells. However, there were no significant non-specific silencing effects on Bcl-2 by the scramble siRNA (Fig. 3.5).

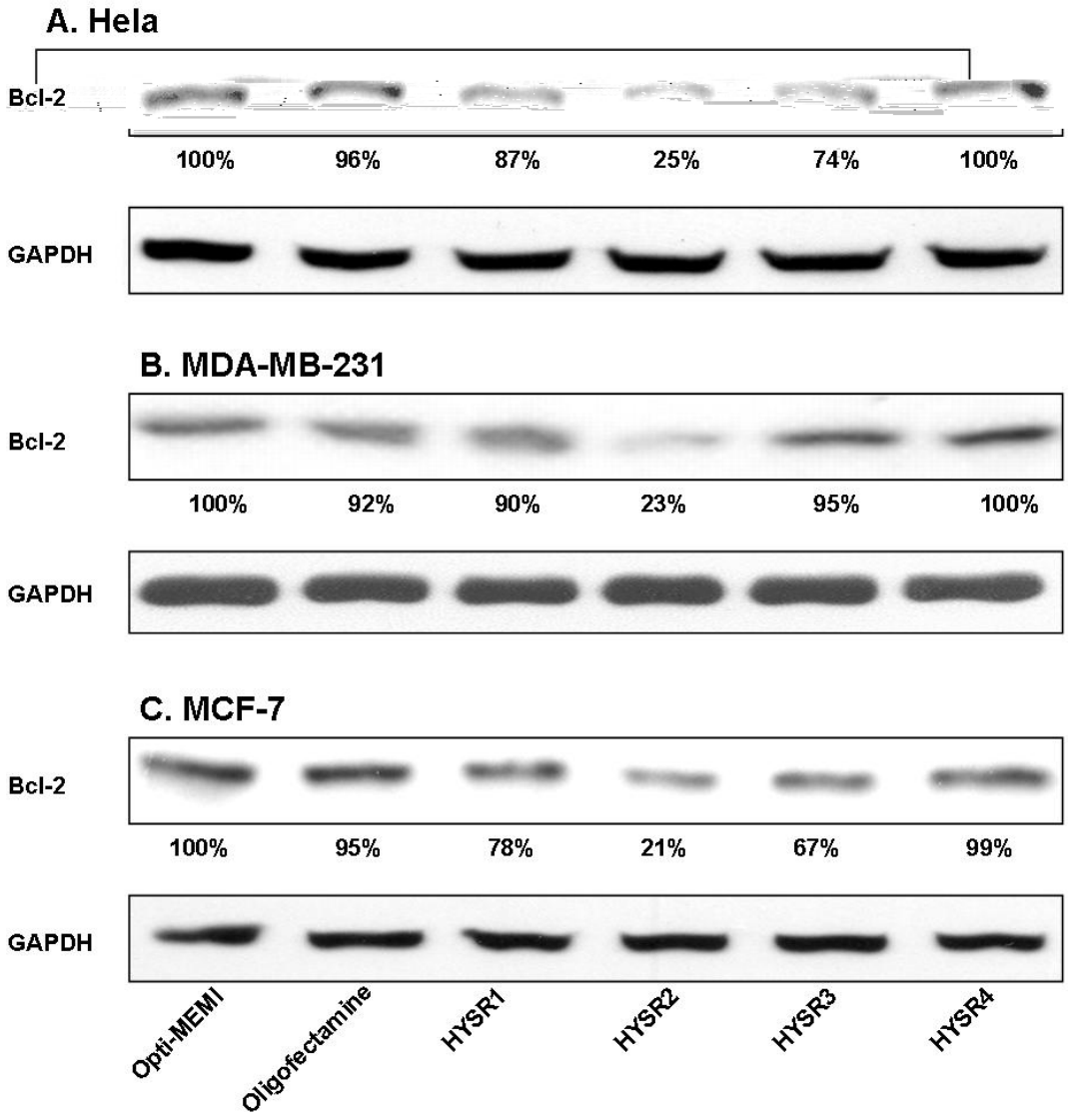

Fig. 3.5 Comparison the silencing effects on Bcl-2 by three siRNAs targeting different sites of Bcl-2 mRNA in three cancer cell lines, HeLa (A), MDA-MB-231 (B), MCF-7 (C). Cells were seeded in a six-well plate (2×10^5 cells/well) and treated with 30 nM siRNA HYSR1, HYSR2, HYSR3 and HYSR4, respectively. Forty-eight hours after the transient transfection, cell lysates were collected and 100 μg of

the total protein from different treatments were separated by 12% SDS-PAGE. The expressions of Bcl-2 protein were checked by western blotting. GAPDH was probed as an internal control. Cells not treated with any siRNA, i.e. Opti-MEM I, were experimental controls. The semi-quantitative assessments of the bands were performed by means of a GS800 densitomer (Bio-Rad). Values were expressed as percentages of the experimental controls (Opti-MEM I), and here showed a representative of three independent experiments.

3.1.6 The detection of Bcl-2 mRNA after siRNAs treatment

In order to check the influence on Bcl-2 mRNA by siRNA HYSR2, the semi-quantitative RT-PCR was performed at 48 hours after the HeLa cells were treated with siRNA. Fig. 3.5 shows that HYSR2 caused significant degradation of Bcl-2 mRNA, whereas, there was no affect on Bcl-2 mRNA by the scramble siRNA (Fig. 3.6).

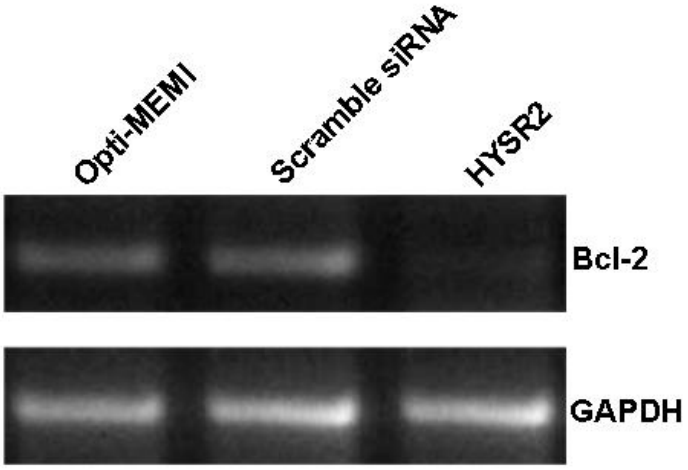

Fig. 3.6 Semi-quantitative RT-PCR analysis on Bcl-2 mRNA after siRNA treatment. HeLa cells were seeded in a six-well plate and treated with 30 nM scramble siRNA and HYSR2 respectively for 48 hours. Total RNAs from Hela cells were isolated with RNeasy Mini Kit (QIAGEN). The

concentrations of total RNAs were measured by DU® 530 UV/Vis spectrophotometer (BECKMAN COULTER$_{TM}$) at 260nm. Semi-quantitative RT-PCR was performed as described in "Materials and Methods". Documentation of the ethidium bromide stained gels were performed with UV illumination on Chemi Genius2.

3.1.7 The RNA interference of Bcl-2 was on concentration- and time-dependent

In order to further check the characteristics of siRNA HYSR2 on Bcl-2 gene silencing, we used HeLa cells as a model cell line and performed Bcl-2 silencing experiments by siRNA HYSR2 to test concentration-dependence and time-dependence. Cells were treated with a series of concentrations of siRNA HYSR2, from 0 to 50 nM, for 48 hours. Western blotting results showed that the down-regulation effects on Bcl-2 depended on the concentrations of siRNA. As a powerful silencing tool, siRNA could significantly silence the targeting gene at a low concentration; about 40% degradation of Bcl-2 occurred with only 10 nM of siRNA HYSR2. The silencing effects were about 80% at 30 nM, and more than 90% at 50 nM of siRNA HYSR2 (Fig. 3.7).

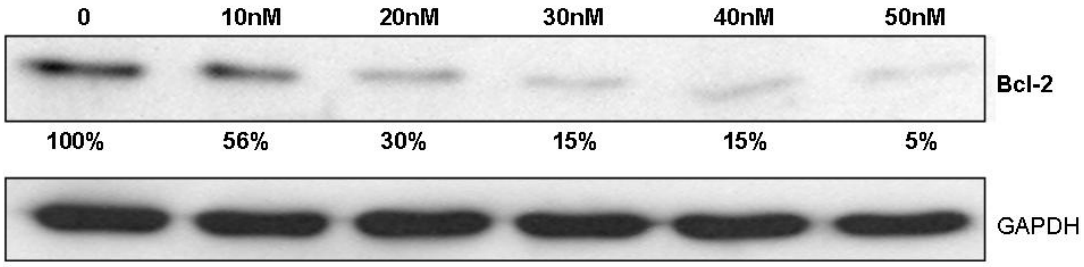

Fig. 3.7 Silencing Bcl-2 by siRNA HYSR2 on concentration-dependent. Cells were seeded on a six-well plate, and transiently treated with a series of concentrations of siRNA HYSR2, from 0 to 50 nM.

Forty-eight hours after the transient transfection, cell lysates were collected and 100 μg of the total protein from different wells were separated by 12% SDS-PAGE and the expressions of Bcl-2 protein were checked by Western blotting. GAPDH was probed as an internal control. The semi-quantitative assessments of the bands were performed by means of a GS800 densitomer (Bio-Rad). Values were expressed as percentages of the experimental controls (opti-MEMI), and the figure shows a representative of three independent experiments.

Although the higher the siRNA concentration was used, the more Bcl-2 decreased, it could not be excluded that there were non-specific cytotoxic effects emerging from too much siRNAs used. Thus, the low amount of siRNA with the significant silencing effect was usually selected for performing experiments. According to this principle, 30 nM siRNA HYSR2 was selected in all of our experiments.

Another feature of siRNA as a powerful silencing tool is its long-lasting silencing effect. In order to check the time course of siRNA HYSR2-induced Bcl-2 suppression, we performed kinetic study on silencing. The results showed that silencing effect on Bcl-2 by transient treatment with 30 nM siRNA HYSR2 could last almost for one week, with the most significant silencing effect appearing 48 hours after transfection (Fig. 3.8).

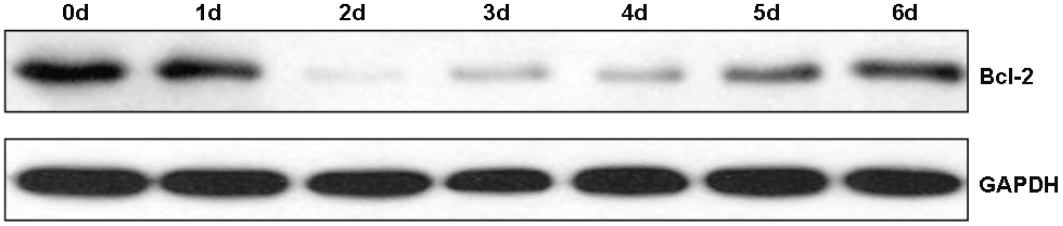

Fig. 3.8 Kinetic study on silencing Bcl-2 by siRNA HYSR2 in HeLa cells. Cells were seeded on a six-well plate, and transiently treated with 30 nM siRNA HYSR2. Cell lysates were collected every 24 hours after transfection until 7 days. 100 μg of the total protein from each well were separated by 12% SDS-PAGE and the expressions of Bcl-2 protein were checked by Western blotting. GAPDH was probed as an internal control. The figure shows a representative experiment that was repeated three times.

3.1.8 Silencing Bcl-2 inhibits cell growth

Bcl-2 is a proto-oncogene with a well-known anti-apoptotic function. Silencing this gene expression will induce cell death through apoptosis. To further investigate the effect of the HYSR2 siRNA on cell growth, we performed cell proliferation study with MTT assay after siRNA HYSR2 treatment. Cells were treated with scramble siRNA or siRNA HYSR2. The cell proliferation at different time points, 0h, 24h, 48h and 72h after siRNAs treatment was checked. Compared to the untreated cells, by 24 hours, the treatment with Bcl-2 siRNA caused about 20% decrease in the cell proliferation, about 35% decrease by 48 hours, and 50% decrease by 72 hours (Fig. 3.9).

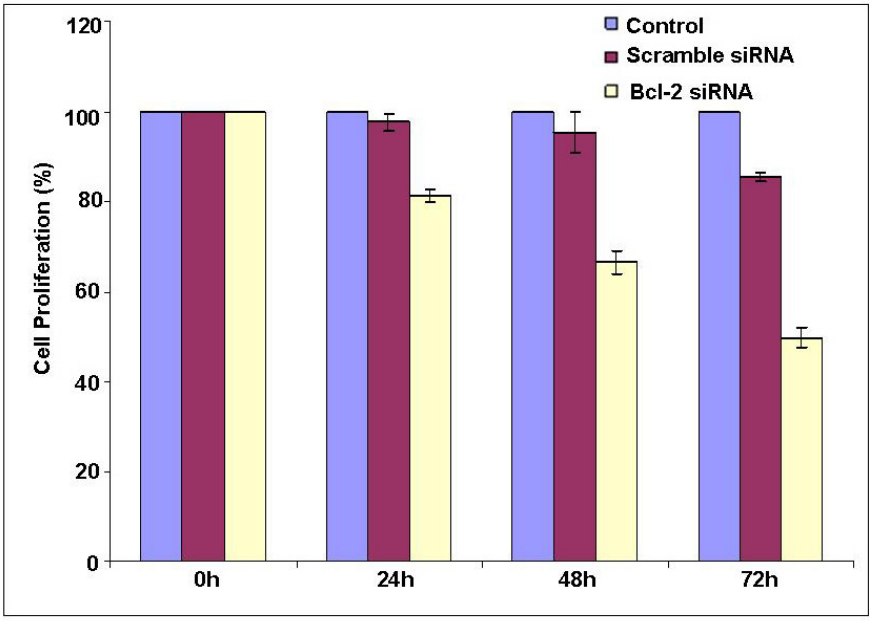

Fig. 3.9 Cell proliferation assay after Bcl-2 siRNA treatment. HeLa cells were seeded in a 96-well plate (5×10^3 cells/well) and treated with 30 nM scramble siRNA or Bcl-2 siRNA on time-dependent, respectively. The cell proliferation at different time points, 0h, 24h, 48h and 72h was analyzed by MTT assay. Absorbances were measured at 490 nm by using microplate reader (Bio Rad). Cells without siRNA treatment were as control (100%). The cell proliferation treated with scramble siRNA or Bcl-2 siRNA were expressed as percentage of control. Values represent the means ± S.D. of three independent experiments.

3.1.9 Silencing Bcl-2 induces caspase-3-dependent apoptosis

In order to identify the characteristics of cell death induced through the suppression of Bcl-2, DAPI staining and annexin-V-FLUOS/PI staining were performed (Fig 3.10) after cells were treated with siRNAs. The changes of the nuclear morphology after treated with Bcl-2 siRNA showed nuclear condensation and chromatin fragmentation (Fig. 3.10A). Cell death was also qualitatively and

quantitatively analyzed by flow cytometry after staining with annexin-V-FLUOS/PI. The results showed that there were about 17% of HeLa cells stained with annexin-V-flourescein after the HYSR2 treatment, while 6% of the cells stained after the scramble siRNA treatment, indicating the HYSR2 treatment increased apoptotic cell death of HeLa cells by about 3 folds. There were still about 3% untreated cells stained with annexin-V-flourescein, which may be caused from the natural cell death (Fig. 3.10B). Meanwhile, some cells were stained with PI, which were the later apoptotic or necrotic cells.

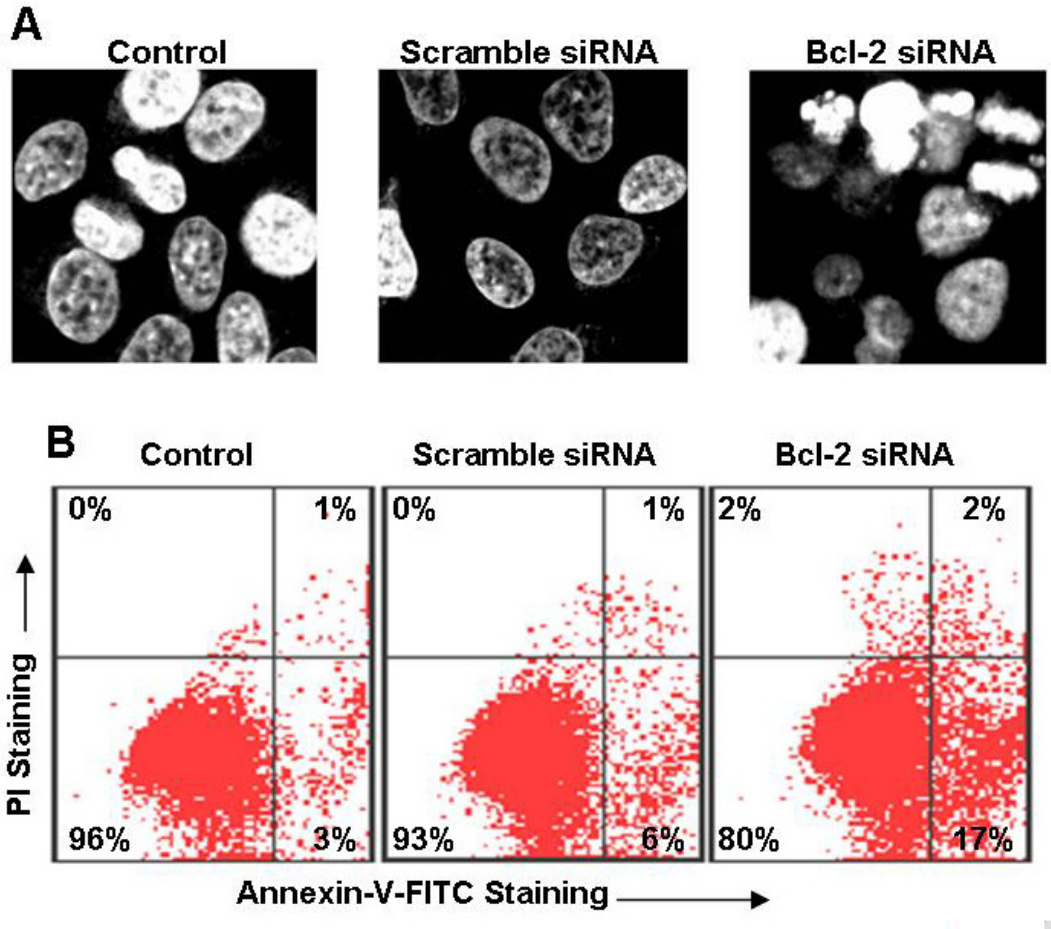

Fig. 3.10 Cell death analyses after Bcl-2 siRNA treatment in HeLa cells. Cells were seeded in a six-well plated and treated with 30 nM scramble siRNA or Bcl-2 siRNA HYSR2 for 48 hours, respectively. **A.** Nuclear morphological study. Cells were stained with DAPI (100 ng/μl) and the nuclear

morphological changes were observed under fluorescent microscope with UV stimulation. **B.** Quantitative analysis of apoptosis with flow cytometry. Cells were harvested by trypsinization and stained with annexin-V-flourescein/propidium iodide (PI) as described in Chapter 2. The apoptotic cell death was quantitatively checked by flow cytometer. Data were analyzed by the Cell Quest Software. Experiments were repeated three times.

Cells undergoing apoptosis display typical features, including cell shrinkage, membrane blebbing, chromatin condensation and nuclear fragmentation. Also during apoptosis, there are some changes in cell membrane. Phosphatidylserine (PS), normally located on the cytoplasmic surface of the cell membrane, becomes exposed to the extracellular environment, which is a characteristic phenomenon during the early stage of apoptosis. Annexin V can specifically binding with PS with the existence of Ca^{2+}. During the later stages of apoptosis, nuclear membrane breaks, chromosomal DNAs leak out and can be easily stained with PI. Here, the analysis of cell death suggests that the cell death induced by siRNA-mediated Bcl-2 suppression mainly through apoptosis.

Furthermore, caspase-3 or caspase-3-like enzymatic activities were determined by checking PARP cleavage and DEVDase activity. PARP is an enzyme that is involved in DNA repair and genomic maintenance. Activated executed caspases, including caspase 3, 6, 7 and 8 can all cleave PARP from its 116 kD form to an 89 kD residual. Here, our data showed that after the treatment with HYSR2 siRNA, PARP was observed as a cleaved fragment about 89 kD and which could be inhibited by the

pan-caspase inhibitor Z-VAD-FMK (Fig. 3.11A), suggesting that the capase activities were activated. The analysis of caspase-3-like enzymatic activities also detected a significant increase of the enzymatic activity (Fig. 3.11B).

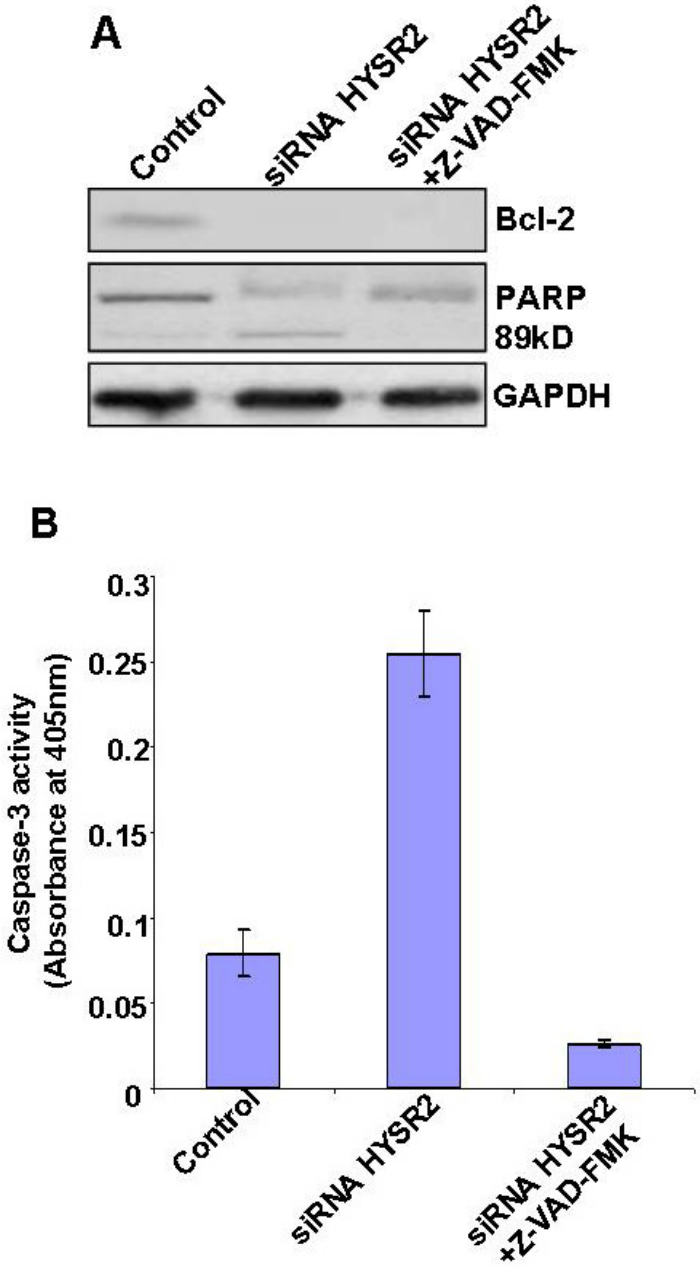

Fig. 3.11 Caspase-3-like activity assay after Bcl-2 siRNA treatment in HeLa cells. Cells were seeded in a six-well plate and treated with 30 nM Bcl-2 siRNA HYSR2 for 48 hours. For the inhibition of apoptosis, 20 μM of the pan-caspase inhibitor Z-VAD-FMK was added into the cell culture media six

hours after siRNA transfection. Cells were continued to be incubated at the same growth condition until analysis. **A.** The expressions of Bcl-2 and PARP cleavage were checked by Western bloting. **B.** The quantitative analysis of caspase-3-like enzymatic activity. The caspase-3-like enzymatic activities were analyzed by using the Promega CaspACE^{TM} assay kit as described in Chapter 2. Values are presented as means ± S.D. of three independent experiments.

3.2 Discussion

3.2.1 RNA interference is post-transcriptional gene silencing (PTGS)

RNA interference is the process by which double-stranded RNA specifically silences the expression of homologous genes through degradation of their cognate mRNA without affecting the chromosomal DNA ((Hammond SM et al., 2001, Hannon GJ, 2002). Through degrading mRNA, protein translation is inhibited, and the interested gene is silenced. Silencing is therefore a post-transcriptional phenomenon. Our data indicated that the distribution of the transfected siRNAs was only in the cytoplasm, not in the nucleus (Fig. 3.3). This observation provides the visible evidence to support that the siRNA-mediated gene knocking-down is at the post-transcriptional level. In addition, the nuclear membrane is a bilayer and separates the interior of the nucleus from a cell's cytoplasm. Although it is marked by a large nuclear pore complex (NPC), the membrane is very selective, permitting only certain molecules and proteins to enter or leave the nucleus (Ribbeck K et al., 2001). This highly

selective transportation mechanism could also contribute the distinct distribution of siRNAs.

3.2.2 Oligofectamine can be applied in siRNA transfection efficiently

Transfection efficiency is a critical element to influence the silencing effect for the transcient transfection. Thus, the high-efficient transfection is the requirement for performing the further experiments. Many methods have been developed for nucleic acids transfection, including calcium phosphate coprecipitation (Pellicer A et al., 1978), electroporation technique (Chu G et al., 1987), diethylaminoethyldextran (DEAE-dextran) delivery (Dubes GR, 1974), and liposome-mediated transfection (Felgner PL et al., 1987). Calcium phosphate co-precipitation is through the formation of calcium phosphate with DNA/RNA to make nucleic acids taken into eukaryotic cells by an endocytotic-type mechanism. Calcium phosphate transfection is used much for the long-term stable transfection. Electroporation technique is based upon perturbation of the cell membrane by an electrical pulse, which forms pores that allow the passage of nucleic acids into the cell. This technique requires fine-tuning and optimization for duration and strength of the pulse for different type of cells to allow efficient delivery without killing the cells. DEAE-dextran is a polymeric cation, which associates tightly with the negatively charged DNA/RNA molecules and carries them into the cell. DEAE-dextran transfection is an efficient DNA/RNA transfection method suitable for transient expression study, however, it may be highly toxic for certain cell lines. Liposome-mediated transfection offers high efficiency for delivery

of nucleotides and proteins to various cell lines including those intransigent to calcium phosphate or DEAE-dextran with low cytotoxicity. Liposome technique can be used for both transient and longer-term transfection. The cell type, the passage number, the confluence of the cells and the concentration of the siRNAs also affect the transfection efficiencies.

In this project, we used oligofectamine to transfect siRNAs into cancer cells, and this is a liposome-mediated transfection. For all the experiments performed in this project, we controlled the cell passage numbers within five and the cell confluences of 50-70%. The liposome-based transfection made the transient transfection efficiency 70-80% after a single transfection, which should be high enough for us to do further experiments with the real working siRNAs targeting Bcl-2 mRNA and FKBP38 mRNA.

3.2.3 The siRNA-mediate silencing of Bcl-2 depends on the mRNA target site

When performing RNAi experiments using siRNA duplexes, the first critical challenge is the design of efficient siRNA. The secondary structure of the target mRNA site significantly influences on the siRNA-mRNA binding activity (Luo KQ et al., 2004). The local secondary structures such as hairpins and internal loops can form through hydrogen bonds between base pairs. A large number of bound bases results in a stable target site with high free energy, which is less accessible for the siRNA because of the unavailable complementary base pairs and spatial obstruction, thus lowering the gene knockdown efficiency. Another important factor that affects the

silencing efficiency is the GC content of siRNAs. The GC content exhibits an important correlation with the stability of the double-stranded siRNAs due to the difference in hydrogen bonding capacity of GC pairs with three H-bonds and AT pairs with two H-bonds. Thus, high GC content of siRNA leads to difficulty in unwinding the double-stranded RNA because of high consumption of ATPs, and reasonably, resulting in decreasing the siRNA efficiency. Among all of the three siRNAs, HYSR2 has the lowest GC content (33%), while HYSR3 has 52% of GC content and HYSR1 has the highest with 62%. Further, the *in silico* analysis showed that the HYSR2-targeting Bcl-2 mRNA region is an open region with low local free energy and a high number of unpaired nucleotides. Therefore, HYSR2 is the easiest to match with the target Bcl-2 mRNA, and leading to easy cleavage and degradation. Thus, the siRNA HYSR2 was chosen to knockdown the expression of Bcl-2 in the further experiments in this project.

3.2.4 RNA interference of Bcl-2 induced caspase-3-dependent apoptosis

The persistence of RNAi activity appears to be another important parameter when the effects of RNAi on the regulation of genes inside cells are considered. Base-paired 21- and 22- nucleotide (nt) siRNAs with overhanging at 3' ends may enhance nuclease resistance of siRNAs in the cells, thus, making the siRNAs stable (Elbashir SM et al., 2001a). This stability also makes it possible for siRNAs entering into the daughter cells with the cell division, which consequently confers the long lasting time of the sequence-specific mRNA degradation (Elbashir SM et al., 2001b). Yet, it is

also conceivable that whenever cell division occurs, the number of RISCs carrying siRNA duplexes decreases in those cells, consequently weakening the siRNA-mediated sequence-specific mRNA degradation effect. This long-lasting silencing property made siRNA to be practical for giving enough time to study gene function.

As an anti-apoptotic protein, overexpression of Bcl-2 has been found in maintaining cell survival ability in various cancers. And Bcl-2 suppression-induced cell death could become a reasonable method for cancer treatment. Our data suggest that 72 hours after Bcl-2 siRNA HYSR2 treatment, cell proliferation decreased, which is consistent with Bcl-2 degradation, suggesting Bcl-2 plays an important role in maintaining HeLa cell survival. Without Bcl-2 expression, cells undergo apoptosis even without extra cell stresses. Bcl-2 is known to localized at the mitochondria and protect the integrity of the mitochondrial outer membrane. Once removing Bcl-2, the mitochondrial outer membrane was broken and several apoptogenic factors will be released from the intermembrane space to the cytosol to activate the caspase cascade and consequently cells undergo apoptosis irreversibly (Muzio M et al., 1997; Enari M et al., 1998; Wang X, 2001). Thus, caspase cascade activities play a critical role in apoptotic pathway. The activation of caspase-3 is essential for various proteases activation, DNA cleavage and cell morphological changes. From our data, we can see that silencing Bcl-2 by the RNA interference induces the activation of caspase-3, which can be the reason for chromosomal DNA cleavage and the morphological changes. Taken together, our results suggest that the HYSR2 siRNA appeared to induce apoptotic cell death through the activation of caspase-3- dependent pathway.

3.3 Conclusion

In conclusion, the double-stranded 21nt-long siRNA-mediated RNA interference is a recently discovered potent and specific gene-silencing tool, which allows us to specifically silence target genes in living cells compared with other existing silencing techniques (Fire A et al., 1998). However, excess siRNAs may also induce non-specific toxicities arising from multiple signaling pathway, thus, using the smallest amount of siRNAs with the most significant silencing effects is essential when using this technique to study gene function (Persengiev SP et al., 2004). In this study, we tested three different siRNAs targeting different sites of Bcl-2 mRNA. With 70 to 80% of transfection efficiency, siRNA HYSR2 showed the best silencing effect by causing about 80% of Bcl-2 degraded only at the concentration of 30 nM. This silencing effect could last for about one week. Also, this siRNA HYSR2 was competent among three different cancer cells. And a caspase-dependent apoptosis induced by Bcl-2 suppression was observed in HeLa cells. Thus, siRNA HYSR2 could be used as a practical gene-silencing tool to further study Bcl-2 function.

Chapter 4 Molecular interaction between Bcl-2 and FKBP38

The immunosuppressant FK-506 binding protein 38 (FKBP38) is expressed in all tissues, particularly highly in brain (Lam E et al., 1995). Recently, it was found that FKBP38 could form a complex with Bcl-2 or Bcl-x_L, and co-localize at the mitochondrial membrane to regulate apoptosis (Shirane M et al., 2003). Also, it was demonstrated that, in neuronal cells, the binding of FKBP38 with Bcl-2 was Ca^{2+}/calmodulin (CaM)-dependent (Edlich F et al., 2005).

Structure studies showed that Bcl-2 contains a long flexible loop comprising about 60 residues, between the BH3 and BH4 regions (Petros AM et al., 2001). It has been shown that the function of Bcl-2 is regulated through the post-translational modifications, including phosphorylation on this loop part (Ruvolo PP et al., 2001; Deng X et al., 2006; Srivastava RK et al., 1999; Haldar S et al., 1998; Lin B et al., 2004). Recently it was found that the loop is important for binding other proteins. This molecular interaction may allow Bcl-2 to undergo conformational changes and subsequently influence Bcl-2's regulatory functions in apoptosis, including changes in the properties of Bcl-2 from an anti-apoptotic protein to a pro-apoptotic protein (Lin B et al., 2004).

The *In vitro* experiments showed that the loop of Bcl-2 also plays an important role in the interaction with FKBP38. And two phosphorylation sites in the loop of Bcl-2, T56 and S87, were shown to be critical for its physical interactions with FKBP38 (Kang CB et al., 2005). Here, in this study, we further investigated the interaction between Bcl-2 and FKBP38 in mammalian cells. The expressions of Bcl-2 and FKBP38 in different cell

lines were checked by Western blotting. In order to examine the role of Bcl-2 loop in binding with FKBP38, several plasmids of Bcl-2 with mutations in its loop domain were constructed as YFP fusions while FKBP38 was inserted into pECFPC1 and pXJ40-FLAG. The distribution of these Bcl-2 mutants inside cells was investigated by using confocal microscopy after staining cells with MitoTracker. The interactions between FKBP38 and Bcl-2 mutants were analyzed by both FRET assay and immunoprecipitation. Our results showed that the loop region of Bcl-2 affects its distribution patterns inside cells and its stability.

4.1 Results

4.1.1 Expression of Bcl-2, Bcl-xL and FKBP38 in cancer cells.

The expression of Bcl-2, Bcl-x_L, FKBP38 and the housekeeping protein in seven different cancer cell lines were checked by Western blotting (Fig. 4.1). In order to compare the expression levels of each protein in different cell lines, the loading amounts of the total proteins from each cell line were the same (100 μg). Results showed that among these seven different cancer cell lines, the expression levels of the anti-apoptotic proteins, Bcl-2 and Bcl-x_L varied significantly. Bcl-2 expression was observed in PC12, HeLa, MDA-MB-231, MCF-7 and Jurkat cells, while there was relatively little expression of Bcl-2 in B104 and A549 cells. The expression level of Bcl-x_L was high in MDA-MB-31, MCF-7, A549, Jurkat, PC12 and B104, while HeLa cells show relatively low level of Bcl-x_L. FKBP38 was abundantly expressed in all of these cells with the

different sizes between rat and human cells. Although all of the cell lines had the expression of the housekeeping protein GAPDH, the expression levels were also different. These different expressions of Bcl-2, Bcl-x_L, FKBP38 and GAPDH maybe related with the differences of the functions of these proteins in cells. And it shoulded also not be excluded the differences of the physiological functions of these cells *in vivo*.

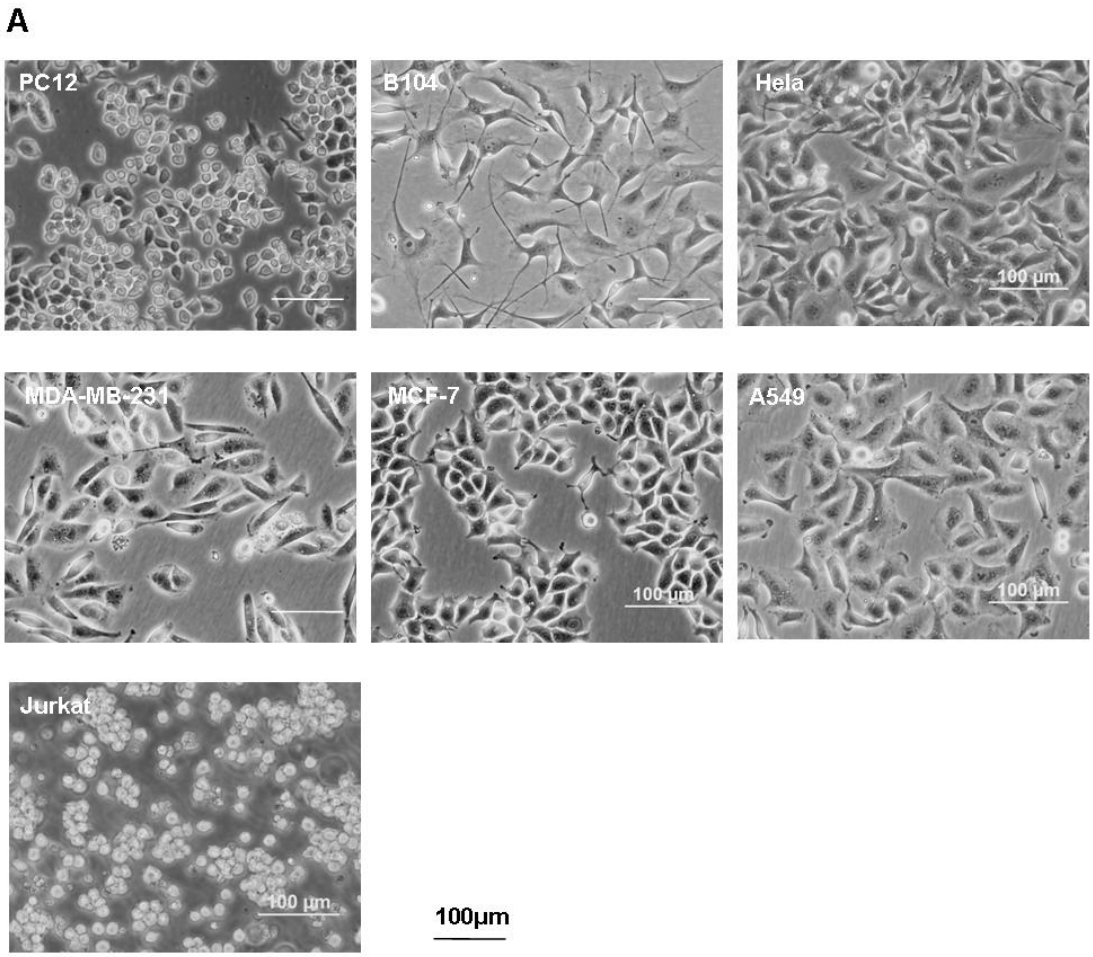

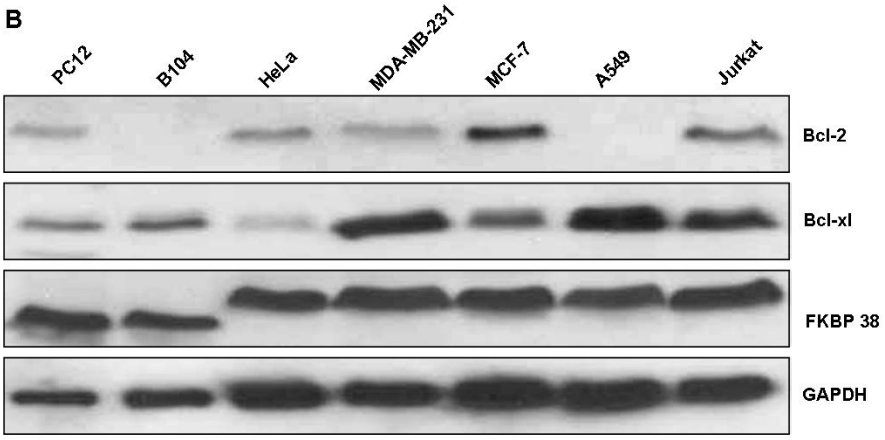

Fig. 4.1 The expressions of Bcl-2, Bcl-x_L, FKBP38 and GAPDH in different cancer cells. Seven different cancer cells were cultured in their proper culture media supplied with 10% FBS and antibiotics, including rat pheochromocytoma cells PC12, rat neuroblastoma cell line, mouse neuroblastoma cell line B104 and human cervical adenocarcinoma cells HeLa, human mammary adenocarcinoma cells MDA-MB-231 and MCF-7, human lung adenocarcinoma cells A549, and human T cell lymphoblast-like cells Jurkat. **A.** Cell images were taken with phase contrast microscopy. **B.** The expressions of Bcl-2, Bcl-xl, FKBP38 and GAPDH were detected by Western blotting. Cell lysates were collected with ice cold lysis buffer. The concentrations of the total proteins were measured with Bio-Rad protein assay dye. 100μg of total proteins from different cells were separated with 12% of SDS-PAGE, and the interested proteins were detected by Western blotting. Here was a representative of three independent experiments.

4.1.2 Co-localization of Bcl-2 and FKBP38 in mammalian cells

In this study, HeLa cells, which express both Bcl-2 and FKBP38, were used for further exploring the biological functions of these two proteins. First, the distributions of the endogenous Bcl-2 and FKBP38 were investigated by subcellular fractionation assay (Fig. 4.2). The results showed that the majority of endogenous Bcl-2 distribution was in mitochondrial part, but there was still some Bcl-2 found in endoplasmic reticulum with two distinct bands. Existence of two bands suggests that Bcl-2 in ER may exist in

unphosphorylated and phosphorylated forms. Another possibility is that the lower band may be caused by Bcl-2 degradation. On the other hand, FKBP38 was only seen in mitochondrial fraction and none was detected in ER, Even though a majority of Bcl-2 and FKBP38 are localized in mitochondria, the localization of Bcl-2 in ER suggests that cells might exert differential regulatory mechanisms to distribute Bcl-2 and FKBP38 in cells.

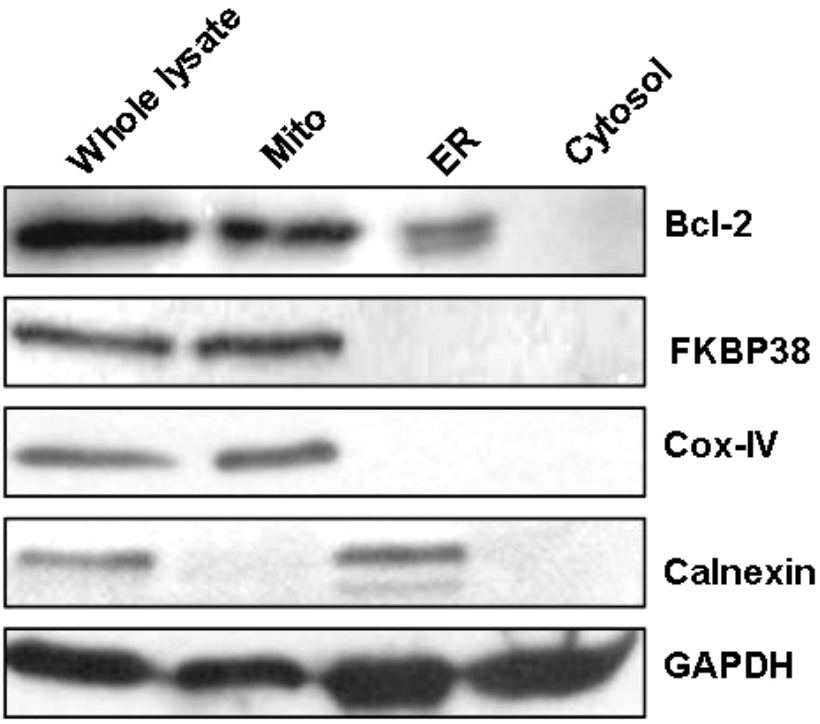

Fig. 4.2 Subcelluar fractionation of endogenous Bcl-2 and FKBP38 in HeLa cells. HeLa cells (1×10^7) were harvested by trypsinization and were washed with cold 1 × PBS three times. Pellets were resuspended in 5 ml of sorbitol-HEPES incubation buffer with complicated protease inhibitors. After homogenized, crude lysates were centrifuged at 1,000 *xg* for 20 min at 4°C to remove nuclei and unbroken cells. The supernatant was collected in a new tube and was centrifuged at 10,000 *xg* for 30 min at 4°C to isolate the mitochondrial part. Then the supernatant was collected and ultra-centrifuged at 100,000 *xg* for 4 hours at 2°C to isolate the endoplasma reticulum (ER) pellets. Final supernatant was collected as the cytosolic fraction. Different parts were collected and the expression of Bcl-2 and FKBP38 were checked by Western blotting. Here was a representative of three independent experiments.

In addition, the localizations of the exogenous Bcl-2 and FKBP38 were checked. The full-length cDNAs of Bcl-2 and FKBP38 were obtained through RT-PCR from the human breast cancer cell MCF-7 (Fig. 4.3). Bcl-2 cDNA is 720 bp and FKBP38 cDNA is 1071 bp. The results were confirmed by DNA sequencing.

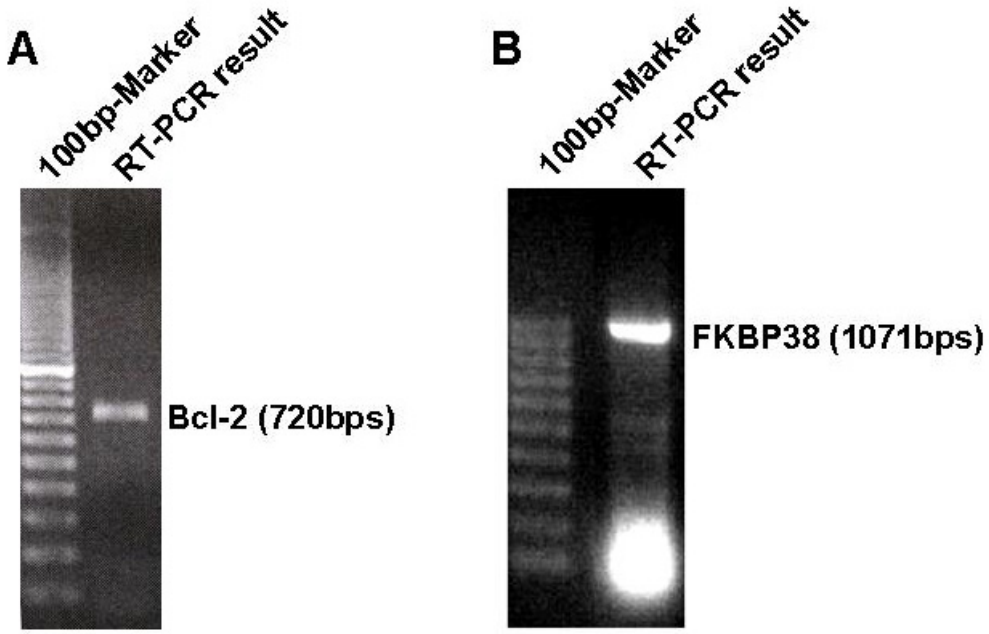

Fig. 4.3 The RT-PCR results of Bcl-2 and FKBP38. Total RNAs were isolated from the human cancer cells with RNeasy® Mini Kit (QIAGEN). Bcl-2 cDNAs were got with the GC-RICH PCR System (Roche). The full length of Bcl-2 cDNA was 720 bps and the full length of FKBP38 cDNA was 1071 bps. The results were confirmed by DNA sequencing.

In order to observe the localizations, YFP-Bcl-2 (wt) and CFP-FKBP38 (wt) were co-transfected into the Hela cells. The localizations of YFP-Bcl-2 and CFP-FKBP38 were checked by confocal microscopy after staining cells with MitoTracker and ERTracker (Fig. 4.4). The results showed that exogenous YFP-Bcl-2 and CFP-FKBP38 merge well with MitoTracker, but poorly with ERTracker, suggesting Bcl-2 and FKBP38 mainly localized at mitochondria, which is consistent with the observation of the endogenous

FKBP38 and Bcl-2. Taken together, these data suggest that these two proteins co-localized at mitochondria and also interacted to each. This is consistent with studies demonstrating the distributions of the endogenous Bcl-2 and FKBP38 from subcellular fractionation assay. Therefore, it is reasonable to speculate that FKBP38 interacts with Bcl-2 and consequently performs its anti-apoptotic function by regulating the localization of Bcl-2 at mitochondrial membrane.

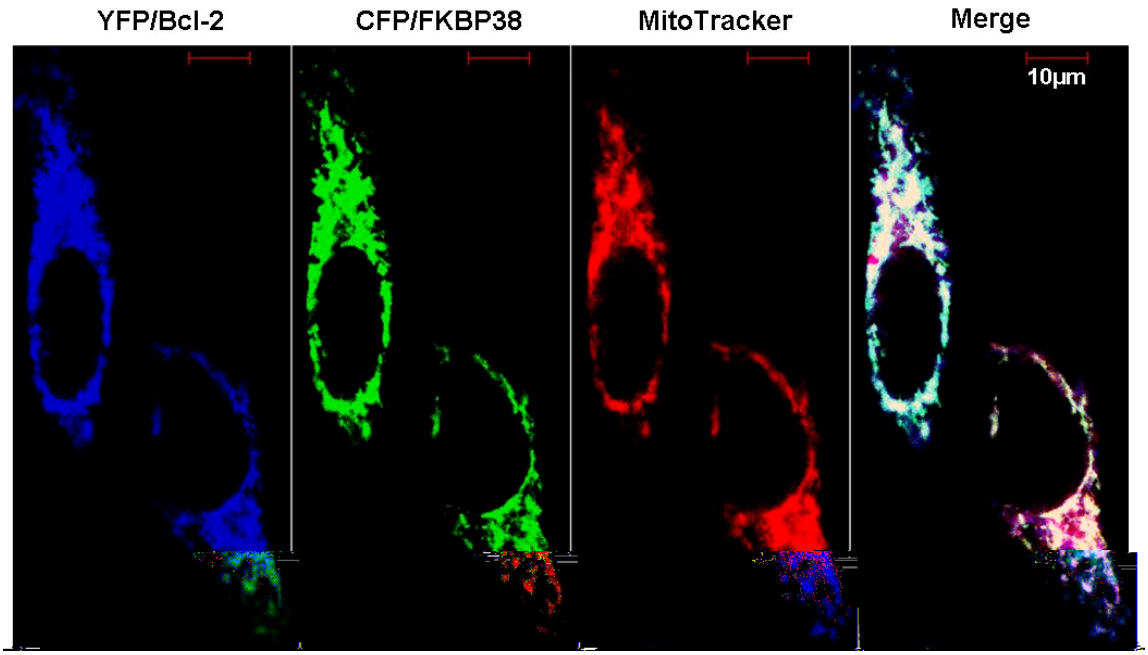

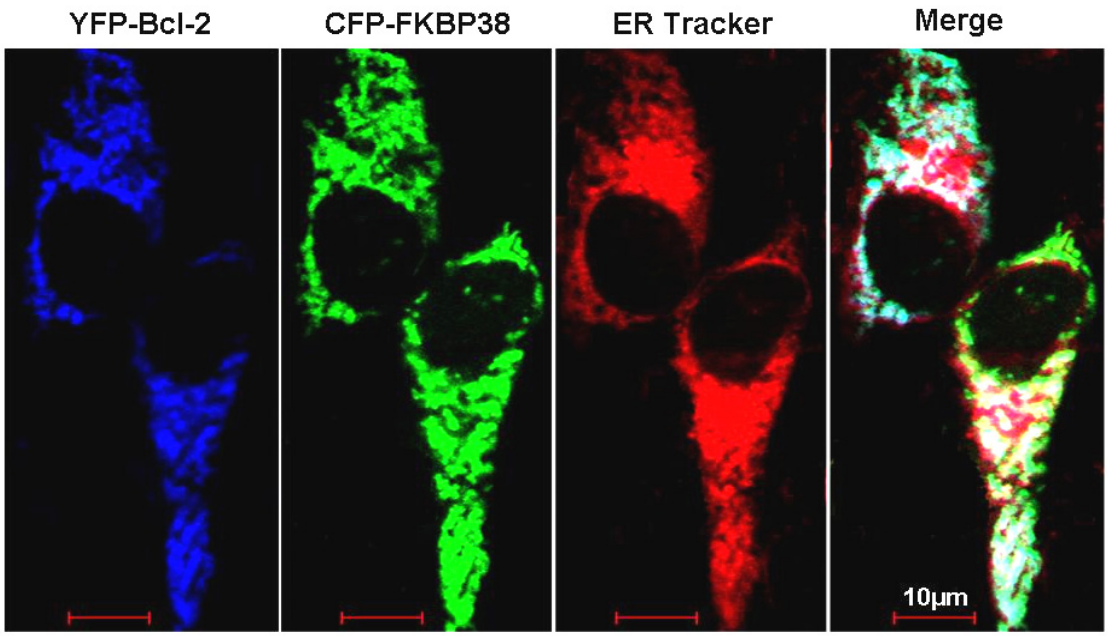

Fig. 4.4 Co-localization of Bcl-2 and FKBP38 in HeLa cells. HeLa cells were seeded on a 22mm^2 cover slip within a six-well plate as 2 × 10^5 cells/well. The plasmids pECFPC1/FKBP38 and pEYFPC1/Bcl-2 were constructed as described in Chapter 2. After confirming the DNA sequencing, pECFPC1/FKBP38 and pEYFPC1/Bcl-2 were co-transfected into cells using the transfection reagent lipofectamine 2000. Twenty-four hours after transfection, cells were stained with 200 nM Mito-Tracker® Deep Red 633 or ER-Tracker™ Blue-White DPX for 30min under the standard growth conditions. Cells were fixed with 3.7% paraformaldehyde for 15 min at 37°C. After washing, the cover slips were mounted with prolong antifade reagent and the slides were sealed with nail polish. Slides were observed with a 60 × oil immersion lens using the Zeiss LSM 510 META confocal microscope. The excitation wavelengths used are 458 nm for CFP, 514 nm for YFP, 633 nm for Mito-Tracker and 405 nm for ER-Tracker. According to the experimental requirements, the corresponding wavelengths were used simultaneously to capture images for the colocalization analysis.

4.1.3 The design and construction of Bcl-2 loop mutants and FKBP38 plasmids

Five plasmids were designed and constructed in this study. The full-length Bcl-2 cDNA was obtained by reverse transcriptase polymerase chain reaction (RT-PCR) from mRNA isolated from MCF-7 breast cancer cells. The NMR experiments showed that there were no structures in the Bcl-2 loop part. And the deletion or the change on the loop part did not affect the three-dimentional structure of Bcl-2 (Petros AM et al., 2001). In order to study the binding activity of the Bcl-2 loop with FKBP38, several Bcl-2 loop mutants were made. According to the length of the loop of Bcl-2 and the phosphorylation sites included, three sites in the loop were selected for the construction of the mutants. One is between D34 and V35, one is between D64 and P65, and one is between P88 and V89 (Fig. 4.5A). And three different Bcl-2 loop mutants were made, including the deletion of the whole loop (V35 to V89), the deletion of the half N-terminal part (V35 to D64) and the deletion of the half C-termianl par (P65 to V89). Also the Bcl-2 transmembrane-deleted plasmid was constructed as well (Fig.4.5B). Bcl-2 and its mutant cDNAs were inserted into the pEYFPC1 (BD Biosciences) with the restriction enzymes *Xho*I and *Sal*I (Fig. 4.5C). This design not only made sure that the loop of Bcl-2 was divided almost evenly, but also ensured that the phosphorylations sites were included in each partial loop remaining plasmids. Finally, there are totally five Bcl-2 mutants plasmids obtained. They are the plasmid of YFP-conjugated full-length Bcl-2 (pEYFPC1/Bcl-2), YFP-conjugated trans-membrane domain-deleted Bcl-2 (pEYFPC1/Bcl-2ΔTM), YFP-conjugated trans-membrane domain and loop-deleted Bcl-2 mutant (pEYFPC1/Bcl-2Δ(TM+Loop)/6A), YFP-conjugated trans-membrane domain

and partial loop-deleted Bcl-2 mutants, pEYFPC1/Bcl-2Δ(TM+(P65-V89)) and pEYFPC1/Bcl-2Δ(TM+(V35-D64)) (Fig. 4.5).

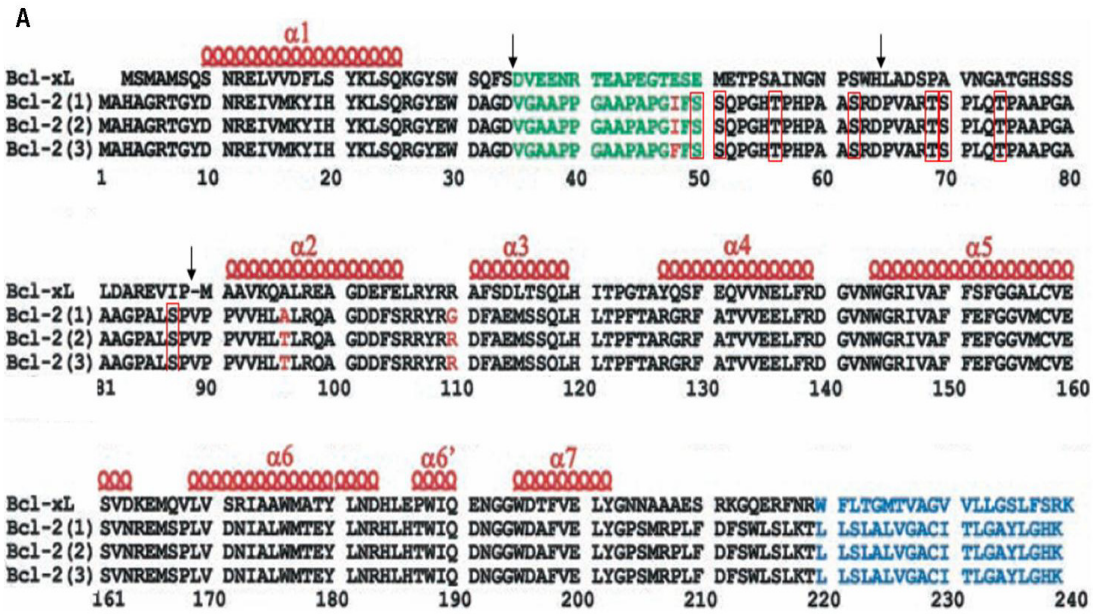

Adapted from Petros AM, et.al (2001). **Solution structure of the antiapoptotic protein bcl-2**. *PNAS.*

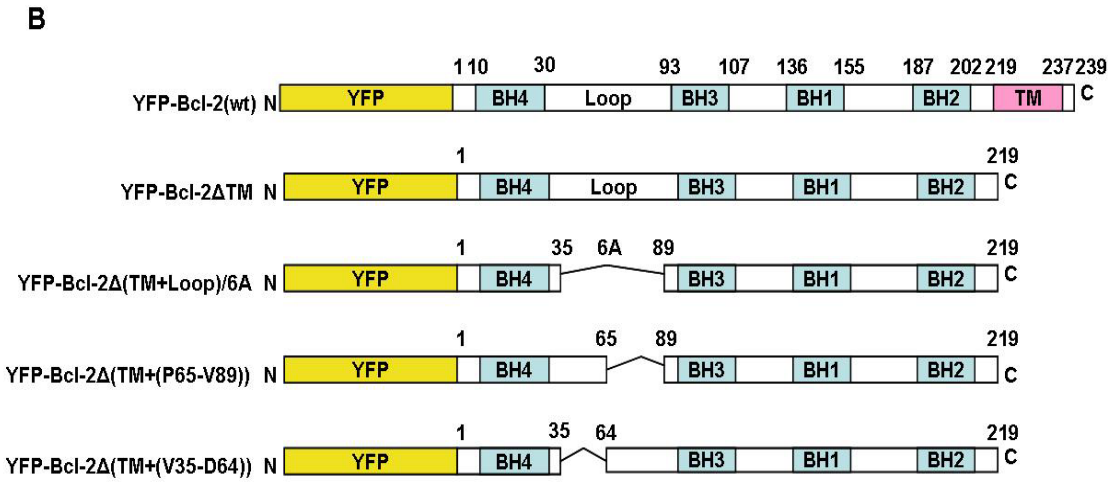

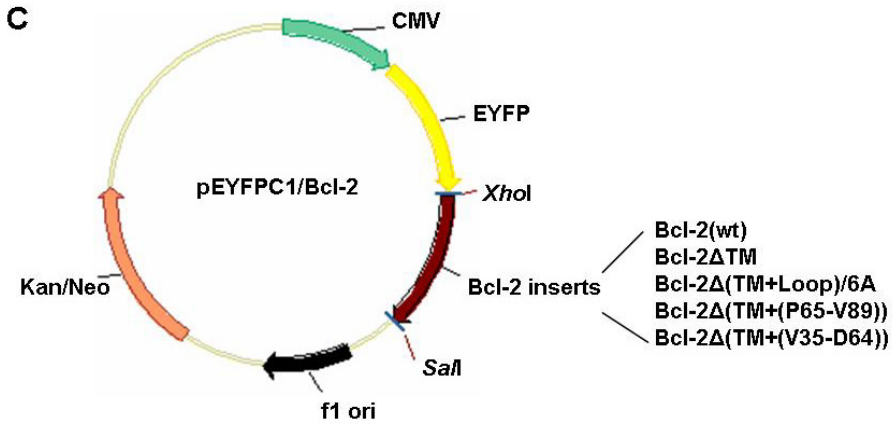

Fig. 4.5 Schematic representations of the plasmids expressing Bcl-2 and its loop mutants in this study. **A.** Sequence alignment of three isoforms of full length Bcl-2 and the full length of another antiapoptotic protein Bcl-x_L (Petros AM et al. 2001). All the serine (S) and the threonine (T) sites in the loop parts of Bcl-2 have been labeled out. The sites for the construction of the Bcl-2 loop mutants were also shown with arrows. **B.** Schematic representations of wild type Bcl-2 and its loop mutants, YFP-Bcl-2 (wt), YFP-Bcl-2ΔTM, YFP-Bcl-2Δ(TM+loop)/6A, YFP-Bcl-2Δ(TM+(P65-V89)) and YFP-Bcl-2Δ(TM+(V35-D64)) with the YFP at the N-terminus of the inserts. BH1-3 domains, loop part and transmembrane domain are indicated. The sites of the main amino acids were also labeled. The full-length Bcl-2 cDNA was obtained by RT-PCR and various Bcl-2 loop mutants were made and inserted into pEYFPC1. **A.** The map of plasmid pEYFPC1. Bcl-2 and loop mutants were inserted into pEYFPC1 with the restriction enzymes *Xho*I and *Sal*I.

The full-length FKBP38 cDNA was obtained by RT-PCR from MCF-7 breast cancer cells and was inserted into the pECFPC1 (BD Biosciences) with the restriction enzymes *Xho*I and *Sal*I to obtain the plasmid of pCFPC1/FKBP38, and inserted into pXJ40-Flag with the restriction enzymes *Bam*HI and *Xho*I to obtain the plasmid pXJ40-Flag/FKBP38 (Fig. 4.6).

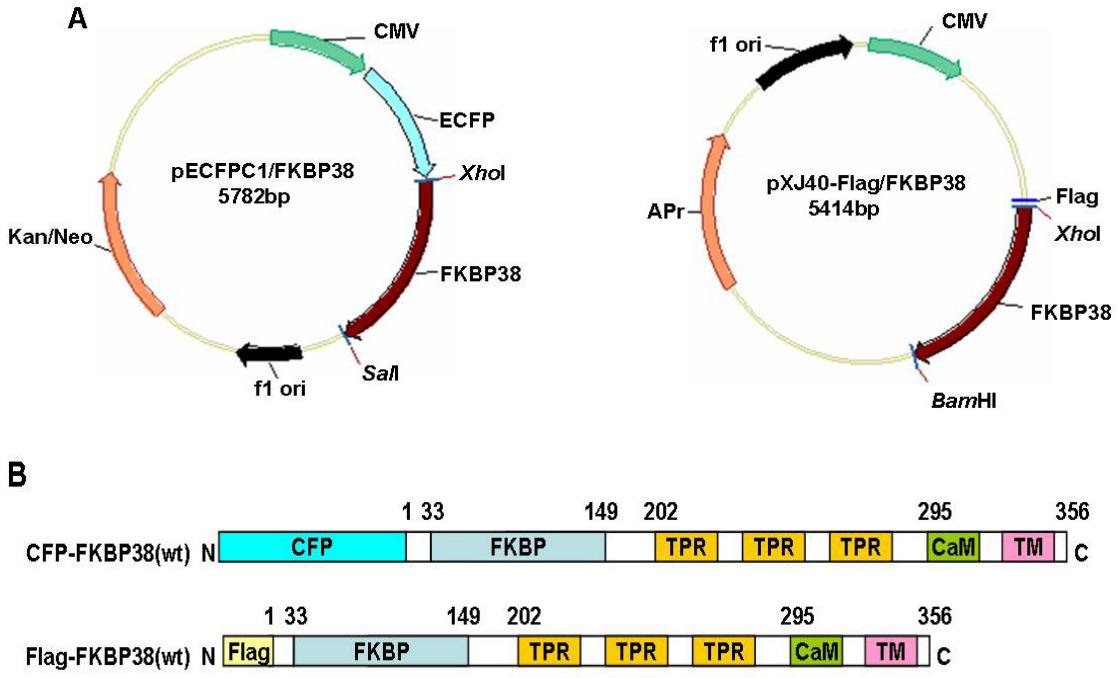

Fig. 4.6 Schematic reprensation of the plasmids expressing FKBP38 in this study. The wild type FKBP38 gene was inserted into pECFPC1 and pXJ40-Flag, respectively. A. The full-length FKBP38 cDNA was obtained by RT-PCR and inserted into pECFPC1 with the restriction enzymes *Xho*I and *Sal*I, And inserted into pXJ40-Flag with the restriction enzymes *Xho*I and *Bam*HI. B. Schematic representations of Flag-FKBP38, CFP-FKBP38 with the Flag tag and CFP localizing at the N-terminus of the inserts. The main domains in FKBP38, FKBP38 domain, TPR domain, CaM domain and transmembrane domain are indicated.

The plasmid with Flag tag was a gift from Dr. Lim's lab [13]. The primers used for constructing the above plasmids are listed in Table 4.1.

Vectors	Primers	Restriction enzymes
pEYFPC1	Forward primer for Bcl-2 and its mutants: 5'-GCGAAGCTCTCGAGGA ATGGCGCACGCTGGGAGAACGGGGTAC-3'	XhoI
	Reverse primer for Bcl-2 wild type: 5'-GCGTGATGTCGACTCACTTGTGGCCCAGATAGGCACCCAG-3'	SalI
	Reverse primer for Bcl-2 mutants: 5'-GCGTGATGTCGACCTATCACCGCATGCTGGGGCCGTACAGTTC-3'	SalI
pECFPC1	Forward primer for FKBP38: 5'-GCGAAGCTCTCGAGGA ATGGGACAACCCCCGGCGGAGGAGGCT-3'	XhoI
	Reverse primer for FKBP38: 5'-GCGTGATGTCGACTCAGTTCCTGGCAGCGATGACCACAGA-3'	SalI
pXJ40-FLAG	Forward primer for FKBP38: 5'-AAGGATCCATGGGACAACCCCCGGCGGAG-3'	BamHI
	Reverse primer for FKBP38: 5'-AAACTCGAGTCAGTTCCTGGCAGCGATGAC-3'	XhoI

Table 4.1 Primers used for plasmids construction in this study. Bcl-2 and its mutants were inserted into the plasmid pEYFPC1 with the restriction enzymes *Xho*I and *Sal*I. FKBP38 was inserted into the plasmid pECFPC1 with the restriction enzymes *Xho*I and *Sal*I. FKBP38 was inserted into the plasmid pXJ40-FLAG with the restriction enzymes *Bam*HI and *Xho*I.

4.1.4 Regulation on the stability of Bcl-2 by its loop

The flexible loop of Bcl-2 between its BH3 and BH4 domain is involved in regulating the functions of Bcl-2 through post-translational modification. In order to study the regulatory function of this loop in the conjunction of Bcl-2 with FKBP38 inside mammalian cells, we constructed several Bcl-2 mutants in the loop region (Fig. 4.7). After transfecting into HeLa cells, the expressions of these Bcl-2 mutants were checked by Western blotting.

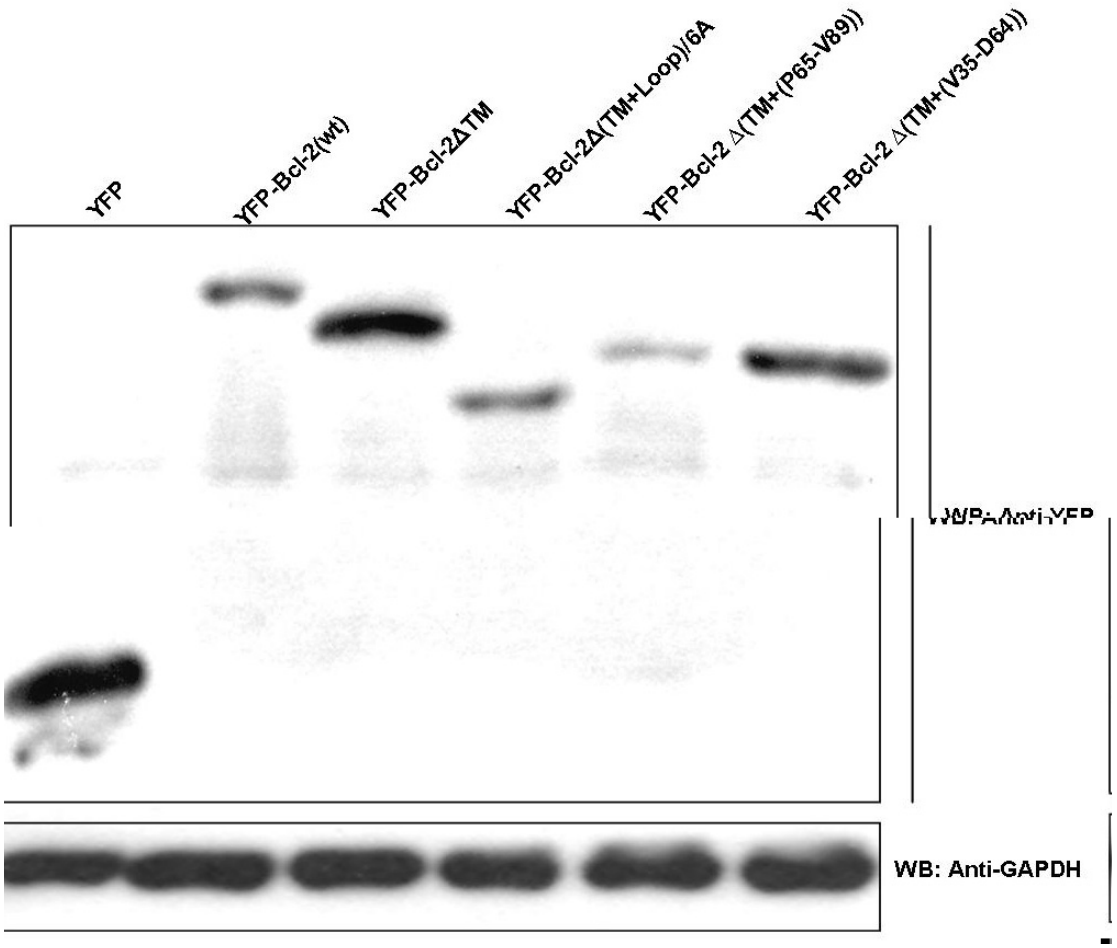

Fig. 4.7 Expressions of YFP conjugated Bcl-2 and its mutants in HeLa cells. Cells were seeded in a six-well plate (2×10^5 cells/well). The plasmids pEYFPC1/Bcl-2(wt), pYFP/Bcl-2ΔTM, pYFP/Bcl-2Δ(TM+Loop)/6A, pYFP/Bcl-2Δ(TM+(P65-V89)) and pYFP/Bcl-2Δ(TM+(V35-D64)) were constructed as described in Chapter 2 and confirmed by DNA sequencing. After measuring the concentrations, equal amounts of plasmids (2μg) were transfected into cells using the transfection reagent lipofectamine 2000. Twenty-four hours after transfection, cells were lyzed and the concentrations of total proteins were measured with protein assay dye. 100 μg of total protein were separated by 12% SDS-PAGE. The expressions of Bcl-2 mutants were checked by Western blotting. GAPDH was probed as an internal control.

4.1.5 Regulation on the distribution of Bcl-2 by its loop

The distribution of proteins inside cells is related to their biological functions. The localization of Bcl-2 at mitochondria is critical for its anti-apoptotic function by protecting the integrity of the mitochondrial membrane. Here the distributions of Bcl-2 mutants were checked by confocal microscopy, and their localizations at mitochondria were examined after staining with MitoTracker in HeLa cells(Fig. 4.8).

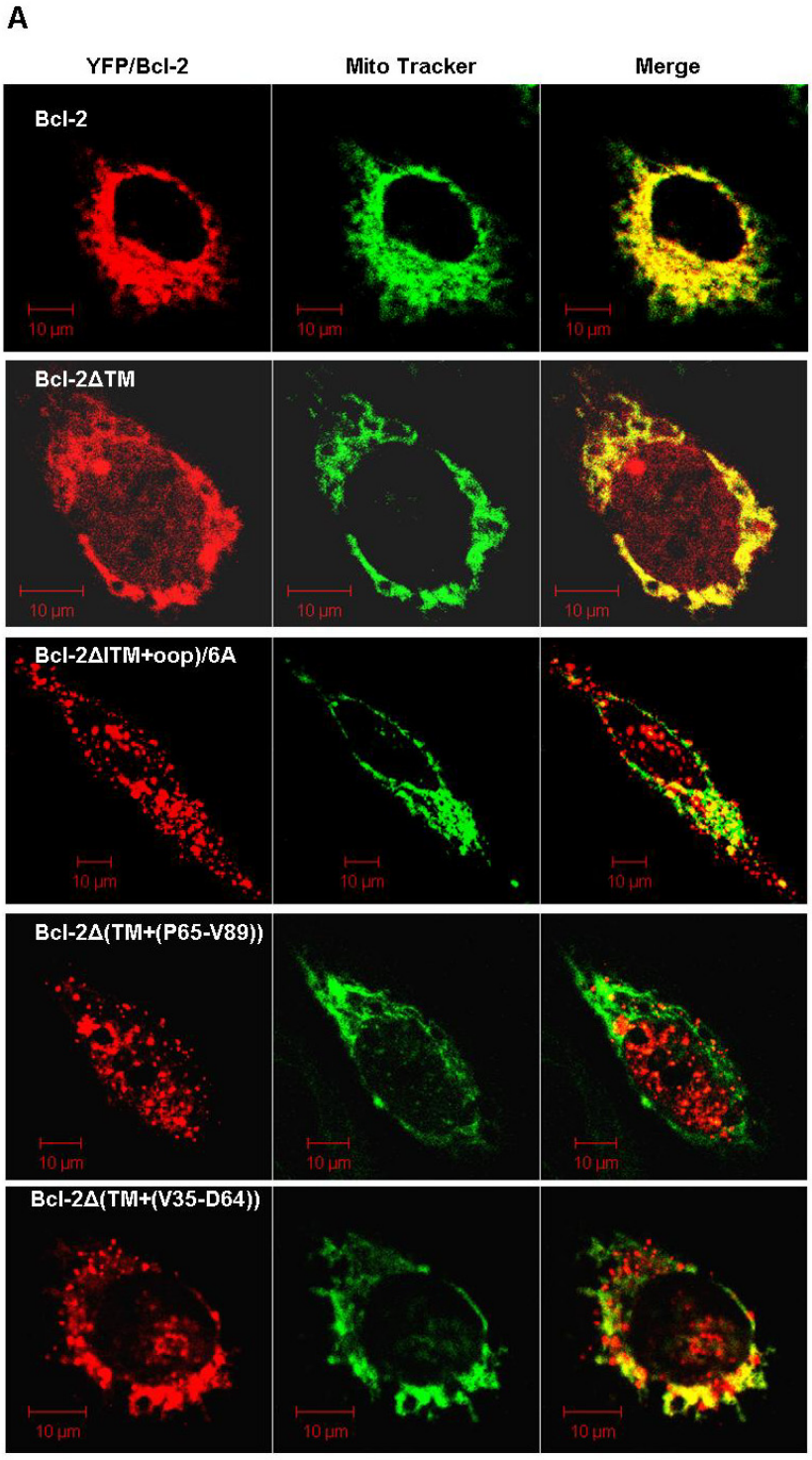

Fig. 4.8 Bcl-2 distribution inside HeLa cells. Cells (2×10^5 cells/well) were seeded on a $22mm^2$ cover slip within a six-well plate and transfected with various Bcl-2 mutant plasmids for 24 hours. After stained with

200 nM Mito-Tracker®, cells were fixed with 3.7% paraformaldehyde. Cell images were observed with a 60 × oil immersion lens under the Zeiss LSM 510 META confocal microscope with the excitation wavelengths 514 nm for YFP and 633 nm for MitoTracker.

The results showed that without the transmembrane domain and the loop region, Bcl-2 was still found targeted to mitochondria, although some were observed inside nucleus. Interestingly, the Bcl-2 distributed inside nucleus showed obvious aggregation. After removing the transmembrane domain, a major fraction of Bcl-2 was still observed to remain localizing at the mitochondria. This suggests that the transdomain is not sole determinant for localization of Bcl-2 to the mitochondrial membrane. Some other proteins may interact with Bcl-2 and help it to localize at the mitochondria. The truncation of the entire loop caused Bcl-2 to be distributed in the nucleus and aggregated, indicating the sign of loss-of-function. However, the removal of V35-D64 caused less aggregating Bcl-2 inside nucleus compared to what was seen in the deletion mutant of P65-V89. These results suggest that the disordered loop might contain locally distinct motifs to differentially modulate Bcl-2 function.

4.1.6 Regulation of Bcl-2 anti-apoptotic function by its loop

Having noticed that the flexible loop of Bcl-2 plays an important role in its stability and cellular distribution, we next examined consequences of the loop deletion mutants on the cell proliferation. YFP-fusion Bcl-2 mutants were overexpressed for 24 hours, and the cell viabilities were analyzed with MTT assay (Fig. 4.9). The results showed that the anti-apoptotic function was slightly weakened after deleting the region of P65-V89. However, the deletion of V35-D64 or the total deletion of the loop part didn't

make this decrease of cell viabilities more significant, suggesting that the residues in different regions made different regulations on the antiapoptotic function of Bcl-2.

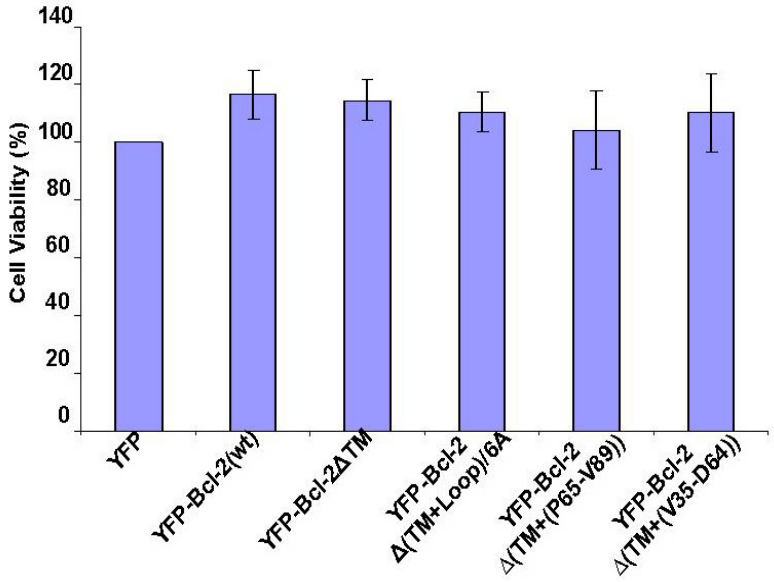

Fig. 4.9 Cell proliferation assay. HeLa cells were seeded in a 96-well plate (5×10^3 cells/well) and treated with YFP-conjugated Bcl-2 mutants' plasmids (0.2μg/well) for 24 hours. Cell viabilities were assessed by MTT assay. Data are presented as means ± S.D. (n = 5).

Together with the data showed in Fig. 4.8, we concluded that the region of P65-V89 not only positively regulated the stability of Bcl-2, but also positively regulated the antiapoptotic function of Bcl-2.

4.1.7 In situ analysis of the interaction between Bcl-2 and FKBP38

FKBP38 is a recently discovered protein with anti-apoptotic function by anchoring Bcl-2 to mitochondria. Without FKBP38, Bcl-2 was found to be misdistributed inside cells and caspase-3-dependent apoptosis was induced. The *in vitro* experiments showed that the loop part of Bcl-2 plays an important role in their binding activity. In

order to *in situ* analyze the spatial interactions between the Bcl-2 loop with FKBP38, FRET were examined after co-transfecting YFP-fusion Bcl-2 mutants and CFP-FKBP38 into Hela cells (Fig. 4.10). The removal of the whole loop decreased FRET by 30% (from about 50% to about 20%). The deletion of P65-V89 led to decrease in FRET by 25% (from about 50% to about 25%); and removal of V35-D64 resulted in a decrease in FRET by about 20%. Thus, based on the results, the C-terminal half part of the loop, which contains the region of P65-V89, appears to be was more important for the binding with FKBP38.

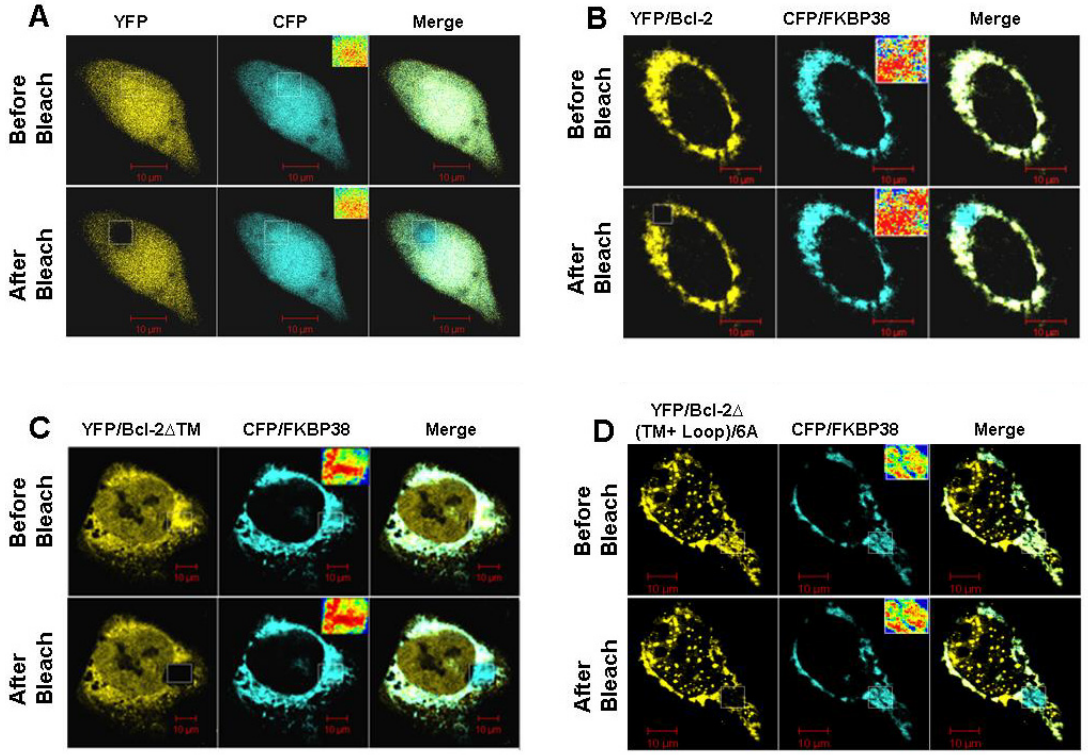

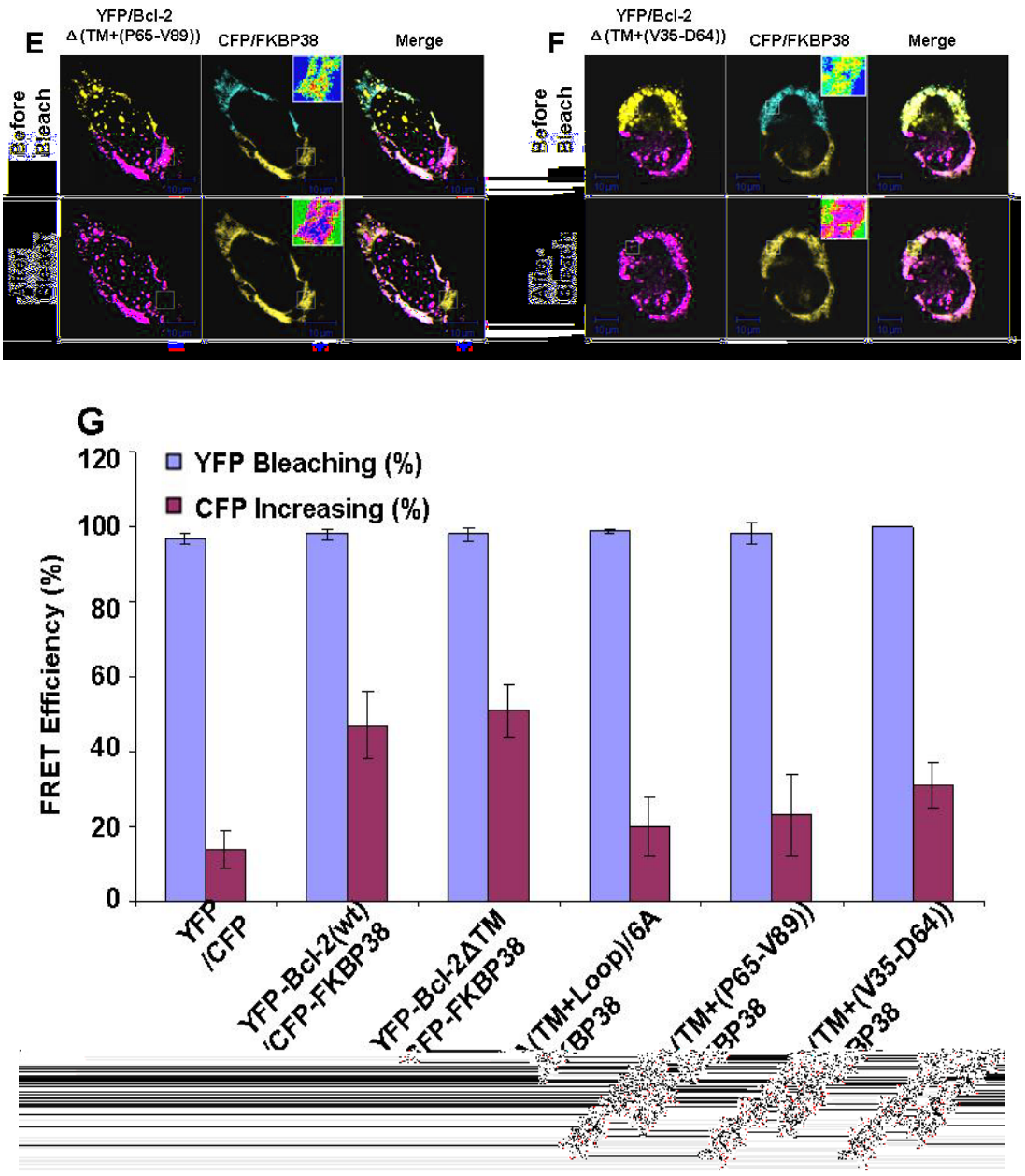

Fig. 4.10 FRET assay between CFP conjugated Bcl-2 mutants and YFP conjugated FKBP38 in HeLa cells. Cells (2×10^5 cells/well) were seeded on a 22 mm^2 cover slip within a six-well plate. The plasmids pEYFPC1/Bcl-2(wt), pEYFPC1/Bcl-2ΔTM, pEYFPC1/Bcl-2Δ(TM+Loop)/6A, pEYFPC1/Bcl-2Δ(TM+(P65-V89)), pEYFPC1/Bcl-2Δ(TM+(V35-D64)) were co-transfected with pECFPC1/FKBP38 into cells, respectively, using the transfection reagent lipofectamine 2000. Twenty-four hours after transfection, cells were fixed with 3.7% paraformaldehyde for 15 min at 37°C. After washing, the cover slips were

mounted with prolong antifade reagent and the slides were sealed with nail polish. Slides were observed with a 60 × oil immersion lens using the Zeiss LSM 510 META confocal microscope. The excitation wavelengths used are 458 nm for CFP, 514 nm for YFP. **A-F.** FRET assay images of FKBP38 and Bcl-2's mutants. A region with both the expression of YFP and CFP was selected as Region Of Interest (ROI), and was photobleached in YFP channel by scanning 10 times. The YFP and CFP images were collected before and after bleach and the fluorescence intensities of YFP and CFP were obtained. **G.** Quantitative analysis of the FRET efficiencies of the results of A-F as described in Chapter 2. Values represented the means ± S.D. of five indival experiments.

4.1.8 Co-immunoprecipitation assay between Bcl-2 and FKBP38

In order to further provide direct evidence for the interactions between Bcl-2 loop mutants and FKBP38, co-immunoprecipitation experiments were performed. Flag-fused FKBP38 was constructed and co-transfected with YFP-fused Bcl-2 loop mutants into HeLa cells for 24 hours. After precipitated by anti-Flag antibody, Bcl-2 mutants were detected by anti-YFP antibody (Fig. 4.11). The results showed that removal of the region of V35-D64 did not abrogate the interaction between FKBP38 and Bcl-2. However, after deleting the region of P65-V89 or the whole loop, there was no Bcl-2 precipitation that could be detected by immunoblotting. Thus, the region of P65-V89 in the Bcl-2 loop part is important for the binding activity between Bcl-2 and FKBP38.

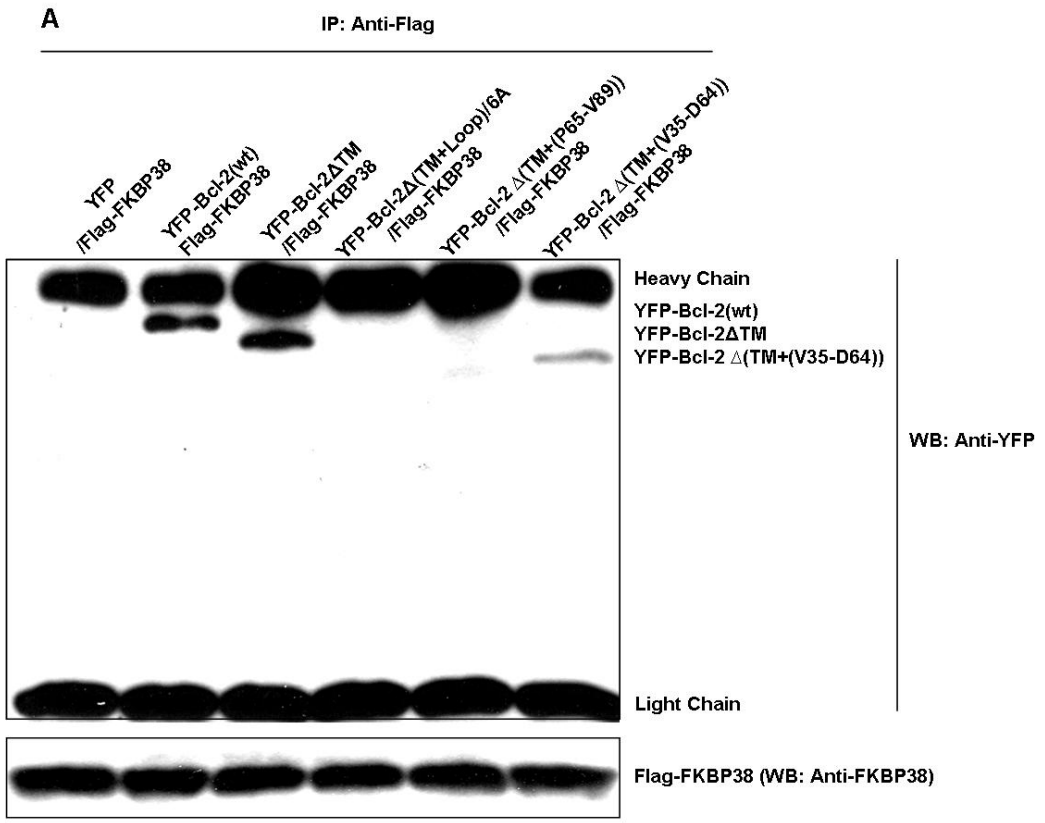

Fig. 4.11 The co-immunoprecipitation between FKBP38 and Bcl-2. HeLa cells were seeded in a six cell plate (2×10^5 cells/well) and co-transfected with the indicated expression vectors (2 μg/well) respectively. Twenty-four hours later, cell lysates were prepared and incubated with anti-Flag antibody (600 μg total proteins: 1 μg antibody) for immunoprecipitation. Immunoprecipitates were subjected to Western blotting using anti-YFP antibody and anti-FKBP38 antibody. Here was a representative of three independent experiments.

4.2 Discussion

4.2.1 Bcl-2 and FKBP38 express vary among different cell lines and localize mainly on the mitochondria

Bcl-2 and/or Bcl-x_L were over-expressed in many cancer cells. Through their anti-apoptotic functions, they are associated with oncogenesis and chemotherapeutic resistance (Reed JC, 1995; Reed JC, 1997). Yet, not all of the cancer cells have the same high expressions of these antiapoptotic proteins. Actually, the expression levels of Bcl-2 and Bcl-x_L varied significantly among different cancer cell lines (Fig. 4.1B). The differences in their expression levels may be attributed to their roles in particular cells (Gottschalk AR et al., 1994). The Bcl-2-binding protein FKBP38 is expressed widely in various tissues, especially highly in the brain (Lam E et al., 1995), suggesting that FKBP38 may be extensively involved in various cellular physiological processes. Although the gene encoding FKBP38 is evolutionarily highly conserved, different open reading frames exist among tissues and species, which cause the differences in the translated products (Jakob V et al., 2003) (Fig 4.1B). And the different phenotype of FKBP38 may be related to its different roles in tissues.

All proteins encoded by nuclear genes are synthesized by 80S ribosomes in the cytoplasm, and the predetermined information contained within the polypeptide sequence guide the proteins to their final destinations. The simplest topogenic signals are single NH2-terminal or COOH-terminal transmembrane (TM) anchor segments. Bcl-2 distribution or localization was also regulated by the 'topogenic' signals. As an anti-apoptotic protein, Bcl-2 was first found in mitochondria (Hockenbery D et al., 1990). Through the protection of the integrity of the mitochondrial outer membrane and the inhibition of the release of apoptogenic factors from mitochondria to cytosol, Bcl-2

performs its anti-apoptotic function (Susin SA et al., 1996; Shimizu S et al., 1998). Recently, another cell-death pathway, the endoplasmic reticulum (ER) stress-mediated apoptotic pathway was revealed. ER-localizing Bcl-2 was found to inhibit Ca^{2+} flux from ER to cytosol (Lam M et al., 1994); ER-localizing Bcl-2 was shown to prevent the release of cytochrome *c* from mitochondria after cells treated with an ER-dilation drug.

However, this distribution of Bcl-2 between mitochondria and ER is tightly regulated (Wang HQ et al., 2005). Different localizations of Bcl-2 can provide a crosstalk between the mitochondria- and ER-dependent apoptotic pathways (Lam M et al., 1994; Hacki J et al., 2000).

FKBP38 was recently found to play a role in anti-apoptosis through anchoring Bcl-2 to the mitochondria, and the removal of FKBP38 resulted in the misdistribution of Bcl-2 inside the cells (Shirane M et al., 2003). Presenilin 1/2 was an ER-localizing integral membrane protein, which was found to reduce the distribution of Bcl-2 on mitochondria and induce apoptosis (Wang HQ et al., 2005). Further study showed that presenilin 1/2 can compete with FKBP38 to regulate Bcl-2's distribution between mitochondria and ER. Presenilin 1/2 promoted the degradation of FKBP38 and Bcl-2 and sequestered these proteins in the ER compartments, thereby inhibiting FKBP38-mediated mitochondrial localization of Bcl-2 and inducing apoptosis. In addition, it was found the exogenous Bcl-2 when distributing inside nucleus (after transient transfection) induced apoptosis, on the other hand, stably expressed exogenous Bcl-2 found in a non-nuclear subcellular localization protected apoptotic cell death induced by staurosporine (Portier BP et al., 2006). Thus, the subcellular localization of Bcl-2 is strictly regulated by various proteins to control its biological functions.

4.2.2 The P65-V89 in the Bcl-2 loop region is in charge of the binding activity with FKBP38

The binding activity between Bcl-2 and FKBP38 was thereby further studied. There is a long flexible loop in Bcl-2 with several potential phosphorylations sites. The loop has been found to be in charge of the interactions between Bcl-2 and various proteins (Lin B et al., 2004; Kang CB et al., 2005; Deng X et al., 2006). The phosphorylation status on different sites of the loop may affect Bcl-2 functions (Haldar S et al., 1998; Deng X et al., 2006). According to our data in this study, the deletion of the loop part from P65 to V89 made Bcl-2 significantly unstable and degraded; yet, deleting the loop part from V35 to D64 didn't affect Bcl-2 stability. Bcl-2 may have undergone some conformational changes after the removal of some critical amino acids in the loop region. And these conformational changes could affect the binding between Bcl-2 peptides with the antibodies. However, since the antibody used in the study was against YFP peptide, not against Bcl-2 peptide, it could be excluded that the difference on the band detection is due to the conformational changes of Bcl-2. Therefore, we concluded that the loop region from V35 to D64 played a role in weakening the stability of Bcl-2 and accelerated its degradation. On the other hand, the loop part from P65-V89 was responsible for the positive regulation of Bcl-2 stability. This difference may be caused by differential phosphorylation sites involved.

The interaction between Bcl-2 and FKBP38 was studied by FRET and co-immunoprecipitaiton. The combination of FRET and co-immunoprecipitation provides a better picture for studying protein-protein interactions in cells. If the interaction between

two proteins is not strong enough, it may not be precipitated by immunoprecipitation. Yet, this interaction still can be detected by FRET as long as the distance between the fluorophores conjugated with the two proteins is less than 80 Å inside cells (Wu P et al., 1994). The different mechanisms of these two experimental methods may be used to explain the different observation of Bcl-2-FKBP38 interaction by FRET and co-immunoprecipitation. After removing the region of P65-V89 and the whole loop, Bcl-2 and FKBP38 still maintain the interactions which could be detected by FRET but the interaction is too weak to precipitate Bcl-2 during the experimental process.

According to our results, the removal of the transmembrane domain of Bcl-2 did not influence its interaction with FKBP38. However, different regions in Bcl-2 loop played different roles in determining its binding with FKBP38. This difference may be attributed to the phosphorylation sites involved. And FKBP38 showed stronger binding ability with the region of P65-V89 in Bcl-2 loop, which contains the phosphorylation sites of T69, S70, T74 and S87. In addition, when replacing the whole loop region with six alanines did not completely abolish the binding activity between Bcl-2 and FKBP38 as observed in FRET, although this binding activity was not strong enough to be detected by the immunoprecipitation. Thus, the loop part may not be the only region in Bcl-2 responsible to the binding activity with FKBP38.

Taken together, we concluded that the region of P65-V89 in the Bcl-2 loop part plays a major role in determining the binding specificity between Bcl-2 and FKBP38.

4.3 Conclusion

The localization of Bcl-2 on mitochondria is essential for its anti-apoptotic function. This localization is regulated by FKBP38. In this current study, we studied the role of the loop part of Bcl-2 in the molecular interaction with FKBP38. Our data demonstrats that the flexible loop between BH4 and BH3 region of Bcl-2 is critical in binding to FKBP38. Especially the region of P65-V89 appears to play a key role in determining their molecular interaction. However, the regulation of the interaction between different regions of the Bcl-2 loop with FKBP38 in response to different stimuli still need to be further studied.

Chapter 5 Regulatory roles of Bcl-2 and FKBP38 on apoptosis and cell cycle

As anti-apoptotic proteins, Bcl-2 and Bcl-x_L exert their anti-apoptotic functions by preventing the mitochondrial outer membrane permeabilization (Hockenbery D et al., 1990). The chaperon protein FKBP38 was recently found to have anti-apoptotic function through the interaction of Bcl-2 and Bcl-x_L. Without FKBP38, Bcl-2 and Bcl-x_L were shown to lose their mitochondrial localization and misdistributed in the cytoplasm (Shirane M et al., 2003). Further experiments showed that the long flexible loop of Bcl-2 played an essential role in determining the binding activity with FKBP38 (Kang CB et al., 2005).

Cell cycle is a highly orchestrated physiological phenomenon. Different cyclins are produced at different cell-cycle phases, resulting in the periodic formation of distinct cyclin-CDK (cylcin-dependent kinase) complexes that trigger different cell-cycle events. Multiple mechanisms contribute to the control of cyclin levels and CDK activities, leading to a complex cyclin-CDK regulatory network. Any abnormality in cell cycle can result in dysregulation in cell proliferation and apoptosis (Rubin LL et al., 1993; Collins K et al., 1997). So far, various experimental results have proved that there are cross-talks existing between apoptosis and cell cycle (Rubin LL et al., 1993; Linette GP et al., 1996).

Previously, it has been shown that the anti-apoptotic proteins Bcl-2 and Bcl-x_L could delay G_0/G_1 or G_1/S transitions by increasing the levels of the regulatory proteins including cyclin-dependent kinase inhibitor p27 or regulating the activation of CDK2 (Linette GP et al., 1996; Greider C et al., 2002; Vairo G et al., 2000;

Janumyan YM et al., 2003; Gil-Gomez G et al., 1998), suggesting the Bcl-2 family proteins were also involved in the regulation of cell cycle. In addition, chaperone proteins were also observed to be involved in regulating cell-cycle proteins. For example, in yeast, it has been demonstrated that a molecular chaperone Ydj1 is essential for the phosphorylation and degradation of a G_1-phase cyclin Cln3 (Yaglom JA et al., 1996); Another chaperone protein heat-shock protein 90 (Hsp90) was shown to have the capacity to interact and stabilize cyclin-dependent kinase 11 (CDK11) (Mikolajczyk M et al., 2004). Given the chaperone features of FKBP38 and its anti-apoptotic function through the interaction with Bcl-2, we hypothesize that FKBP38 may also function as a regulator on cell cycle.

In this study, we further explored the interaction between Bcl-2 and FKBP38, and their regulatory activities in both cell death and cell cycle. The expressions of Bcl-2 and FKBP38 were checked by Western blotting. Apoptosis and cell cycle were analyzed with flow cytometry. The ROS level and the mitochondrial membrane potential were also investigated with flow cytometry.

5.1 Results

5.1.1 Bcl-2 degradation caused by FKBP38 suppression

FKBP38 acts as an anti-apoptotic protein by interacting with Bcl-2, and co-localizing at mitochondria. Without FKBP38, Bcl-2 was found misdistributed inside cells. Here, to understand the role of FKBP38, we first treated cells with FKBP-specific siRNA (30 nM) and then kinetically monitored the expression of the endogenous Bcl-2, the expression of the pro-apoptotic protein Bax, and the cleavage

of PARP (Fig. 5.1B). FKBP38 decreased significantly 24 hours after transfection. Bcl-2 was observed degraded about 48 hours after FKBP38 siRNA treatment, which is about 24 hours later than the level of FKBP38 decrease. Correspondingly, the increase of the pro-apoptotic protein Bax and the cleavage of PARP, which is substrate of the active caspase-3, were observed.

Meanwhile, the parallel changes of FKBP38, Bcl-2, Bax and PARP by silencing Bcl-2 with siRNA were also checked (Fig. 5.1A). The expected increase of the pro-apoptotic and the cleavage of PARP were observed. Yet, there was no influence on the expression of FKBP38 by silencing Bcl-2.

The FKBP38-siRNA-induced Bcl-2 degradation was inhibited by the caspase inhibitor and the lysosomal inhibitor, but little inhibited by the ubiquitin-proteasome inhibitor (Fig. 5.1C).

Our immunofluorescence data showed that after the suppression of Bcl-2, FKBP38 still localized on the mitochondria with no obvious changes in its expression level (Fig. 5.1D and E). However, the knocking-down of FKBP38 resulted in a dramatic decrease in the endogenous expression of Bcl-2, consistent with immunoblotting results.

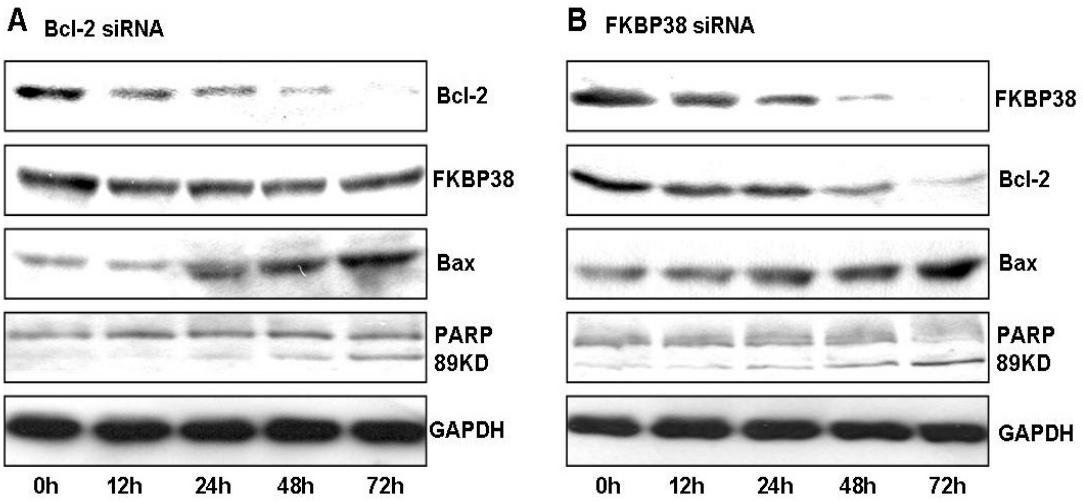

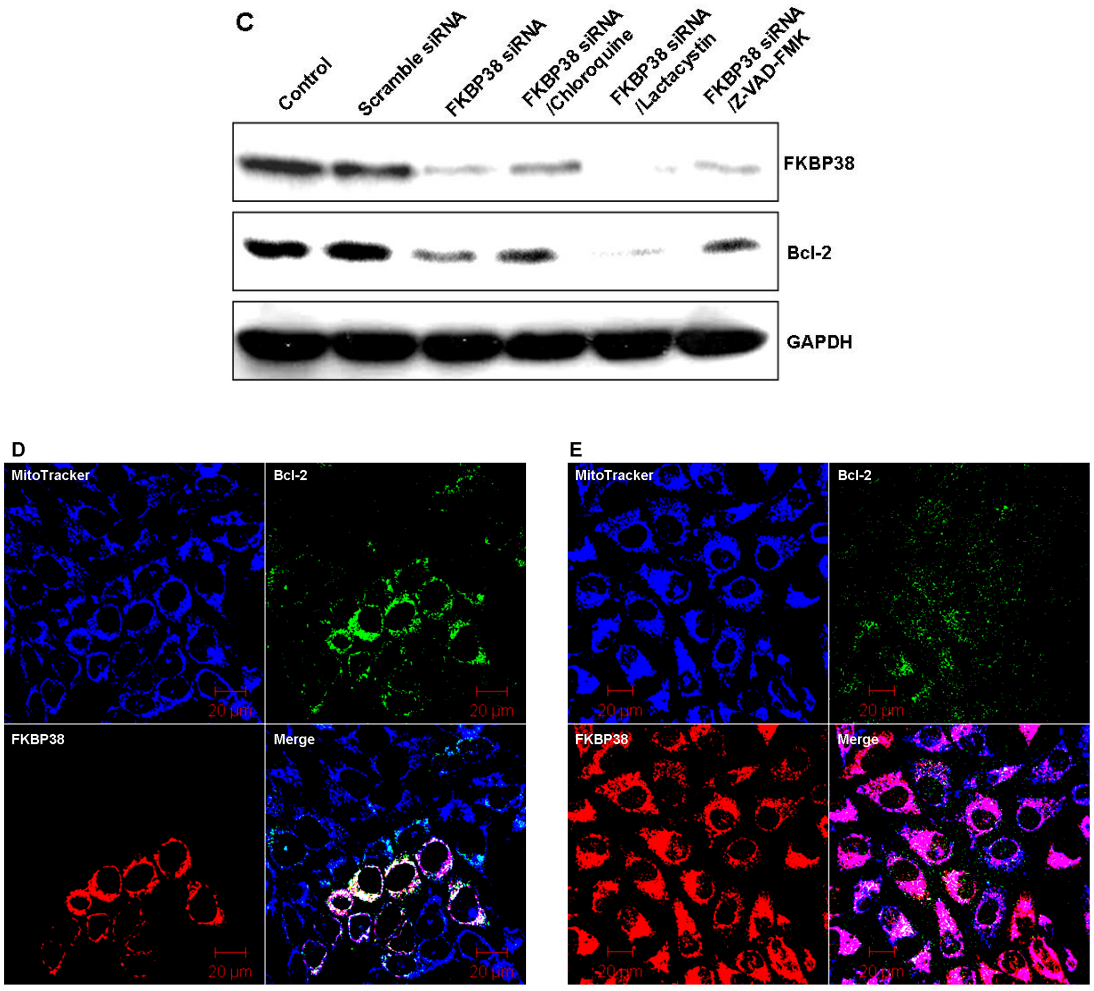

Fig. 5.1 The suppression of Bcl-2 or FKBP38 by RNA interference in HeLa cells. Cells were seeded in a six-well plate (2×10^5 cells/well), and were treated with 30 nM Bcl-2 siRNA (**A**) or FKBP38 siRNA (**B**). Cell lysates were collected at 0h, 12h, 24h, 48h and 72h after transfection. After measuring the concentration, 100 μg of the total proteins were separated by 12 % SDS PAGE and transferred to the membrane. The expressions of FKBP38, Bcl-2, Bax and PARP were checked by Western blotting. **C**. The inhibition on the Bcl-2 degradation. Cells were seeded in a six-well plate (2×10^5 cells/well), and treated with 30 nM Scramble siRNA and FKBP38 siRNA only, or together with the lysosomal inhibitor chloroquine (20 μM), the ubiquitin-proteasome inhibitor lactacystin (1 μM) and caspase inhibitor Z-VAD-FMK (20 μM), respectively, for 72 hours. The expressions of FKBP38 and Bcl-2 were checked by Western blotting. GAPDH was used as an internal control. Experiments were repeated three times. (**D**) and (**E**) The *in situ* expressions of FKBP38 and Bcl-2 after treated with FKBP38 siRNA and Bcl-2 siRNA. Cells were seeded in a six-well plate with a cover slip inside and treated with 30 nM FKBP38 siRNA (**D**) or Bcl-2 siRNA (**E**) for 72 hours. Cells were stained with 100 nM

MitoTracker and fixed with 3.7% paraformaldehyde at 37°C for 15 min. After permeabilized with 0.5% Triton, cells were first incubated with anti-FKBP38 primary antibody (from Rabbit, 1:500) at 4°C overnight, and detected with FITC-labeled secondary antibody (Goat anti-rabbit, 1:500). Then cells were incubated with anti-Bcl-2 primary antibody (from Mouse, 1:500) at 4°C overnight, and detected with Cy5-labeled secondary antibody (Goat anti-mouse, 1:500). Slides were observed under a confocal microscope with the exciting wave length 633 nm for MitoTracker, 488 nm for FITC and 543 nm for Cy5.

5.1.2 Apoptosis induced by RNA interference of Bcl-2 and FKBP38

In order to study the cell death caused by the suppression of Bcl-2 and FKBP38, cell death was analyzed by flow cytometry after treating cells with the equal amount (30 nM) of Bcl-2 siRNA or FKBP38 siRNA.

First, cell viabilities were assessed by MTT assay (Fig. 5.2A). At the early time period (within 48 hours), the treatment with Bcl-2 siRNA led to a more decrease on cell viability than that of FKBP38 siRNA. At 72 hours, the down-regulation of FKBP38 siRNA caused cell viability to decrease to about 30%, much significant than what caused by Bcl-2 siRNA (Fig. 5.2A).

The quantitative apoptotic analysis showed that by 48 hours 18% of cells underwent apoptosis (stained with annexin-V-fluorescein only), while Bcl-2 siRNA resulted in apoptosis with 8% of cell population. By 72 hours, the population of the apoptotic cells induced by FKBP38 siRNA increased to about 32%, accompanied by 10% of later apoptotic cells or necrotic cells, which were stained both with annexin-V-flourescein and PI. However, the population of apoptotic cells induced by Bcl-2-specific siRNA was 18% with about 3% of necrotic cells. Thus, the silencing of FKBP38 by siRNA generated stronger cytotoxic effects than the silencing of Bcl-2 by siRNA.

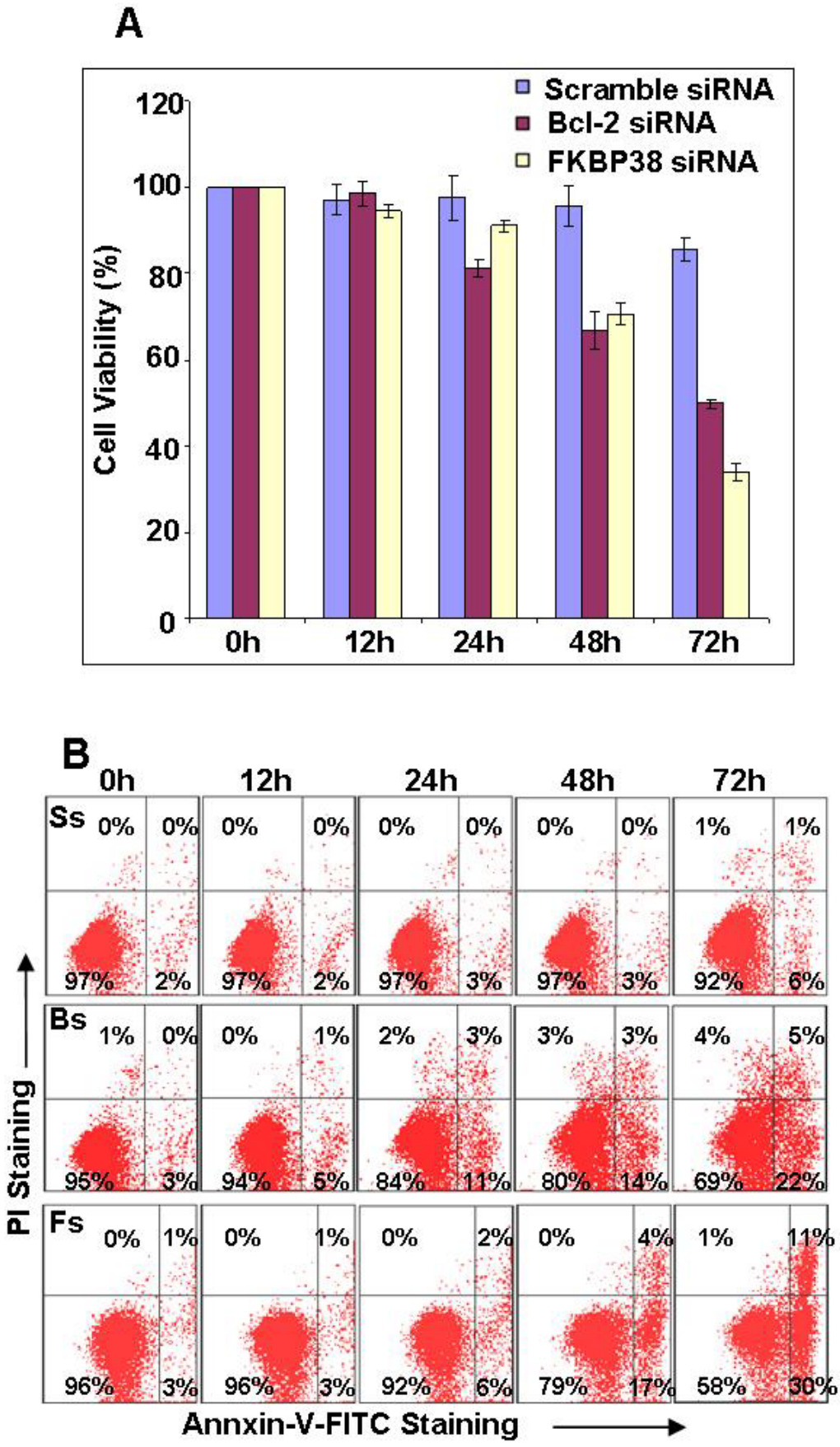

Fig. 5.2 A. Cell proliferation assay by using MTT after siRNA treatment. HeLa cells were seeded in a 96-well plate (5×10^3 cells/well) and treated with scramble siRNA (Ss), Bcl-2 siRNA (Bs) and FKBP38 siRNA (Fs) as the indicated time periods, respectively. The cell proliferations of 0h, 12h, 24h, 48h and 72h were analyzed using MTT assay as described in Chapter 2. Values represent means ± S.D. of three independent experiments. **B.** Apoptotic analysis by flow cytometry after staining with annexin-V-fluorescein/PI in Hela cells. Cells were seeded in a six-well plate (2×10^5 cells/well) and treated with scramble siRNA, Bcl-2 siRNA and FKBP38 siRNA as the indicated time periods, respectively. After staining with annexin-V-fluorescein/PI, apoptosis was analyzed by flow cytometry as described in Chapter 2. Data were analyzed using CELLQuest software. Here is a representative of three independent experiments.

5.1.3 Regulation of cell size and cellular granularity by Bcl-2 and FKBP38

Bcl-2 controls cell size. Overexpression of Bcl-2 retards cell cycle in G_0/G_1 phase and results in a smaller cell size. FKBP38 was also reported to be involved in Tuberous Sclerosis Complex (TSC) gene-dependent cell size regulation [15]. After cells treated with Bcl-2 or FKBP38-specific siRNA, HeLa cells showed morphological changes (Fig. 5.3). As fibroblastic cells, HeLa cells changed from elongated spindle shapes to rounded and flattened shapes, and become larger in the size. By 72 hours, many cells died, which were characterized as shrinking and bubbles protruding from the membrane.

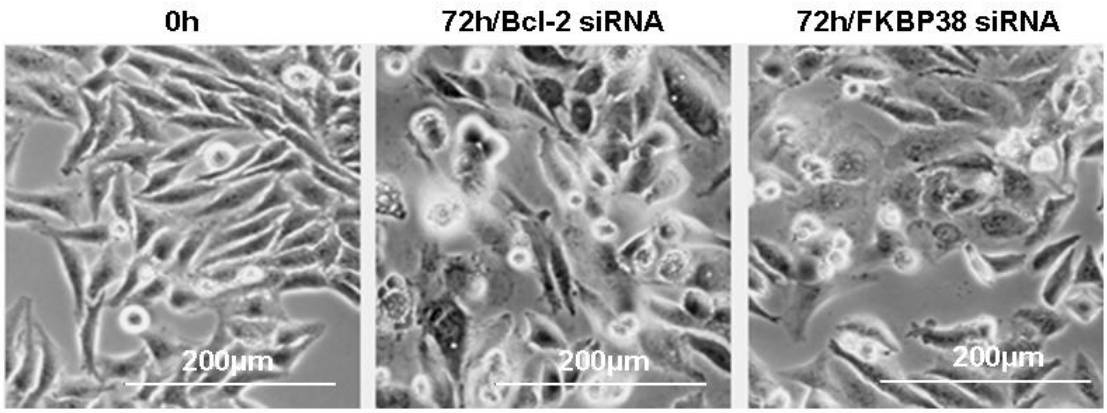

Fig. 5.3 HeLa cell morphological changes after treated with Bcl-2 siRNA or FKBP38 siRNA. Cells were seeded in a six-well plate (2×10^5 cells/well) and treated with 30 nM of Bcl-2 siRNA and FKBP38 siRNA, respectively. The morphological changes were observed under phase-contrast microscope. By 72 hours, many cells underwent apoptosis and cell images were captured.

In addition, the cell size and cellular granularity/complexity of annexin-V-flourescein/PI-gated cells were quantitatively investigated via forward scatter (FSC) and side scatter (SSC) of flow cytometry, respectively (Fig. 5.4). Both mean FSC histograms and mean SSC histograms showed rightward shifts after cells were treated with either Bcl-2 or FKBP38 siRNA. Thus, the suppression of either Bcl-2 or FKBP38 promoted the increase of cell size and cellular granularity before apoptosis happening. The quantitative analysis of the means of histograms indicated that silencing of Bcl-2 induced about 50% increase in the cellular granularity by 72 hours, which is slightly more than what caused by the silencing of FKBP38 (about 40% increase by 72 hours). However, silencing FKBP38 resulted in much significant increase on cell size (about 20% of increase by 72 hours) than what caused by silencing Bcl-2 (about 15% of increase by 72 hours).

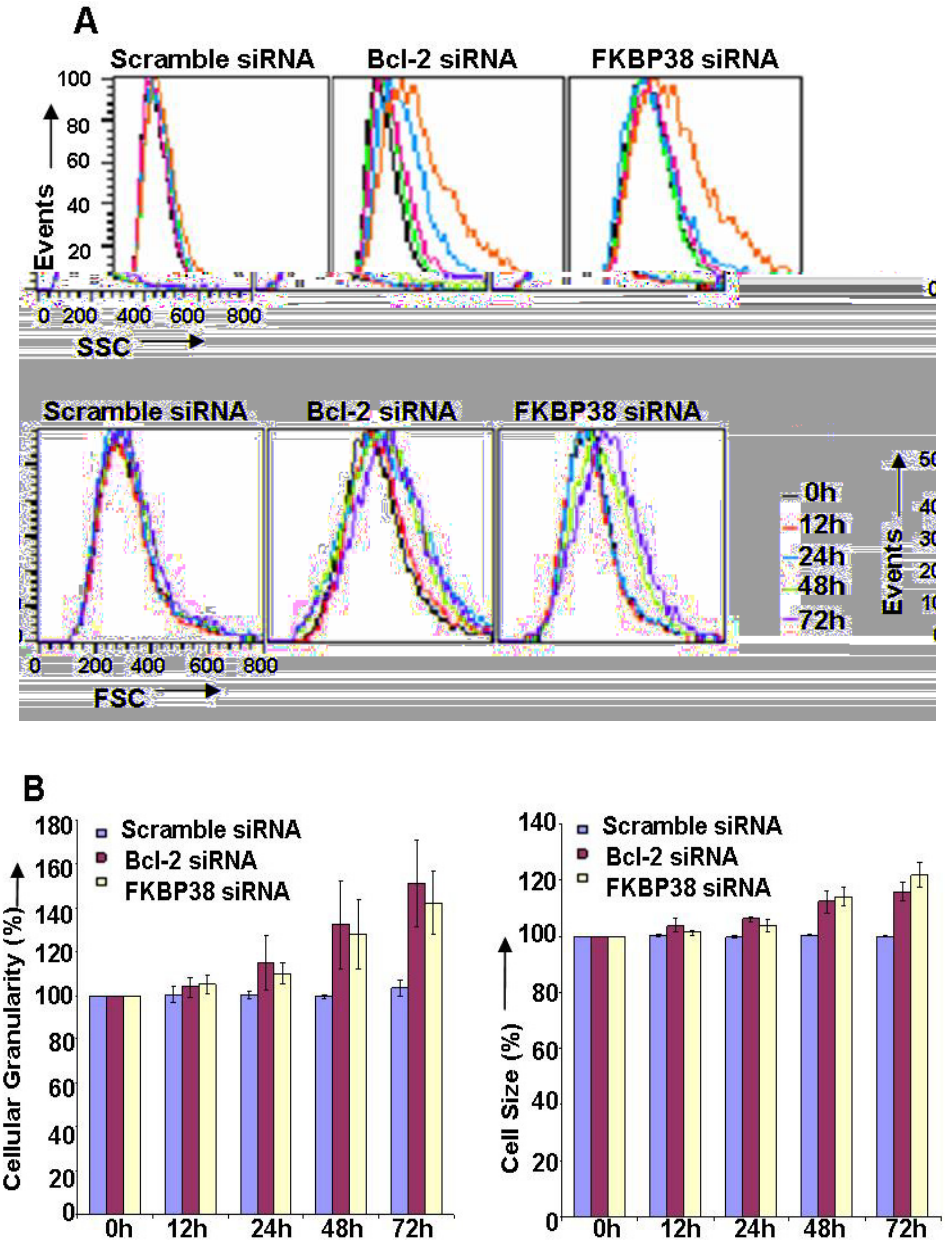

Fig. 5.4 Cell size and cellular granularity analyses after siRNA treatments. HeLa cells were seeded in a six-well plate (2×10^5 cells/well) and treated with 30 nM scramble siRNA, Bcl-2 siRNA, FKBP38 siRNA at the indicated time periods, respectively. **A.** The cell size and cellular granularity of the annexin-V-fluorescein/PI-gated cells were investigated via FSC and SSC, respectively. Data were analyzed using CELLQuest software. Here was a representative of three independent experiments. **B.** Quantitative analysis of the mean of SSC and FSC of the three independent experiments performed as described in (A).

5.1.4 Regulation of cell cycle progression by Bcl-2 and FKBP38

To further explore the mechanisms under these physiological changes in cell size and cellular granularity, cell cycle progressions were kinetically analyzed by flow cytometry after staining with propidium iodide (PI).

As seen in Fig. 5.5, the majority (about 65%) of the asynchronously growing cells containing 2N DNA was in the G_1-phase. After cells were treated with Bcl-2 or FKBP38 siRNA, the sharp narrow peak representing G_1-phase cells became thick and broad; much significantly in cells treated with Bcl-2 siRNA (indicated as arrow 1). The quantitative analysis showed that after treated with Bcl-2 siRNA for 72 hours, the population of G_1-phase cells decreased to about 9%. Yet, there were about 20% of G_1-phase cells decreasing 72 hours after treated with FKBP38 siRNA. This result means that the removal of Bcl-2 can not completely initiate the G_1-S transition to the same degree as what caused by FKBP38 siRNA.

Interestingly, a new peak (indicated as arrow 2') representing S-phase cells appeared at 72 hours after the treatment with FKBP38 siRNA. Although this distinct peak was not observed in those cells treated with Bcl-2 siRNA, it could be seen that the angle between the G_1 and S phase turned from sharp to obtuse. Thus, Cells could not completely move from G_1 into S phase after treated with Bcl-2 siRNA. In another words, the G_1-S transition was not complete. The quantitative analysis indicated about 15% increase in S-phase cells after treated with FKBP38 siRNA and about 10% increase after treated with Bcl-2 siRNA.

After treating with Bcl-2 siRNA, the peak (indicated as arrow 3) representing the cells in G_2/M-phase decreased. Together with the delay of G_1-S transition, it is easy to understand that the G_2/M-phase cells decreased, thus, the suppression of Bcl-2 could not completely initiate cell cycle progression. Yet, this peak could still be

detected after treated with FKBP38 siRNA as a round-turning shape (indicated as arrow 3').

The pre-G_1-phase cells, which represented the population of dead cells, increased to more than 20% in both siRNA treatments.

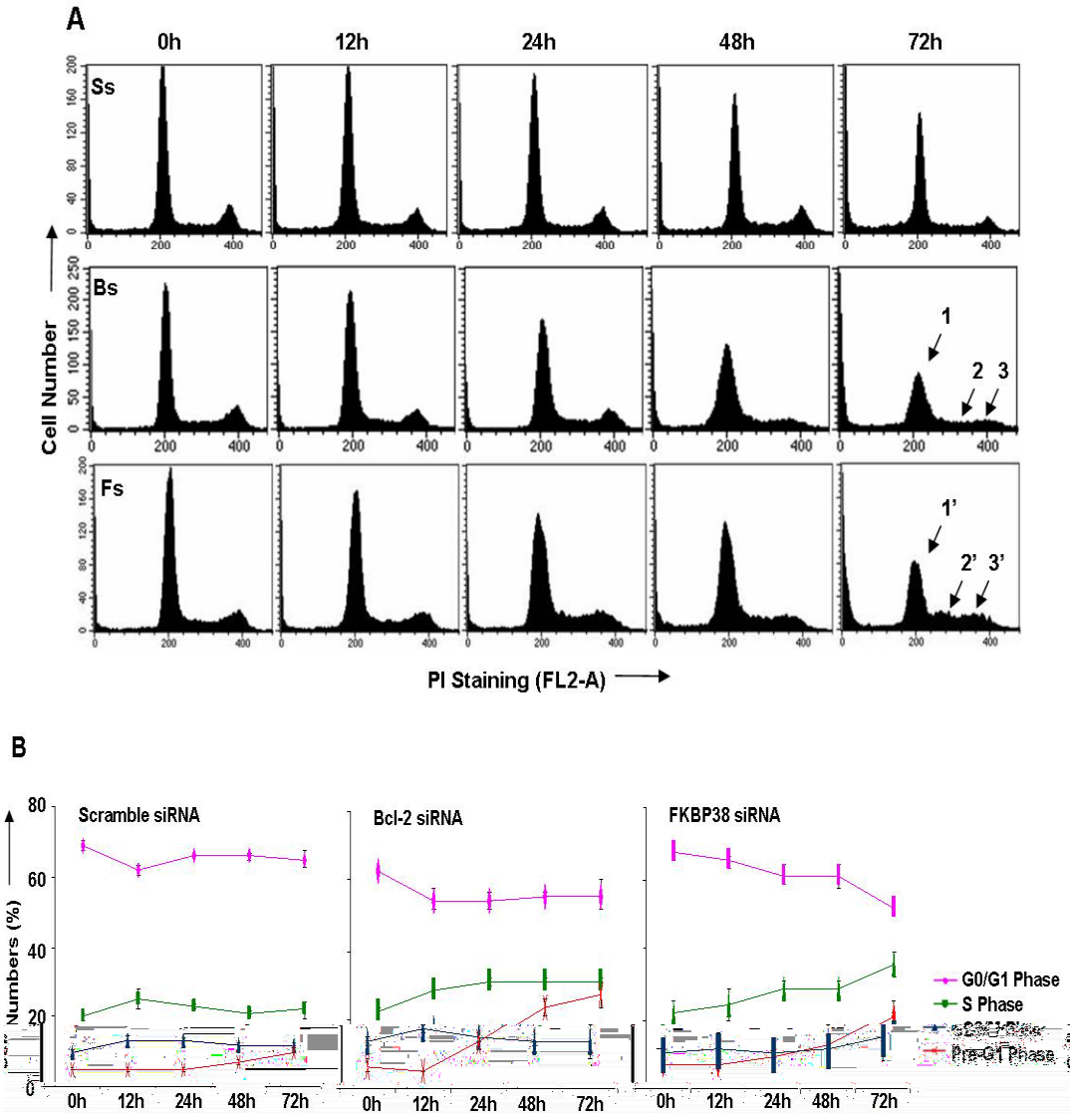

Fig. 5.5 The cell cycle analysis after siRNA treatment. HeLa cells were seeded in a six-well plate (2×10^5 cells/well) and treated with 30nM scramble siRNA (Ss), Bcl-2 siRNA (Bs), FKBP38 siRNA (Fs) at the indicated time periods. Cells were stained with propidium iodide (PI), and cell cycles were analyzed by flow cytometry. **A.** A representative histogram of three independent experiments. **B.** Quantitative analysis of the cell population in different cell cycle phases described in (A) with ModFit LT cell cycle analysis software. The peaks representing cells in different phases are indicated as arrows.

Like apoptosis, cell cycle progression is another fundamental and ubiquitous process in multicellular organisms for cell growth and proliferation. Cyclins and cyclin-dependent kinases (CDKs), which regulate cell cycle progression, are well characterized (Hill DA et al., 2004; Ben-Ze'ev A et al., 1980). Cyclins bind and activate CDKs, and target CDKs to specific substrates or subcellular localizations. The expression levels of cyclins varied in cell cycle stages. For example, cyclin Ds (D1, D2 and D3) appeared in early G_1-phase, cyclin E in late G_1- and early S-phase, cyclin A in S- and G_2-phase, and cyclin B1 in G_2/M-phase (Fig. 1.3).

In order to provide more evidence for the changes of cell cycle progression, and confirm the observation of cell cycle analysis by flow cytometry, those cell cycle-related biomarkers were further checked by Western blotting analysis (Fig. 5.6).

The results showed that either the suppression of Bcl-2 or the suppression of FKBP38 caused the decrease in cyclin D1 (the specific indicator of the early G_1-phase). Although the increase of cyclin E (the specific indicator of the late G_1- and early S-phase) was observed in both cases, the cyclin A (the specific indicator of the S- and G_2/M-phase) and cyclin B1 (the specific indicator of the G_2/M-phase) decreased after treating cells with the Bcl-2 siRNA. However, the treatment with FKBP38 siRNA resulted in the increases in expression levels of both cyclin A and B1. The cyclin-dependent kinase 2 (CDK2) was observed activated by the treatment with FKBP38 siRNA; But there was no significant activation of CDK2 by the treatment with Bcl-2 siRNA. In addition, p27, which is a cyclin-dependent kinase inhibitor, decreased in both two experimental conditions.

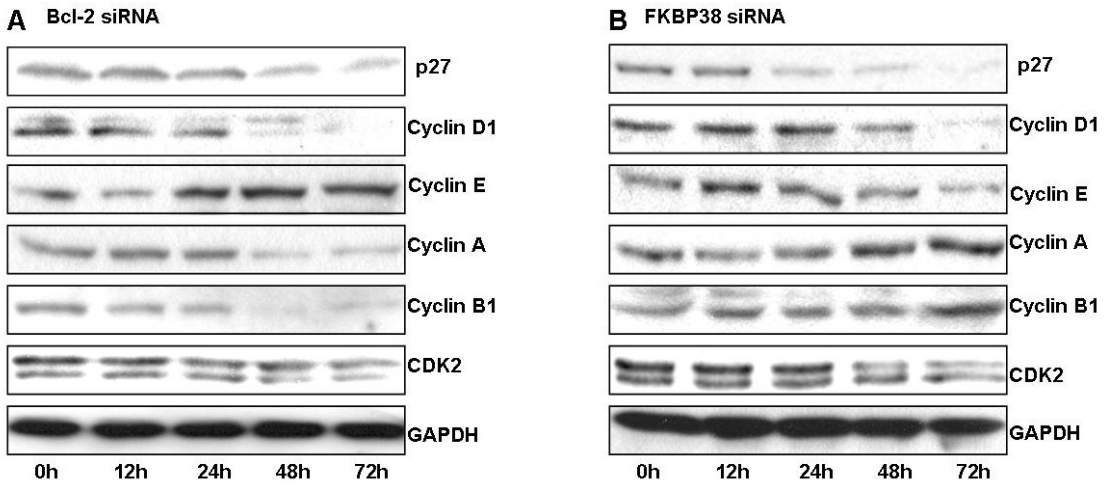

Fig. 5.6 The expression of the cell cycle progression regulators after siRNA treatment. HeLa cells were seeded in a six-well plate (2×10^5 cells/well) and treated with 30 nM Bcl-2 siRNA, FKBP38 siRNA at the indicated time periods, respectively. Cell lysates were prepared. After measuring the concentrations, 100 μg of total proteins were separated by 12% SDS PAGE and transferred to membrane. The expressions of the cyclins, CDK2 and p27 were checked by Western blotting. GAPDH was used an internal control. Here is a representative of three independent experiments.

Combining the cell cycle analysis by flow cytometry with the expressions of specific indicators of cell cycle, it can be concluded that the suppression of Bcl-2 by siRNA induced the cell cycle arrest in the later G_1- or early S-phase. However, FKBP38 siRNA led to the cell cycle arrest in S- and G_2/M-phase.

In order to confirm the regulatory roles of Bcl-2 and FKBP38 in cell cycle, cells were first synchronized with aphidicolin (Aph) before treated with Bcl-2 or FKBP38 siRNA (Fig. 5.7). The results showed that more than 95% of the cells were synchronized in the boundary of G_1/S-phase 24 hours after treated with Aph without affecting the expressions of Bcl-2 and FKBP38.

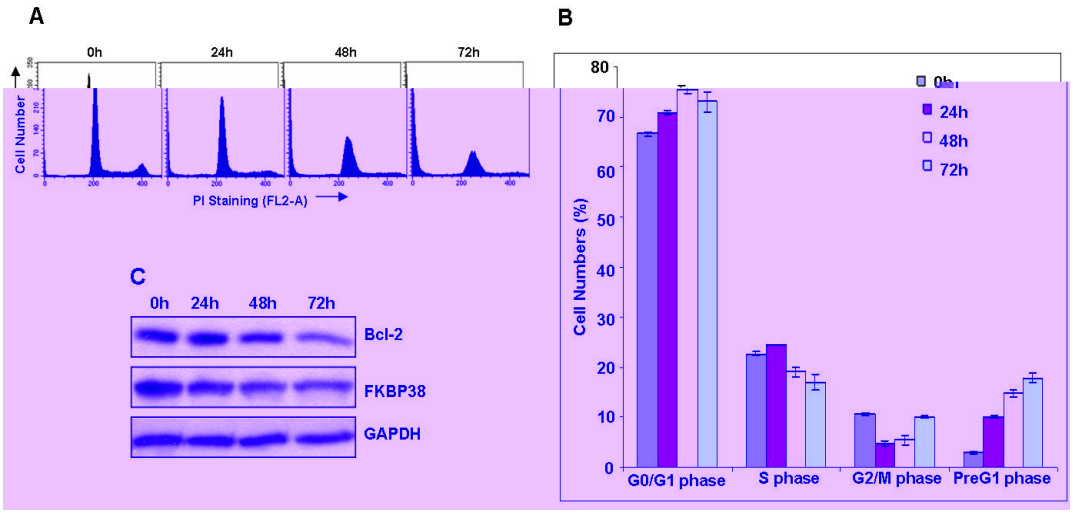

Fig. 5.7 Synchronization of cell cycle. Cells were seeded in a six-well plate as 2×10^5 cells/well and incubated with 5 μg/ml of aphidicolin in DMEM without FBS for 24 hr, 48 hr and 72 hr, respectively. Cell cycle was analyzed by flow cytometry after staining with PI. **A.** A presentative histogram of three independent experiments. **B.** Quantitative analysis of the cell population in different cell cycle phases described in (A) with ModFit LT cell cycle analysis software. C. Expressions of Bcl-2 and FKBP38 were checked by Western blotting. GAPDH was used as an internal control. Experiments were repeated three times.

Aphidicolin (Aph) is a tetracyclic diterpene-tetraol produced by several fungi, and blocks DNA synthesis by interfering with the activity of DNA polymerase α. Aphidicolin prevents G_1-phase cells from entering the DNA synthetic period, blocks cell in S-phase, allows G_2-, M- and G_1-phase to continue the cell cycle and to accumulate at the G_1/S border. According to the above results, the regulations on cell cycle progression by Bcl-2 and FKBP38 were compared after synchronization with aphidicolin (Fig. 5.8).

The results showed that once releasing cell cycle without influencing the expressions of Bcl-2 and FKBP38, the majority of cell population was in G_0/G_1 phase (about 55%), the S-phase cells were about 33% and the G_2/M-phase cells were about 12%. However, when knocking down Bcl-2, G_0/G_1-phase cells decreased to about

39% with the dramatic increase of S-phase cells to about 45% and a slight increase of G2/M-phase cells (about 16%). Although a significant decrease on G_0/G_1-phase cells was also observed by down-regulating FKBP38 (about 36%), different from Bcl-2, down-regulation on FKBP38 caused the synchronized cells mainly arresting in G_2/M phase (about 25%) with a slight increase of S-phase cells (about 38%) (Fig. 5.8B).

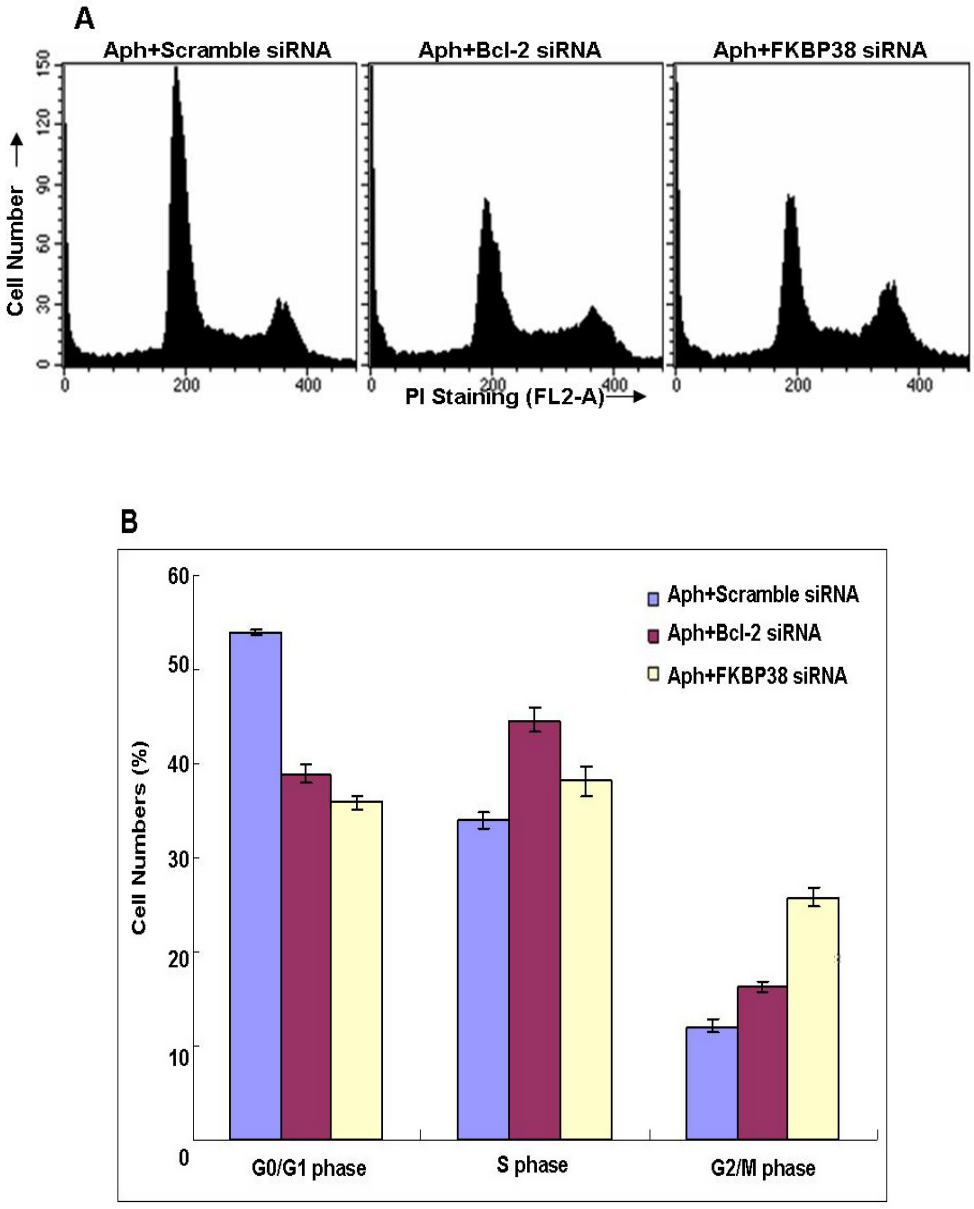

Fig. 5.8 Comparison of the regulatory effects on synchronized cells by FKBP38 and Bcl-2. Cells were seeded in a six-well plate (2×10^5 cells/well) and incubated with 5 μg/ml of aphidicolin in DMEM without FBS for 24 hours. Then, cells were treated with 30 nM FKBP38 siRNA or Bcl-2 siRNA.

Seventy-two hours later, cell cycle was analyzed by flow cytometry after staining with PI. **A.** A presentative histogram of three independent experiments. **B.** Quantitative analysis of the cell population in different cell cycle phases described in (A) with ModFit LT cell cycle analysis software.

Apoptosis and cell cycle are two fundamental cell processes. The balance between apoptosis and cell proliferation is essential for tissue homeostasis (Norbury C et al., 1992). Both apoptotic and mitotic cells lose substrate attachment and become rounded. During both processes, cells were observed shrinking, condensing their chromatin, and displaying membrane blebbing. The similarity of the morphological characteristics between apoptosis and mitosis suggested these two antagonistic processes may involve the same regulators or biochemical changes inside cells (Morgan DO, 1995).

As an anti-apoptotic protein, Bcl-2 was also found in regulating cell cycle process, and the overexpression of Bcl-2 delayed the G_1-S transition with the smaller cell size (Janumyan YM et al., 2003). Although the detail mechanisms are still not very clear, Bcl-2 was found to regulate the activation of CDK2 in thymocyte apoptosis (Gil-Gomez G et al., 1998). Thus, it may act as a link between apoptosis and cell cycle.

According to our results, FKBP38 also had the function in controlling cell cycle progression in HeLa cells. After suppressing FKBP38, cell cycle progression was initiated. Cells rapidly entered into S- and G_2/M-phase. Thus, both FKBP38 and Bcl-2 may act as cell cycle progression inhibitor. And the suppression on either of these two proteins initiates cell cycle progression. However, the down-regulation of Bcl-2 caused cells to be mainly arrested in the later G_1- or the early S-phase without entering G_2/M-phase, while the down-regulation of FKBP38 resulted in cells arrested in S-phase and G_2/M-phase. Consistent with these cell cycle analysis results, the

suppression of FKBP38 induced an increase in cyclin E, A, and B1 and the activation of CDK2; yet, the suppression of Bcl-2 only induced an increase in cyclin E with a decrease in cyclin A and B1 and without the activation of CDK2.

Thus, both Bcl-2 and FKBP38 maintain cells survival in a stable quiescent status. The inhibition of either Bcl-2 or FKBP38 initiated cell cycle progression, and subsequently cells became unstable in proliferating status and committed apoptosis.

In addition, both Bcl-2 and FKBP38 play their anti-apoptotic functions by controlling cell cycle progression. The initiation of cell cycle progression is a highly regulated process. During this process, the genetic information is duplicated and proteins are orderly assembled to form a competent and replicative chromosomal state before mitosis. Although different pathways were involved, the abnormal initiation of cell cycle progression by the treatments of Bcl-2 and FKBP38 siRNA brought various disordered biological activities inside the cells, which accelerated cell death. And these changes of cell cycle progression also give one possible explanation for the changes in cell size and cellular granularity.

5.1.5 Modulation of ROS by Bcl-2 and FKBP38

The abnormal cell cycle progression initiated by the suppression of Bcl-2 and FKBP38 could make various biological activities deregulated and initiate apoptosis. The reactive oxygen species (ROS) are toxic by-products of normal cell growth and metabolism. The intracellular amount of ROS was found to be synchronous with the cell population at specific phases (S and G_2/M). The dramatic increase in cell population in S and G_2/M-phase means high metabolic activities inside cells after suppressing Bcl-2 and FKBP38, which prompted us to check the changes of the intracellular ROS.

The quantitative assessment of the intracellular ROS demonstrated an increase of the intracellular ROS level with the down-regulation of Bcl-2 and FKBP38 (Fig. 5.9). A significant increase in ROS was observed as early as 24 hr following FKBP38 siRNA treatment. At 72 hr, the level of ROS increased to more than 9 folds compared to that of control (0 hr). However, the maximal production of ROS induced by the treatment of Bcl-2 siRNA appeared at 48 hours, which was about 3-fold increase compared to that of control. These data indicate that FKBP38 appears to be a more potent inhibitor of ROS generation than Bcl-2.

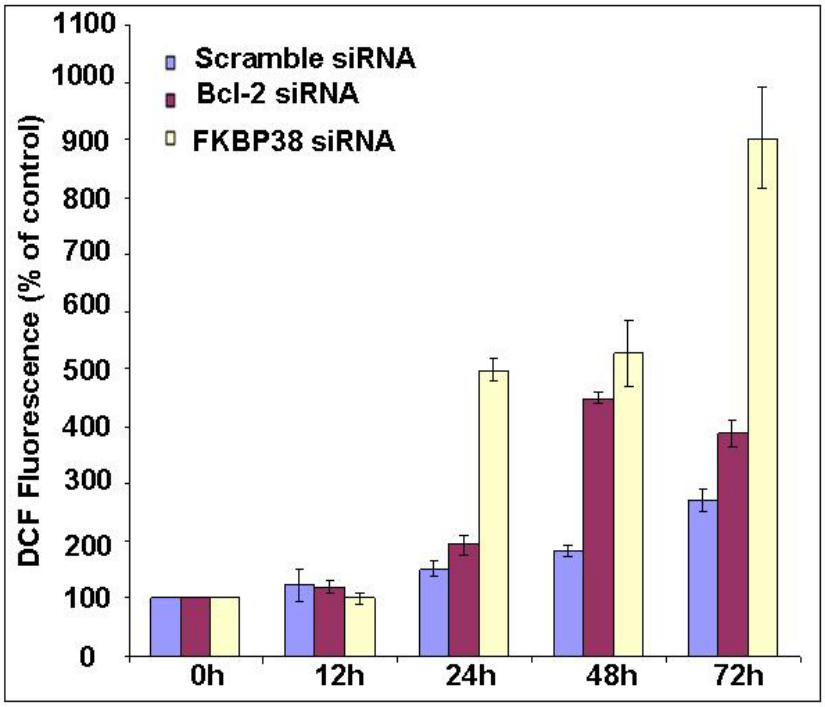

Fig. 5.9 The generation of Reactive Oxygen Species (ROS) by the suppression of Bcl-2 and FKBP38 in HeLa cells. Cells were seeded in a six-well plate (2×10^5 cells/well) and treated with 30 nM scramble siRNA, Bcl-2 siRNA and FKBP38 siRNA at the indicated time periods, respectively. Cells were stained with 10 μM DCHF-DA for 1 hour at 37°C. Then cells were collected by trypsinization and resuspended in 1× PBS. The green fluorescence of DCF was excited by using an argon laser and was detected using FL1 channel of a flow cytometer. The ROS amounts were quantitatively analyzed by the CELLQuest software and expressed as percentages of control (0h).

5.1.6 Influence on the mitochondrial function by Bcl-2 and FKBP38

The mitochondrion is the organelle to provide energy for maintaining cell survival. In addition to their critical role in energy metabolism, mitochondria are major regulators of apoptosis. The mitochondrial membrane potential (MMP) reflects the mitochondrial status. Bcl-2 is a mitochondria-anchoring protein and well known for its anti-apoptotic function through the protection of the integrity of the mitochondrial outer membrane. In order to evaluate and compare the protective effects on the mitochondria by Bcl-2 and Bcl-2-binding protein FKBP38, the MMP was quantitatively assessed by flow cytometry after stained with JC-1 (Fig. 5.10).

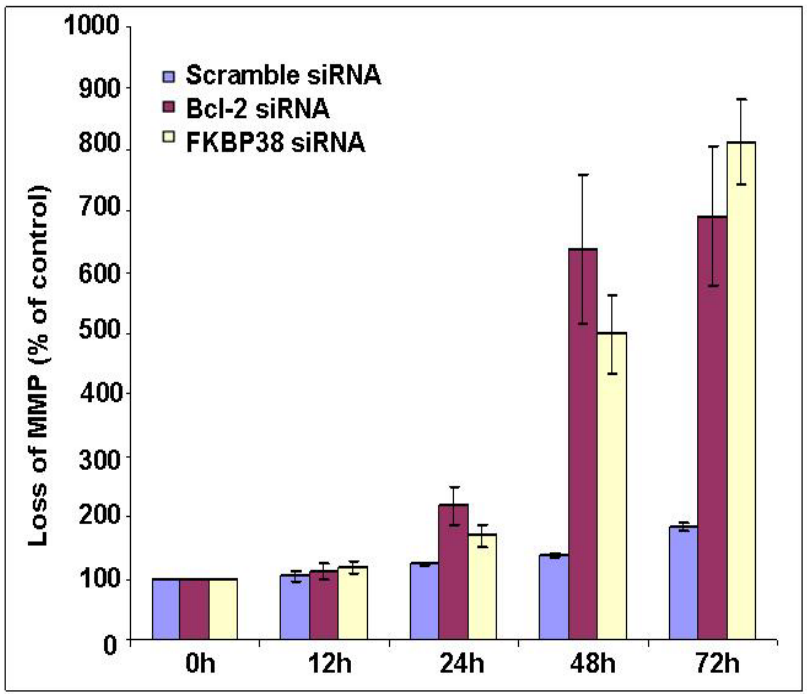

Fig. 5.10 The mitochondrial membrane potential (MMP) analysis after the suppression of Bcl-2 and FKBP38 in HeLa cells. Cells were seeded in a six-well plate (2×10^5 cells/well) and treated with 30 nM scramble siRNA, Bcl-2 siRNA and FKBP38 siRNA at the indicated time periods, respectively. Cells were collected by trypsiniation and stained with 5, 5', 6, 6'- tetrachloro- 1, 1', 3, 3'- tetraethylbenzimidazolylcarbocyanine iodide/chloride (JC-1) for 15 min at 37°C. The MMP was detected with flow cytometry with FL2 channel for the gated cells containing red JC-1 aggregates. The

loss of the MMP was quantitatively analyzed by the CELLQuest software and expressed as percentages of control (0h).

The result showed that the loss of MMP was observed at 24 hr after cells were treated with either Bcl-2 siRNA or FKBP38 siRNA. By 48 hr, the loss of MMP was more than 6 times by the suppression of Bcl-2 compared to the control, and less than 5 times by the suppression on FKBP38. However, at 72 hours, the treatment with FKBP38 siRNA induced the loss of MMP quickly reaching more than 8 times compared to that of control. Thus, the suppression of Bcl-2 caused a rapider damage on the mitochondrial function than what caused by the suppression of FKBP38. And this means that Bcl-2 plays a direct role on protecting the mitochondrial function. The suppression of FKBP38, however, finally resulted in severer damage on the mitochondrial activity.

5.1.7 Role of Antioxidants on ROS

There were lots of ROS generated by either Bcl-2 suppression or FKBP38 suppression as reported in the part 5.5. In order to determine the relationship between ROS and apoptosis and to better understand the protective function on the mitochondria by Bcl-2 and FKBP38, the antioxidant Tiron was used together with the RNA interference of Bcl-2 and FKBP38. Cells were treated with scramble, Bcl-2 or FKBP38 siRNA molecules together with Tiron for 72 hours. ROS were analyzed by flow cytometry after incubating with DCHF-DA (Fig. 5.11). A significant leftward shifts in the histogram peaks indicated that the generation of ROS induced by either Bcl-2 or FKBP38 suppression could be inhibited by Tiron.

Next, the role of ROS in the apoptosis induced by RNA interference of Bcl-2 and FKBP38 was explored by flow cytometry after the combination of Tiron with Bcl-2 and FKBP38 siRNA, respectively (Fig. 5.12). Although Tiron could inhibit the ROS generated from the RNA interference of Both Bcl-2 and FKBP38, Tiron could only protect apoptotic cell death induced by FKBP38 siRNA. The quantitative analysis after staining with annexin-V-fluorescein showed that the apoptotic cells caused by the FKBP38 siRNA was considerably reduced to more than 10% (from 28% to 16%) by the co-treatment of Tiron (6mM). On the other hand, Tiron failed to inhibit apoptosis induced by Bcl-2 siRNA, instead, enhanced annexin-V-fluorescein-labeling apoptotic cells to about 20% (from 19% to 38%). Meanwhile, some dead cells were observed when Tiron was combined with the scramble siRNA, which may be caused by the non-specific cytotoxic effect from Tiron.

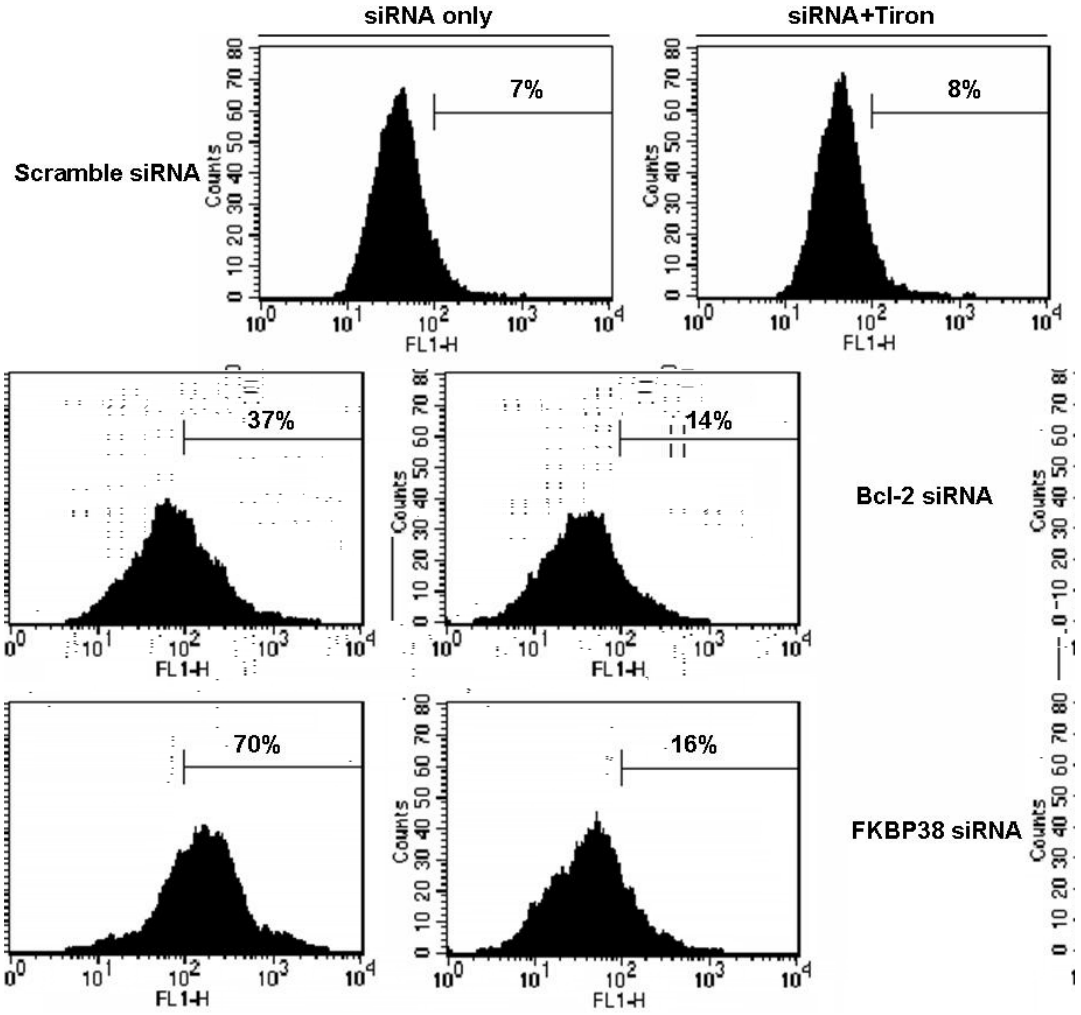

Fig 5.11 The inhibition of the generation of ROS by the antioxidant. HeLa cells were seeded in a six-well plate (2×10^5 cells/well) and treated with 30nM scramble siRNA, Bcl-2 siRNA and FKBP38 siRNA, respectively, together with 6mM of the antioxidant Tiron for 72 hours. Then cells were stained with 10 μM of DCHF-DA for 1 hour at 37°C and were collected by trypsinization, and resuspended in 1× PBS. The green fluorescence of DCF was excited by using an argon laser and was detected using FL1 channel of a flow cytometer. Data were analyzed with CELLQuest software. A representative histogram plot of three independent experiments was shown here.

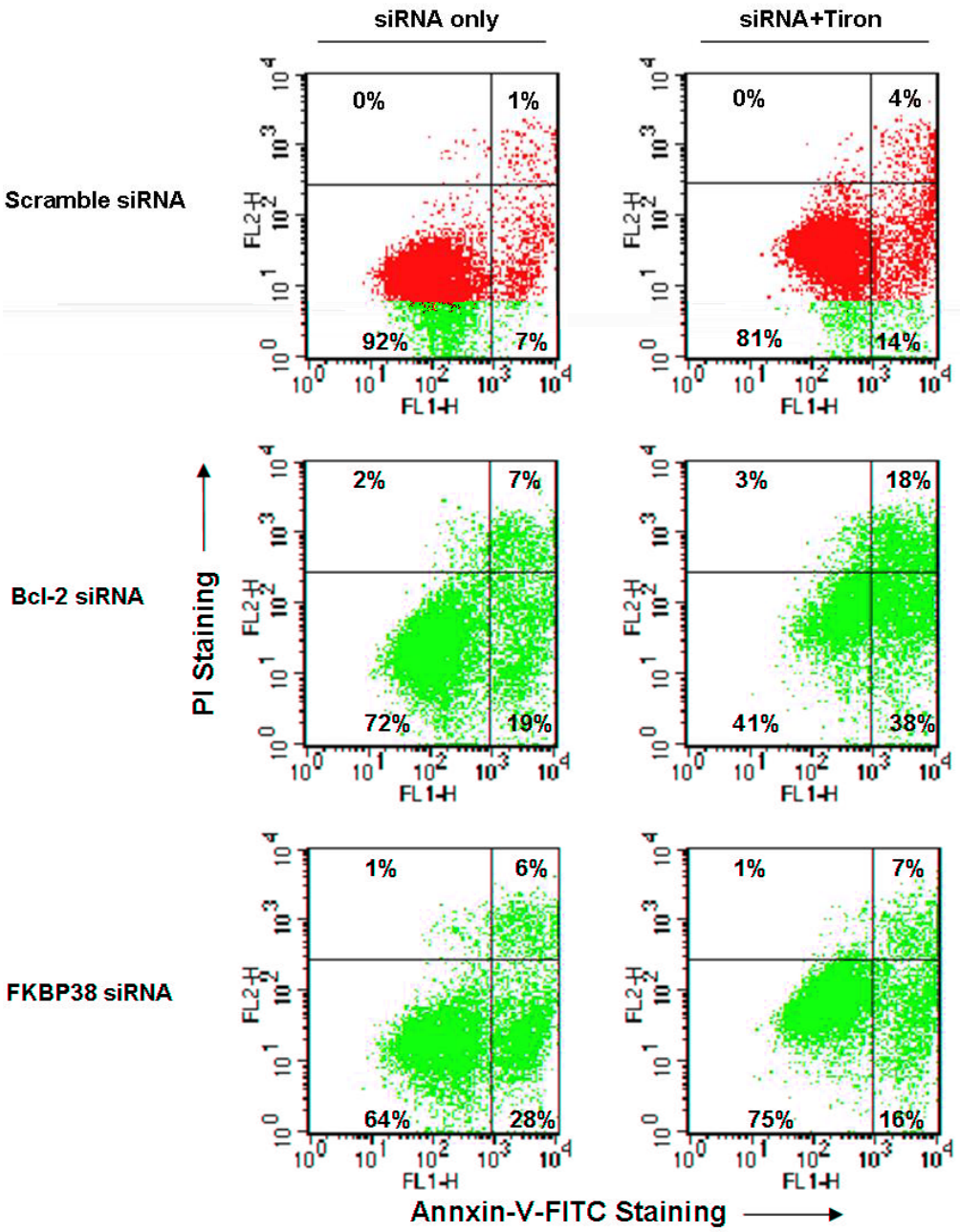

Fig. 5.12 Apoptosis was influenced by the antioxidant in HeLa cells. Cells were seeded in a six-well plate (2×10^5 cells/well) and treated with 30 nM scramble siRNA, Bcl-2 siRNA and FKBP38 siRNA, respectively, together with 6 mM of the antioxidant Tiron for 72 hours. Then, cells were stained with annexin-V-fluorescein/PI and apoptosis was analyzed by flow cytometry with FL1 channel for the detection of green fluorescence and FL2 channel for the detection of red fluorescence. Data were analyzed using CELLQuest software. A representative dot plot of three independent experiments was shown here.

5.1.8 Influence on MMP by antioxidant

During the aerobic respiration, mitochondria generate ATP as well as the by-product ROS. Mitochondria are the major source of ROS and also the main target of ROS. Bcl-2 and FKBP38 were known to localize at the mitochondrial outer membrane. The removal of either Bcl-2 or FKBP38 resulted in the increase of ROS and apoptosis. Yet, the inhibition of ROS could only prevent apoptosis induced by FKBP38 siRNA, not by Bcl-2 siRNA. Thus, there must be different pathways involved in FKBP38-siRNA-induced apoptosis and Bcl-2-siRNA-induced apoptosis.

In order to distinguish the mechanisms of apoptosis induced by the suppression of Bcl-2 and FKBP38, the relationship between ROS and MMP was analyzed through the combination of RNA interference with the antioxidant Tiron (Fig. 5.13).

The quantitative analysis by using JC-1 staining showed that the treatment of Tiron prevented the loss of MMP caused by FKBP38 suppression to about 30% (from 67.1% to 40.1%), while it rather enhanced the loss of MMP induced by removing Bcl-2 to about 10% (from 55.6% to 66.9%) (Fig. 5.13). Meanwhile, some non-specific cytotoxic effect was observed. Thus, the antioxidant Tiron could only prevent the loss of MMP caused by the suppression of FKBP38, but could not prevent the Bcl-2-suppression-induced the loss of MMP. In another words, the increase of ROS after the suppression of FKBP38 was responsible for the damage of the mitochondrial function. Yet, the generation of ROS induced by Bcl-2 siRNA was not the main reason for the Bcl-2-suppression-induced mitochondrial damage. One possible reason is that the removal of Bcl-2 caused a direct damage on the integrity of the mitochondrial outer membrane and the MMP. This damage could not be reversed by the inhibition of the ROS generation.

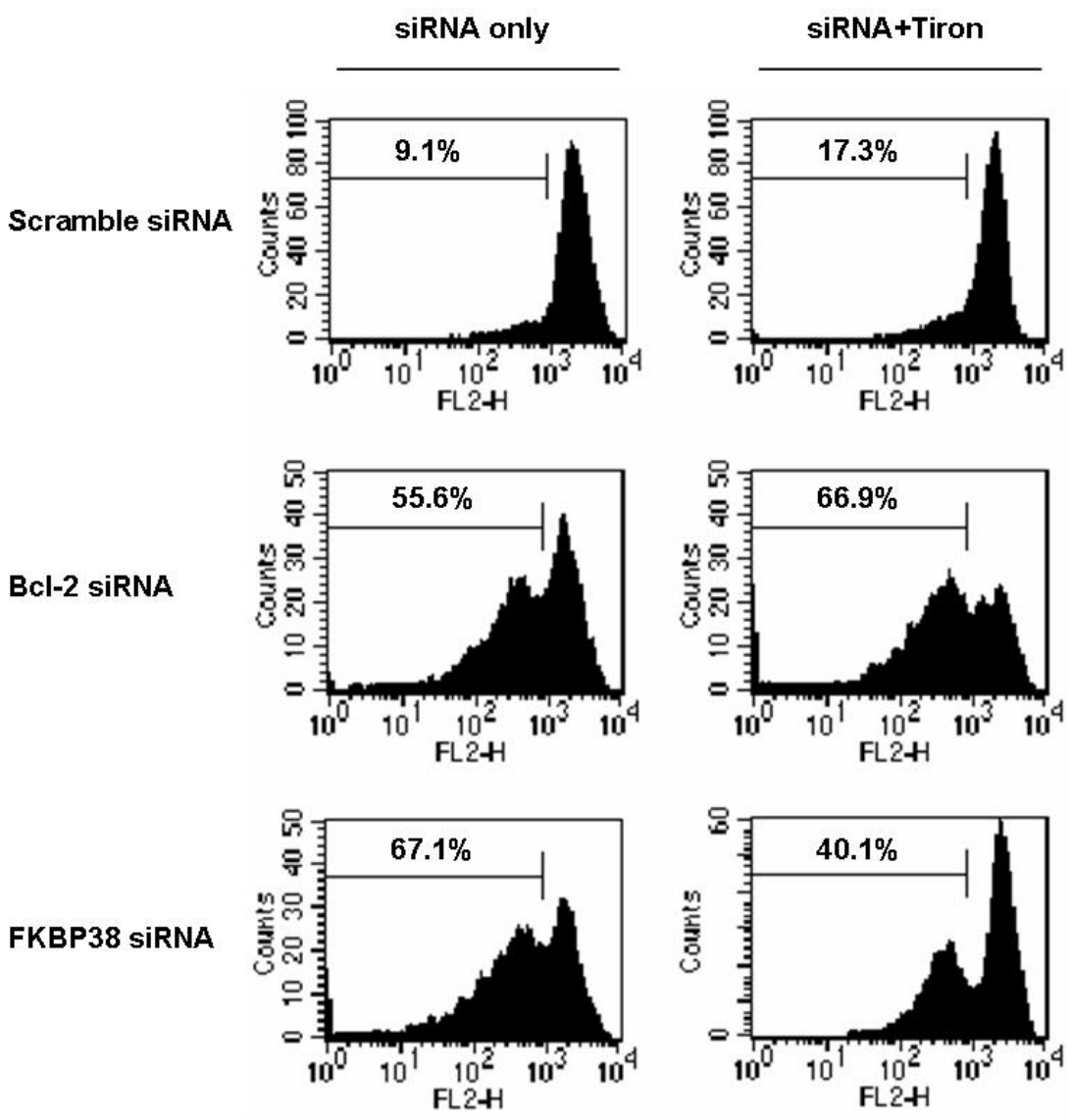

Fig.5.13 The mitochondrial membrane potential (MMP) was influenced by the antioxidant in HeLa cells. Cells were seeded in a six-well plate (2×10^5 cells/well) and treated with 30 nM scramble siRNA, Bcl-2 siRNA and FKBP38 siRNA, only or together with 6 mM of the antioxidant Tiron for 72 hours. Cells were collected by trypsiniation and stained with 5, 5', 6, 6'- tetrachloro- 1, 1', 3, 3'- tetraethylbenzimidazolylcarbocyanine iodide/chloride (JC-1) for 15 min at 37°C. The MMP was detected with flow cytometry with FL2 channel for the gated cells containing red JC-1 aggregates. Data were analyzed by Cell Quest Software. Here is a representative histogram plot of three independent experiments.

5.1.9 Influence on Bcl-2 expression by antioxidant

The suppression of FKBP38 induced apoptosis with the degradation of Bcl-2 and the increase of ROS. In order to study the relationship between the Bcl-2 and the ROS, the expression of Bcl-2 was checked by Western blotting after the treatment of FKBP38 siRNA together with the antioxidant Tiron (Fig. 5.14). The result showed that the degradation of Bcl-2 caused by FKBP38 siRNA could not be prevented by the antioxidant Tiron. Thus, the ROS pathway is Bcl-2-independent.

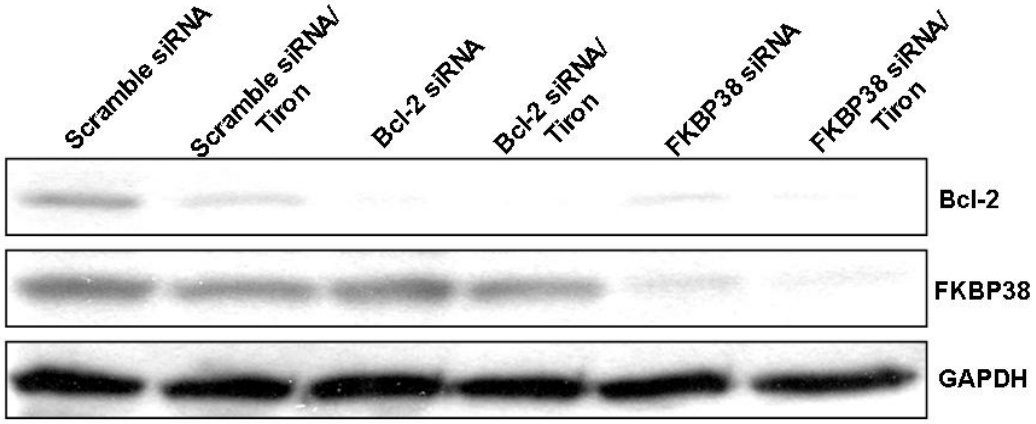

Fig. 5.14 The expression of Bcl-2 was influenced by the antioxidant in HeLa cells. Cells were seeded in a six-well plate (2×10^5 cells/well) and treated with 30 nM scramble siRNA, Bcl-2 siRNA and FKBP38 siRNA, only or together with 6 mM of antioxidant Tiron for 72 hours. Cell lysates were obtained and 100 μg of the total proteins were separated by 12% of SDS-PAGE. The expression levels of Bcl-2 and FKBP38 were checked by Western blotting. GAPDH was used as an internal control. Experiments were repeated for three times.

5.2 Discussion

5.2.1 FKBP38 determines Bcl-2 stability

The siRNA-mediated RNAi exerts gene silencing by specifically cleaving and degrading the target mRNA (Hannon GJ, 2002). According to the results, the

suppression of FKBP38 with the specific FKBP38 siRNA caused Bcl-2 degradation. However, when cells were treated with Bcl-2 siRNA, there was no influence on FKBP38 expression. Thus, FKBP38 plays a role in regulating the stability of Bcl-2. Before it has been shown that FKBP38 bound Bcl-2 and targeted it to mitochondria, without FKBP38, Bcl-2 was found to aggregate in perinuclear compartments, and subsequently induced a caspase-dependent apoptosisV (Shirane M et al., 2003). Combining with out data in this study, FKBP38 not only acts as an anchor of Bcl-2 to localize at the mitochondria, but also serves as a protector of Bcl-2 from degradation. It is reasonable to conclude that both of these two factors account for the anti-apoptotic function of FKBP38. Yet, since the RNA interference of FKBP38 led to severer cytotoxic effects than what caused by Bcl-2 siRNA, it can be concluded that besides Bcl-2, there should be other downstream targets involved in the FKBP38-siRNA-induced apoptosis.

5.2.2 FKBP38 acted as a linker between cell cycle and apoptosis through the ROS-mediated damage on MMP, and this appeared to be Bcl-2-indpendent

The mitochondrial respiratory chain at the inner mitochondrial membrane is a major intracellular source of ROS (Raha S et al., 2001). After silencing FKBP38 by RNA interference, a dramatic increase of ROS was detected. We noticed that the amount of ROS generated from the treatment of FKBP38 siRNA was much more than what caused by the Bcl-2 siRNA treatment. Under normal physiological conditions, about 85% of all oxygen used by the cells is consumed by the mitochondrial electron transport system; and up to 5% of the oxygen consumed by mitochondria is converted into superoxide, hydrogen peroxide, and other reactive oxygen species (Boveris A et al., 1973; Boveris A, 1977; Liu Y et al., 2002). Also, ROS can be generated during

diverse biological and cellular reactions. Depending on its level, ROS has dual roles; it can play positive roles for biological activities or can result in cytotoxic effects. At a very low concentration, ROS may act as a second messenger in interfering with kinases such as JNK or some other biomolecules in signal transduction pathway (Suzuki YJ et al., 1997; Liu SL et al., 2002). Also, the low concentration of ROS plays a role in the normal cell cycle progression (Takahashi Y et al., 2004). However, when unregulated and excessive ROS are produced in a very short period of time, it turns to be highly toxic to cells, damaging many vital molecules and cell components, including lipid peroxidation, mitochondria fission and DNA damage, which finally result in the breakdown of normal cellular activities and subsequently induce cell death (Kannan K et al., 2000; Simon HU et al., 2000).

Recently it is found that ROS is generated synchronously with the cell cycle progression (Takahashi Y et al., 2004). The level of ROS reflects the metabolic activities inside the cells, and is proportional to the S-phase cell population. The rapid increase of the cell population in S- and G_2/M-phase induced by the FKBP38 suppression resulted in the increase of the activity of the mitochondrial respiration, which could be one of the reasons to cause such a high-level intracellular ROS. In contrast, Bcl-2 suppression did not result in that high increase of S-phase cells, therefore, not that dramatic increase of ROS as what seen in FKBP38 suppression. Tiron is an efficient antioxidant capable of scavenging a variety of biological oxidants, such as ·OH and $O_2{\cdot}^-$ and therefore protects against intracellular oxidative damage. Although Tiron could inhibit the generation of ROS in cells treated with both Bcl-2 siRNA and FKBP38 siRNA, interestingly, only the apoptosis induced by the FKBP38 siRNA could be inhibited by Tiron. The addition of Tiron even enhanced Bcl-2-

siRNA-induced cell death. Thus, ROS appeared to be directly associated with apoptosis induced by FKBP38 siRNA, not by Bcl-2 siRNA.

The integrity of the mitochondrial outer membrane is essential to maintain cell survival. The damage on the mitochondrial outer membrane results in the releases of several apoptogenic proteins from the mitochondria to the cytosol and initiates apoptosis by activating caspase cascades or neutralizing apoptosis inhibitors (Green DR et al., 2000). Mitochondrial membrane potential (MMP) is generated by mitochondrial electron transport chain, which drives a proton flow from matrix through inner mitochondrial membrane to cytoplasm, thus creating an electrochemical gradient with negative inside of about 180-200 mV. A variety of pathophysiological conditions can influence MMP. And the increase in MMP may be a sign of mitochondrial swelling/hyperpolarization and disruptions of the outer mitochondrial membrane, which is an early event in the apoptotic caspase cascade (Kannan K et al., 2000). Although silencing either Bcl-2 or FKBP38 by RNA interference could result in the loss of MMP and the increase of ROS, the antioxidant Tiron could only prevent the loss of MMP from FKBP38 suppression, and could not prevent the loss of MMP induced by Bcl-2 siRNA. Therefore, the ROS-mediated damage on the mitochondria could be another reason for FKBP38-suppression-induced apoptosis. Bcl-2, on the other hand, just played a direct role in protecting the mitochondrial function. However, although the inhibition on ROS could prevent apoptosis, it could not prevent Bcl-2 degradation caused by FKBP38 suppression. Thus, this ROS-mediated apoptotic pathway is Bcl-2-independent.

5.3 Conclusion

Regulatory roles of Bcl-2 and one of Bcl-2-binding protein FKBP38 on apoptosis and cell cycle are explored in this study. The suppression of Bcl-2 by RNA interference caused the damage of the mitochondrial outer membrane and the loss of MMP. Although cells were detected to be arrested in later G_1- and early S-phase with the increase of ROS, the antioxidant Tiron treatment could not prevent Bcl-2-siRNA-induced loss of MMP and apoptosis. Thus, Bcl-2 played a direct role on protecting the mitochondria. Different from Bcl-2, the suppression of FKBP38 induced cells arrested in S- and G_2/M-phase with a dramatic increase of ROS. The inhibition on the ROS with the antioxidant Tiron could prevent the loss of MMP induced by FKBP38 siRNA and consequently prevent apoptosis without influencing Bcl-2 expression. Thus, the ROS-mediated damage on the mitochondrial membrane potential provides another pathway in apoptosis caused by FKBP38 suppression, which is independent of Bcl-2 (Fig.5.15). Yet, the detail mechanisms of the protection on the mitochondria by FKBP38 still need to be further studied.

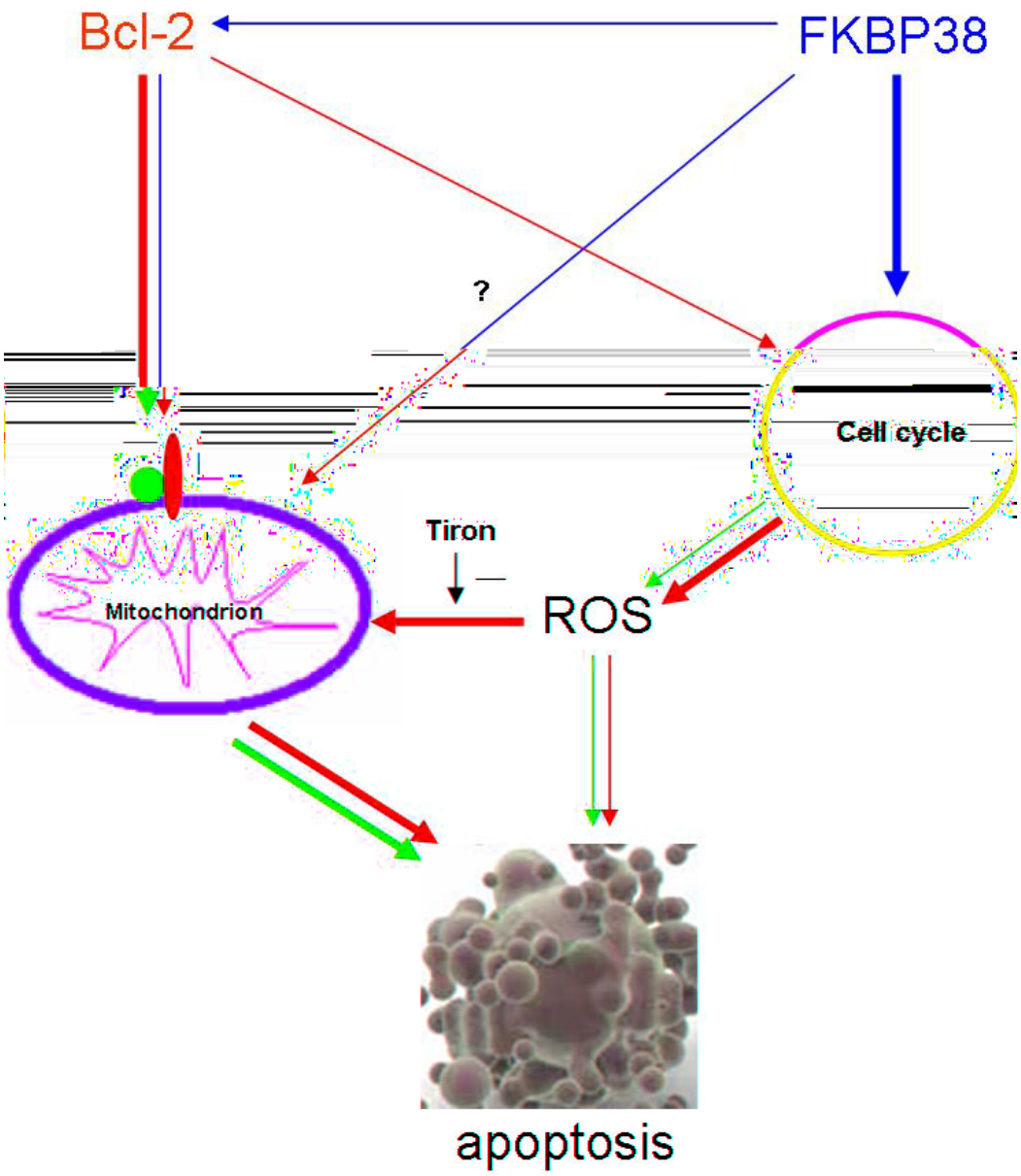

Fig. 5.14 Mechanisms of Bcl-2 and FKBP38 in regulating apoptosis. Both Bcl-2 and FKBP38 were found localizing on the mitochondrial membrane and involved in the regulation of cell cycle progression. Yet, different pathways were involved in the regulation of apoptosis by Bcl-2 and FKBP38. The removal of Bcl-2 showed direct damage on the integrity of the mitochondrial outer membrane. The removal of FKBP38 led to the disruption of the mitochondrial outer membrane through ROS, which was generated by a dramatic increase in S-phase cells. This damage on the mitochondria could be inhibited by the antioxidant and was independent from Bcl-2.

Chapter 6 RNA interference of Bcl-2 and chemosensitivity of cancer cells

Bcl-2 is a major regulatory protein in apoptosis with anti-apoptotic function (Tsujimoto Y et al., 1984). Bcl-2 belongs to a big family, named Bcl-2 family. The Bcl-2 family proteins include anti-apoptotic and pro-apoptotic members sharing sequence-homology domains, BH1, 2, 3, and 4 (Kelekar A et al., 1998). Members are able to interact with each other through heterodimerization or homodimerization to modulate each others' functions. Thus, their relative concentrations are important in determining the fate of the apoptosis (Oltvai ZN et al., 1993).

Bcl-2 is a proto-oncogene, and its up-regulation has been found in various tumours. Bcl-2 exerts its tumorigenesis through prolonging cell survival (Tsujimoto Y et al., 1985; Coultas L et al., 2003). Because of its anti-apoptotic function, the overexpression of Bcl-2 correlates with resistance to conventional chemo- and radiotherapies and poor prognosis in a wide spectrum of human cancers. Bcl-2 can limit the therapeutic effects of many currently available anti-cancer drugs. Therefore, the functional blockade of Bcl-2 or Bcl-x_L should either restore the apoptotic process in tumor cells or sensitize these tumors to chemo- and radio-therapies. Bcl-2 is hence one of the major targets in anti-cancer therapy (Reed JC, 1995; Bettaieb A et al., 2003).

Several strategies, including anti-sense, small molecules, and peptide mimetics, have been developed to modulate the expression of Bcl-2 protein (Dorai T et al., 1997; Gautschi O et al., 2001; Nahta R et al., 2003). It has been reported that the use of chemically synthesized small interfering RNA (siRNA) in mammalian cells offers an

alternative way of regulating therapeutic targets due to its specific silencing effect (Hannon GJ, 2002; Shen WG, 2004).

In this study, we evaluated the effects of siRNA-induced Bcl-2 suppression in three cancer cell lines: Hela, MDA-MB-231 and MCF-7. The changes in chemosensitivities of three cancer cells to four anti-cancer drugs, Paclitaxel, Camptothecin, Betulinic Acid and Cisplatin were subsequently assessed after Bcl-2 down-regulation in these cells. Our results showed cell-dependent enhancements of chemosensitivities after silencing Bcl-2 by RNA interference.

6.1 Results

6.1.1 Influences on Bcl-2 family proteins by Bcl-2 siRNA

First, the influences on Bcl-2 family proteins by Bcl-2 siRNA were evaluated in three cancer cells: HeLa, MDA-MB-231 and MCF-7. Based on the earlier results, for studying chemosensitivity, the Bcl-2 siRNA HYSR2, which showed the best silencing effects on Bcl-2, was selected and was used in this anticancer study (Fig. 3.5). The expressions of Bcl-2 family proteins after the treatment of Bcl-2 siRNA were checked by Western blotting (Fig. 6.1). The results showed that after silencing Bcl-2 with siRNA HYSR2, Bcl-x_L expression showed no obvious changes, but Bax expression increased.

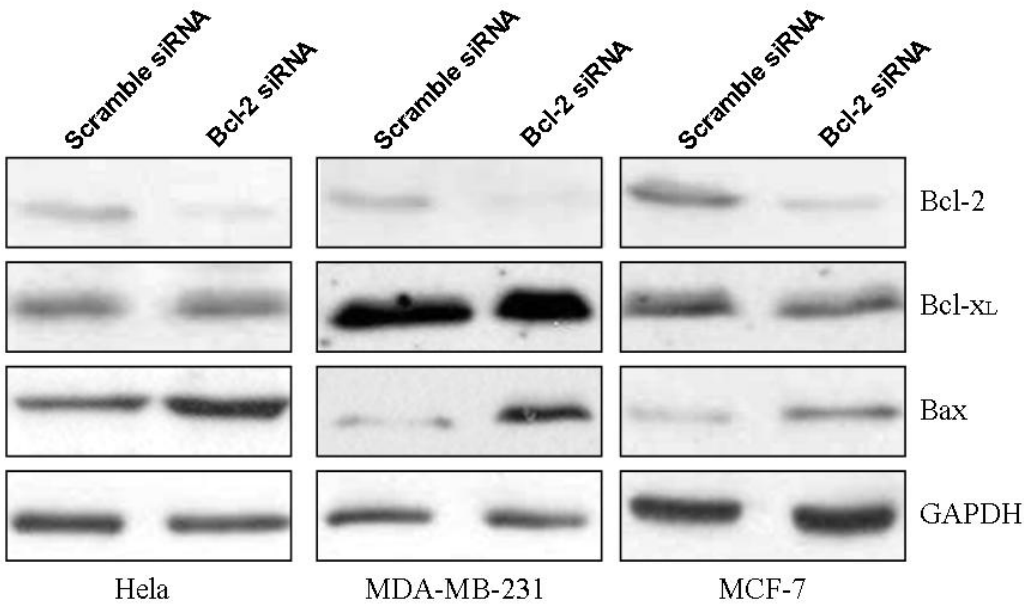

Fig. 6.1 The influences of Bcl-2 family proteins after silencing Bcl-2 by RNA interference in HeLa, MDA-MB-231 and MCF-7 cells. Cells were seeded in a six-well plate (2×10^5 cells/well), and were treated with 30 nM scramble siRNA and Bcl-2 siRNA for 72 hours, respectively. Cells were lyzed and cell lysates were centrifuged. After measuring concentrations, 100 µg of the equal amounts were separated by 12% of SDS PAGE, and transferred to a membrane. The expressions of Bcl-2, Bcl-x_L and Bax were checked by Western blottings.

6.1.2 Inhibitions of cell growth by Bcl-2 siRNA

After Bcl-2 is suppressed, cells undergo apoptosis. The increase in the expression of Bax accelerated the cell death. Next, we examined the effect of RNA interference of Bcl-2 on cell viabilities. The results showed that upon silencing Bcl-2, cell growth was inhibited to about 60% in Hela cells, 50% in MDA-MB-231 cells and 40% in MCF-7 cells (Fig. 6.2). There were little non-specific cytotoxic effects from the scramble siRNA.

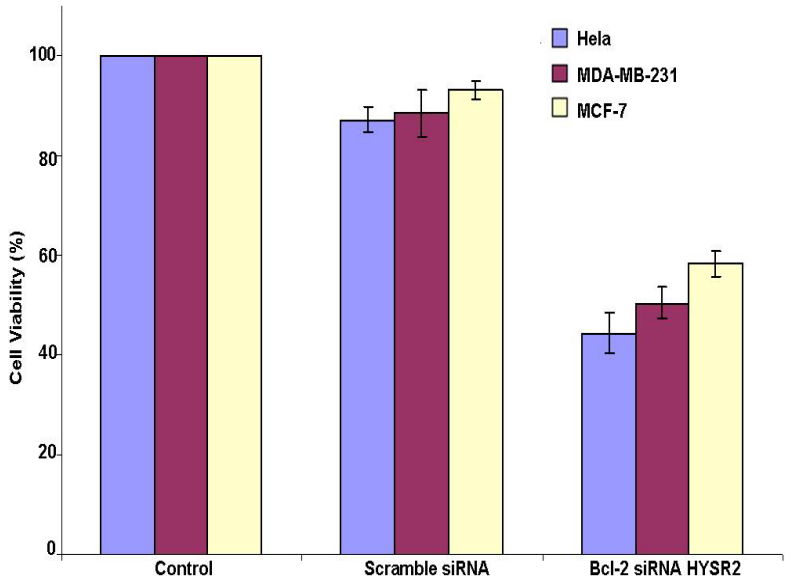

Fig. 6.2 Cell proliferation assay after suppressing the expression of Bcl-2 in HeLa, MDA-MB-231 and MCF-7 cells. Cells were seeded in a 96-well plate (5×10^3 cells/well), and were treated with 30 nM scramble siRNA and Bcl-2 siRNA for 72 hours. Cell proliferation was analyzed with MTT assay. Values represent means ± S.D. of three independent experiments.

6.1.3 RNA interference of Bcl-2 in chemosensitivities of cancer cells

In order to assess the influence of Bcl-2 siRNA on the chemosensitivities of cancer cells to anti-cancer drugs, IC_{50} values were investigated in HeLa, MDA-MB-231 and MCF-7 cells. After silencing Bcl-2 with siRNA, cells were exposed to the anti-cancer drugs including cisplatin, betulinic acid, camptothecin and paclitaxel. The cell growth rates were measured with MTT assay and the IC_{50} values were calculated (Table 6.1). Compared with the IC_{50} values in the absence of Bcl-2 suppression (treated with scramble siRNA), enhancements on the chemosensitivities to different anti-cancer drugs after the suppression of Bcl-2 varied in different cancer cell lines. HeLa cells showed the highest increase in sensitivities to all of the four anti-cancer drugs, paclitaxel (3.5-fold increase), camptothecin (2.7-fold increase), betulinic acid (2.1-fold increase) and cisplatin (1.6-fold increase). However, neither MCF-7 nor

MDA-MB-231 showed such similar significant enhancements as HeLa cells did to the anti-cancer drugs tested, although the down-regulation of Bcl-2 in MDA-MB-231 showed a 1.8-fold increase to cisplatin.

Drugs	Cell lines	IC_{50}		
		Scramble siRNA	Bcl-2 siRNA	Fold increase*
Paclitaxel (nM)	Hela	18.3±2.8	5.3±0.9	3.5
	MDA-MB-231	23.3±0.6	23.1±1.6	1.0
	MCF-7	42.9±1.7	32.4±4.1	1.3
Camptothecin (nM)	Hela	685.8±4.7	251.7±8.3	2.7
	MDA-MB-231	1902.7±31.6	1607.0±130.0	1.2
	MCF-7	1181.6±30.0	1002.3±84.3	1.2
Betulinic Acid (μM)	Hela	39.1±3.5	18.9±3.0	2.1
	MDA-MB-231	41.4±5.4	25.8±2.5	1.6
	MCF-7	67.1±10.1	49.8±5.6	1.3
Cisplatin (μM)	Hela	45.3±2.1	28.1±6.2	1.6
	MDA-MB-231	246.2±15.0	139.7±18.2	1.8
	MCF-7	205.8±5.1	181.4±6.8	1.1

* Fold increase was defined as IC50 (Scramble siRNA) / IC_{50} (Bcl-2 siRNA).

Table 6.1 The assessments of chemosensitivities to anti-cancer drugs by silencing Bcl-2 in HeLa, MDA-MB-231 and MCF-7 cells. Cells were seeded in a 96-well plate (5×10^3 cells/well), and treated with 30 nM scramble siRNA or Bcl-2 siRNA for 48 hours. Then cells were treated with different anti-cancer drugs from low to high concentrations, including paclitaxel (0-100 nM), camptothecin (1-10 μM), betulinic acid (0-100 μM) and cisplatin (0-500 μM) for 24 hours, respectively. Cell growths were analyzed with MTT assay and cell growth curves were got. IC_{50}s were calculated by Kaleida Graph software. Experiments were repeated five times.

6.1.4 Morphological studies of HeLa cells

Different anti-cancer drugs killed cancer cells through different mechanisms. Here we explored the morphological changes in HeLa cells treated with low doses of

the four anti-cancer drugs with or without the combination of Bcl-2 siRNA (Fig. 6.3). Apoptotic changes such as membrane blebbling and cell fragmentation were seen in HeLa cells. In addition, special morphological characteristics were also observed, after HeLa cells were treated with different anti-cancer drugs. For example, the treatments with camptothecin and cisplatin made cells bigger both in the cell overall cell dimension and in the nucleus size. The treatment with paclitaxel made the cells smaller; and the cell shapes turned from fibroblast-like to round. Although there was not much change in the size and the shape after betulinic acid treatment, an obvious condensation and cleavage on the chromosome was observed, and the treatment with Bcl-2 siRNA enhanced this cytotoxity in HeLa cells.

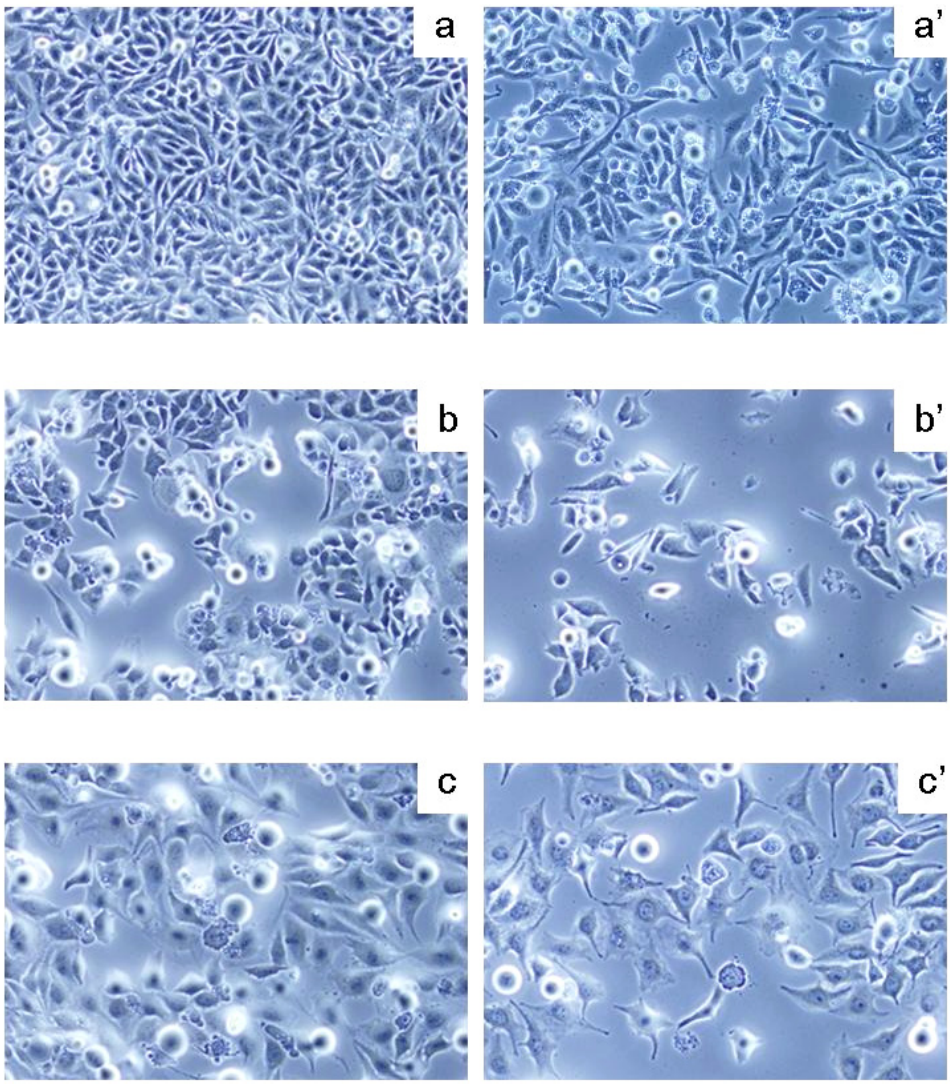

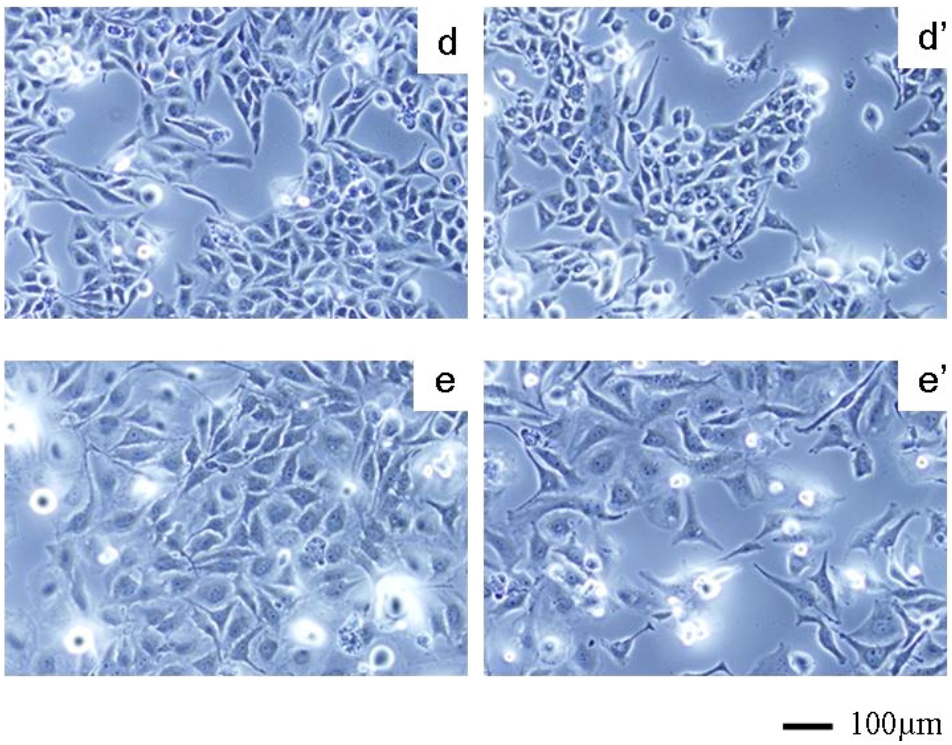

Fig. 6.3 The morphological changes of Hela cells after treated with anti-cancer drugs with/without the combination of Bcl-2 siRNA. Cells were seeded in a six-well plate (2×10^5 cells/well), and were first treated or not treated with 30 nM Bcl-2 siRNA for 48 hours. Cells were then treated with various low-concentation anti-cancer drugs, Paclitaxel (4 nM), Camptothecin (100 nM), Betulinic Acid (10 μM) and Cisplatin (20 μM), for another 24 hours. The morphological changes of the cells were observed and captured with phase-contrast microscopy.

6.2 Discussion

6.2.1 Expressions of Bcl-2 family proteins vary among different cancer cells and influence cell survival abilities

Bcl-2 is localized at the mitochondrial outer membrane and functions as an anti-apoptotic protein by protecting the mitochondria. The suppression of Bcl-2 resulted in an increase in the mitochondrial outer membrane permeabilization, and the

release of the mitochondrial apoptogenic proteins to the cytoplasm. The pro-apoptotic protein Bax is usually localized in the cytoplasm in an inactive form. During the apoptotic process, it is activated and moved to the mitochondrial outer membrane to interact with other Bcl-2 family proteins. Thus, the ratio between anti-apoptotic proteins and pro-apoptotic proteins is critical for the determination of cell fate. The increases of Bax observed in the cancer cells after suppressing Bcl-2 with RNA interference contribute to apoptotic cell death.

6.2.2 Enhancements of chemosensitivities by Bcl-2 suppression are cancer-cell-line dependent

Apoptosis-related proteins, especially anti-apoptotic proteins are molecular targets for anti-cancer therapy. Various reagents, including ribozyme, anti-sense oligonucleotide, peptidomimetics and small molecules, have been developed for the down-regulation of the expression of Bcl-2. Here, we studied the effects of siRNA on chemosensitivity of cancer cells, demonstrating that the effects are cell line-dependent. Previously it has been demonstrated that sensitivities to anti-cancer drugs cannot be always predicted by Bcl-2 alone. For example, in the cells with the expression of wild-type p53, levels of Bcl-2, Bcl-x_L and Bax were correlated to determine the chemosensitivity to long-term 5-FU treatment (Luo D et al., 1999; Inoue S et al., 2001; Violette S et al., 2002). In our study, reason for differential sensitivity of cancer cells to the anti-cancer drugs in Bcl-2-siRNA-treated cancer cells could be attributed to the residual amount of Bcl-2 still providing the cancer cells with the capacity to be chemo-resistant. MCF-7 cells show the highest expression of Bcl-2 protein among all of these three cell lines. MDA-MB-231 demonstrated a significant silencing effect on

Bcl-2, but the high-level expression of Bcl-$x_{L,}$ which was not affected by Bcl-2 siRNA, may still played an important role in drug resistance.

Bcl-2 was found protecting the integrity of the mitochondrial membrane and delaying the cell cycle progression. Suppression Bcl-2 resulted in the damage on the mitochondrial membrane and the initiation of G1 → S transition. It is generally observed that resting or slowly growing cancer cells are more resistant than rapidly growing cells to external stresses such as radiation and anti-cancer drugs, because most anti-cancer drugs target the proliferation-associated events such as DNA replication and mitosis. Paclitaxel induces the polymerization of tubulin, which results in the formation of abnormally stable and nonfunctional microtubules, thereby inhibiting cellular replication in the G_0/G_1 and G_2/M phases, thus cells lose the normal long spindle shapes and become round and smaller in size. The suppression of Bcl-2 initiates cell cycle progression, which requires microtubules for the assembly of cytoskeleton. Thus, it is conceivable that the combination of Bcl-2 siRNA with paclitaxel enhances the misregulation of cell cycle progression and promoted cell death.

Both camptothecin and cisplatin interrupt DNA replication. Camptothecin specially targets and inhibits human DNA topoisomerase I (Topo I) by binding noncovalently to the Topo I-DNA complex (Fan Y et al., 1998). As a result, single- and double-strand DNA breaks are generated, leading to premature termination of DNA replication and inhibition of DNA transcription (Bendixen C et al., 1990). Cisplatin can form cisplatin-DNA adducts by 1,2-intrastrand crosslinks between adjacent purines in DNA or 1,3-interstrand crosslinks and monoadducts; and all of these adducts could inhibit DNA replication and transcription (Zamble DB et al., 1995). Without DNA duplication, cells cannot undergo cell division, and cell cycle

progression is interrupted with an increased cell volume. The deregulation of cell cycle progression caused by Bcl-2 siRNA treatment appears to enhance the cytotoxities by camptothecin and cisplatin.

Betulinic acid was first reported in 1995 as a selective inhibitor of human melanoma (Pisha E et al., 1995). Betulinic acid showd its cytotoxic effect in the mitochondria and induced depolarization of mitochondrial membrane potential, which led to apoptosis by the release of apoptogenic factors from mitochondria to cytosol. Further insight into the mechanism of betulinic acid action in melanoma cells revealed that betulinic acid activated pro-apoptotic mitogen-activated protein kinases and induced the expression of the anti-apoptotic protein Mcl-1. There were no apparent affects on the cell size and shape by betulinic acid. In this study we showed that the treatment with betulinic acid resulted in a condensed and cleaved nucleus, which could be one of the apoptotic characteristics for betulinic acid. The depletion of Bcl-2 enhanced this damage on chromosome DNA, and the increase of the mitochondrial membrane permeabilization, thus, it is reasonable to conclude that silencing Bcl-2 could enhance the cytotoxity of betulinic acid.

6.3 Conclusion

Chemotherapy is a conventional method in the cancer therapy. However, the development of drug resistance limits the effects of the treatment, and also the nonspecific cytotoxities from a wide variety of anti-cancer drugs could result in severe side effects on the normal cells. Thus, increasing the efficacy of drug will reduce the side-effects from drugs and beneficial for individuals suffering from cancers.

The specifically silencing Bcl-2 expression by RNA interference not only promotes cell death, but also reduces the amounts of drugs used. According to our results, the enhancements of sensitivity of cancer cells to the anti-cancer drugs by silencing Bcl-2 are cell line-dependent. Further studies and understanding on the mechanisms of the involvement of Bcl-2 in apoptotic pathways triggered by various anti-cancer drugs could contribute to designing novel approaches in overcoming chemoresistance.

Chapter 7 General Discussion

The balance of cell death and cell growth is essential for normal embryonic development and tissue homeostasis. Apoptosis and cell cycle are the two fundamental biological processes directly responsible for the control of cell death and cell growth (Rubin LL et al., 1993).

Apoptosis or Programmed Cell Death (PCD) is a highly regulated process, which involves a systematic disassembly of an unwanted cell without causing damage or stress to neighboring cells in a multi-cellular organism. Cell cycle includes an orderly sequence of events in which a cell duplicates its contents and then divides into two daughter cells. These two processes are regulated in a coordinated fashion in order to maintain the balance between the cell growth and the cell death.

Many proteins are involved in apoptotic regulation and cell cycle. Bcl-2 is a well-known anti-apoptotic protein localized at the mitochondrial outer membrane. During apoptosis, several apoptogenic proteins are released from the intermembrane space of the mitochondria to the cytoplasm to initiate the down-stream caspase cascade, which is responsible for the final degradation of various proteins and the disassembly of the cells and execution of apoptosis (Hengartner MO, 2000). The mitochondrial localization of Bcl-2 prevents the release of those apoptogenic proteins by protecting the integrity of the mitochondrial outer membrane (VanderHeiden MG et al., 1999).

Besides its anti-apoptotic function, Bcl-2 also plays a role in regulating cell cycle progression. Bcl-2 expression delays $G_1 \rightarrow S$ transition and inhibits cell growth and cell proliferation (Mazel S et al., 1996; Huang DC et al., 1997). The down-regulation of Bcl-2 led to a perturbation in the cell cycle transition: the initiation of cell cycle progression and the increase of S-phase cell population.

Chaperon proteins help in folding of nascent polypeptide chains, refolding of denatured proteins, and preventing the aggregation of surface-exposed hydrophobic parts of proteins. In addition, chaperon proteins are also involved in protein stabilization, degradation and transferring inside cells.

As a novel chaperon protein, FKBP38 was observed to interact with Bcl-2 and help the mitochondrial localization of Bcl-2 (Shirane M et al., 2003; Kang CB et al., 2005). After suppressing FKBP38, the Bcl-2 was found misdistributed in the cytoplasm and also around the nucleus. Also, we showed that FKBP38 protects the endogenous Bcl-2 from degradation. Like Bcl-2, FKBP38 is involved in the regulation of cell cycle by retarding $G_1 \rightarrow S$ transition. The down-regulation of FKBP38 initiated the cell cycle progression and a significant increase of S-phase cell population.

Thus, our data suggest that Bcl-2 and FKBP38 regulate both apoptosis and proliferation. And these two functions may orchestrate each other to maintain cell survival. Dysregulation of either one may result in the breakdown of cellular homeostasis. By delaying $G_1 \rightarrow S$ transition, Bcl-2 and FKBP38 may provide a longer time for cells to check the chromosome to ensure the correctness of genome before

cell division. The delay in the cell cycle transition would prolong the survival time of cancer cells by reducing oxygen and nutrient consumption especially in hypoxic conditions, which may give enough time for new capillary growth into the tumor tissue. In the rapidly dividing and growing cells generate reactive oxygen species (ROS), which is toxic to cells. The overexpression of Bcl-2 and FKBP38 may reduce cell proliferation and consequently contribute to maintaining cells healthy by keeping ROS under control.

Although both Bcl-2 and FKBP38 play a role in the regulation of apoptosis and cell cycle progression, they act through different pathways. The silencing of FKBP38 resulted in a greater number of cells arrested in S- or G_2/M-phase with a significant increase of cyclin A and activation of CDK2; whereas the silencing of Bcl-2 resulted in cells arrested in the late G_1- or early S-phase with an increase of cyclin E, and without obvious influence on CDK2.

We showed that the antioxidant was able to protect the mitochondrial membrane from damage and inhibit the apoptotic cell death initiated by FKBP38 suppression. However, it showed little effect on the Bcl-2-suppression-induced mitochondrial damage and apoptosis. Thus, we believe that the suppression of FKBP38 may lead to a ROS-mediated damage on the mitochondria, independent on Bcl-2.

In conclusion, cell growth or proliferation and cell death are not absolutely independent events. These events communicate with each other through a diversity of range of proteins involved in the signaling pathways of both cell cycle and apoptosis.

Besides the involvement of the Bcl-2 family proteins in cell cycle progression (Janumyan YM et al., 2003), cell cycle-related molecules, such as p27 and CDK2 were also involved in apoptosis (Gil-Gomez G et al., 1998). Furthermore, the novel finding which involves FKBP38 in the regulation of both the cell cycle and apoptosis suggests the existence of a new pathway connecting these two processes. It is conceivable that the crosslink between these two fundamental biological processes plays an essential role in maintaining tissue homeostasis and in maintaining normal embryonic development. The better understanding of the biochemical and molecular regulations of Bcl-2 and FKBP38 in apoptosis and cell cycle not only can give valuable suggestions in understanding tissue growth and development, but also can provide new idea in developing anti-cancer drugs.

References

Adams JM: **Ways of dying: multiple pathways to apoptosis**. *Genes Dev* 2003, **17**(20):2481-2495.

Aisenberg AC, Wilkes BM, Jacobson JO: **The bcl-2 gene is rearranged in many diffuse B-cell lymphomas**. *Blood* 1988, **71**(4):969-972.

Alberici A, Moratto D, Benussi L, Gasparini L, Ghidoni R, Gatta LB, Finazzi D, Frisoni GB, Trabucchi M, Growdon JH *et al*: **Presenilin 1 protein directly interacts with Bcl-2**. *J Biol Chem* 1999, **274**(43):30764-30769.

Ameisen JC, Groux H, Capron A: **[Programmed death (apoptosis) of T CD4 lymphocytes and AIDS pathogenesis]**. *C R Acad Sci III* 1992, **314**(9 Suppl):47-50.

Annis MG, Soucie EL, Dlugosz PJ, Cruz-Aguado JA, Penn LZ, Leber B, Andrews DW: **Bax forms multispanning monomers that oligomerize to permeabilize membranes during apoptosis**. *Embo J* 2005, **24**(12):2096-2103.

Antonsson B, Conti F, Ciavatta A, Montessuit S, Lewis S, Martinou I, Bernasconi L, Bernard A, Mermod JJ, Mazzei G *et al*: **Inhibition of Bax channel-forming activity by Bcl-2**. *Science* 1997, **277**(5324):370-372.

Antonsson B, Montessuit S, Lauper S, Eskes R, Martinou JC: **Bax oligomerization is required for channel-forming activity in liposomes and to trigger cytochrome c release from mitochondria**. *Biochem J* 2000, **345 Pt 2**:271-278.

Aravin AA, Lagos-Quintana M, Yalcin A, Zavolan M, Marks D, Snyder B, Gaasterland T, Meyer J, Tuschl T: **The small RNA profile during Drosophila melanogaster development**. *Dev Cell* 2003, **5**(2):337-350.

Ashkenazi A, Dixit VM: **Death receptors: signaling and modulation**. *Science* 1998, **281**(5381):1305-1308.

Bendixen C, Thomsen B, Alsner J, Westergaard O: **Camptothecin-stabilized topoisomerase I-DNA adducts cause premature termination of transcription**. *Biochemistry* 1990, **29**(23):5613-5619.

Bettaieb A, Dubrez-Daloz L, Launay S, Plenchette S, Rebe C, Cathelin S, Solary E: **Bcl-2 proteins: targets and tools for chemosensitisation of tumor cells**. *Curr Med Chem Anticancer Agents* 2003, **3**(4):307-318.

Bhardwaj A, Aggarwal BB: **Receptor-mediated choreography of life and death**. *J Clin Immunol* 2003, **23**(5):317-332.

Blaszczyk J, Tropea JE, Bubunenko M, Routzahn KM, Waugh DS, Court DL, Ji X: **Crystallographic and modeling studies of RNase III suggest a mechanism for double-stranded RNA cleavage**. *Structure* 2001, **9**(12):1225-1236.

Boldin MP, Goncharov TM, Goltsev YV, Wallach D: **Involvement of MACH, a novel MORT1/FADD-interacting protease, in Fas/APO-1- and TNF receptor-induced cell death**. *Cell* 1996, **85**(6):803-815.

Bouillet P, Strasser A: **BH3-only proteins - evolutionarily conserved proapoptotic Bcl-2 family members essential for initiating programmed cell death**. *J Cell Sci* 2002, **115**(Pt 8):1567-1574.

Boulares AH, Yakovlev AG, Ivanova V, Stoica BA, Wang G, Iyer S, Smulson M: **Role of poly(ADP-ribose) polymerase (PARP) cleavage in apoptosis. Caspase 3-resistant PARP mutant increases rates of apoptosis in transfected cells**. *J Biol Chem* 1999, **274**(33):22932-22940.

Boveris A, Chance B: **The mitochondrial generation of hydrogen peroxide. General properties and effect of hyperbaric oxygen**. *Biochem J* 1973, **134**(3):707-716.

Boveris A: **Mitochondrial production of superoxide radical and hydrogen peroxide**. *Adv Exp Med Biol* 1977, **78**:67-82.

Breitschopf K, Haendeler J, Malchow P, Zeiher AM, Dimmeler S: **Posttranslational modification of Bcl-2 facilitates its proteasome-dependent degradation: molecular characterization of the involved signaling pathway**. *Mol Cell Biol* 2000, **20**(5):1886-1896.

Bright J, Khar A: **Apoptosis: programmed cell death in health and disease**. *Biosci Rep* 1994, **14**(2):67-81.

Buxbaum JD, Choi EK, Luo Y, Lilliehook C, Crowley AC, Merriam DE, Wasco W: **Calsenilin: a calcium-binding protein that interacts with the presenilins and regulates the levels of a presenilin fragment**. *Nat Med* 1998, **4**(10):1177-1181.

Carson DA, Ribeiro JM: **Apoptosis and disease**. *Lancet* 1993, **341**(8855):1251-1254.

Carter WO, Narayanan PK, Robinson JP: **Intracellular hydrogen peroxide and superoxide anion detection in endothelial cells**. *J Leukoc Biol* 1994, **55**(2):253-258.

Cheng EH, Kirsch DG, Clem RJ, Ravi R, Kastan MB, Bedi A, Ueno K, Hardwick JM: **Conversion of Bcl-2 to a Bax-like death effector by caspases**. *Science* 1997, **278**(5345):1966-1968.

Chinnaiyan AM, O'Rourke K, Tewari M, Dixit VM: **FADD, a novel death domain-containing protein, interacts with the death domain of Fas and initiates apoptosis**. *Cell* 1995, **81**(4):505-512.

Chipuk JE, Kuwana T, Bouchier-Hayes L, Droin NM, Newmeyer DD, Schuler M, Green DR: **Direct activation of Bax by p53 mediates mitochondrial membrane permeabilization and apoptosis**. *Science* 2004, **303**(5660):1010-1014.

Chu G, Hayakawa H, Berg P: **Electroporation for the efficient transfection of mammalian cells with DNA**. Nucleic Acids Res 1987, **15**(3): 1311–1326.

Collins K, Jacks T, Pavletich NP: **The cell cycle and cancer**. *Proc Natl Acad Sci U S A* 1997, **94**(7):2776-2778.

Coultas L, Strasser A: **The role of the Bcl-2 protein family in cancer**. *Semin Cancer Biol* 2003, **13**(2):115-123.

Crompton M: **The mitochondrial permeability transition pore and its role in cell death**. *Biochem J* 1999, **341 (Pt 2)**:233-249.

Danial NN, Korsmeyer SJ: **Cell death: critical control points**. *Cell* 2004, **116**(2):205-219.

Davies TH, Sanchez ER: **Fkbp52**. *Int J Biochem Cell Biol* 2005, **37**(1):42-47.

Del Maestro R, McDonald W: **Subcellular localization of superoxide dismutases, glutathione peroxidase and catalase in developing rat cerebral cortex**. *Mech Ageing Dev* 1989, **48**(1):15-31.

Deng X, Gao F, Flagg T, Anderson J, May WS: **Bcl2's flexible loop domain regulates p53 binding and survival**. *Mol Cell Biol* 2006, **26**(12):4421-4434.

Deng X, Gao F, May WS, Jr.: **Bcl2 retards G1/S cell cycle transition by regulating intracellular ROS**. *Blood* 2003, **102**(9):3179-3185.

Dennis PB, Jaeschke A, Saitoh M, Fowler B, Kozma SC, Thomas G: **Mammalian TOR: a homeostatic ATP sensor**. *Science* 2001, **294**(5544):1102-1105.

Dillin A: **The specifics of small interfering RNA specificity**. *Proc Natl Acad Sci U S A* 2003, **100**(11):6289-6291.

Dimmeler S, Breitschopf K, Haendeler J, Zeiher AM: **Dephosphorylation targets Bcl-2 for ubiquitin-dependent degradation: a link between the apoptosome and the proteasome pathway**. *J Exp Med* 1999, **189**(11):1815-1822.

Doan A, Thinakaran G, Borchelt DR, Slunt HH, Ratovitsky T, Podlisny M, Selkoe DJ, Seeger M, Gandy SE, Price DL *et al*: **Protein topology of presenilin 1**. *Neuron* 1996, **17**(5):1023-1030.

Dorai T, Goluboff ET, Olsson CA, Buttyan R: **Development of a hammerhead ribozyme against BCL-2. II. Ribozyme treatment sensitizes hormone-resistant prostate cancer cells to apoptotic agents**. *Anticancer Res* 1997, **17**(5A):3307-3312.

Du C, Fang M, Li Y, Li L, Wang X: **Smac, a mitochondrial protein that promotes cytochrome c-dependent caspase activation by eliminating IAP inhibition**. *Cell* 2000, **102**(1):33-42.

Dubes GR: **Strong inhibition of transfection by critical low concentration of diethylaminoethyl-dextran**. *Acta Virol* 1974,**18**(6):457-66.

Edlich F, Weiwad M, Erdmann F, Fanghanel J, Jarczowski F, Rahfeld JU, Fischer G: **Bcl-2 regulator FKBP38 is activated by Ca2+/calmodulin**. *Embo J* 2005, **24**(14):2688-2699.

Edlich F, Weiwad M, Wildemann D, Jarczowski F, Kilka S, Moutty MC, Jahreis G, Lucke C, Schmidt, triggow F *et al*: **The specific FKBP38 inhibitor N-(N',N'-dimethylcarboxamidomethyl)cycloheximide has potent neuroprotective and neurotrophic properties in brain ischemia**. *J Biol Chem* 2006, **281**(21):14961-14970.

Edlich F, Erdmann F, Jarczowski F, Moutty MC, Weiwad M, Fischer G: **The Bcl-2 Regulator FKBP38-Calmodulin-Ca^{2+} Is Inhibited by Hsp90.** *J Biol Chem* 2007, **282**(21): 15341-15348.

Elbashir SM, Harborth J, Lendeckel W, Yalcin A, Weber K, Tuschl T: **Duplexes of 21-nucleotide RNAs mediate RNA interference in cultured mammalian cells**. *Nature* 2001, **411**(6836):494-498.

Elbashir SM, Lendeckel W, Tuschl T: **RNA interference is mediated by 21- and 22-nucleotide RNAs**. *Genes Dev* 2001, **15**(2):188-200.

Enari M, Sakahira H, Yokoyama H, Okawa K, Iwamatsu A, Nagata S: **A caspase-activated DNase that degrades DNA during apoptosis, and its inhibitor ICAD**. *Nature* 1998, **391**(6662):43-50.

Fan Y, Weinstein JN, Kohn KW, Shi LM, Pommier Y: **Molecular modeling studies of the DNA-topoisomerase I ternary cleavable complex with camptothecin**. *J Med Chem* 1998, **41**(13):2216-2226.

Fan Z, Beresford PJ, Oh DY, Zhang D, Lieberman J: **Tumor suppressor NM23-H1 is a granzyme A-activated DNase during CTL-mediated apoptosis, and the nucleosome assembly protein SET is its inhibitor**. *Cell* 2003a, **112**: 659-672.

Fan Z, Beresford PJ, Zhang D, Lieberman J: **HMG2 interacts with the nucleosome assembly protein SET and is a target of the cytotoxic T-lymphocyte protease granzyme A**. *Mol Cell Biol* 2002, **22**:2810-2820.

Fan Z, Beresford PJ, Zhang D, Xu Z, Novina CD, Yoshida A, Pommier Y, Lieberman J: **Cleaving the oxidative repair protein Ape1 enhances cell death mediated by granzyme A**. *Nat Immunol* 2003b, **4**:145-153.

Felgner PL, Gadek TR, Holm M, Roman R, Chan HW, Wenz M, Northrop JP, Ringold GM, Danielsen M: **Lipofection: a highly efficient, lipid-mediated DNA-transfection procedure**. Proc Natl Acad Sci U S A 1987, **84** (21):7413-7417.

Ferri KF, Kroemer G: **Organelle-specific initiation of cell death pathways**. *Nat Cell Biol* 2001, **3**(11):E255-263.

Filippov V, Solovyev V, Filippova M, Gill SS: **A novel type of RNase III family proteins in eukaryotes**. *Gene* 2000, **245**(1):213-221.

Fire A, Xu S, Montgomery MK, Kostas SA, Driver SE, Mello CC: **Potent and specific genetic interference by double-stranded RNA in Caenorhabditis elegans**. *Nature* 1998, **391**(6669):806-811.

Freeman BC, Toft DO, Morimoto RI: **Molecular chaperone machines: chaperone activities of the cyclophilin Cyp-40 and the steroid aporeceptor-associated protein p23**. *Science* 1996, **274**(5293):1718-1720.

French LE, Tschopp J: **Protein-based therapeutic approaches targeting death receptors**. *Cell Death Differ* 2003, **10**(1):117-123.

Furukawa Y, Iwase S, Kikuchi J, Terui Y, Nakamura M, Yamada H, Kano Y, Matsuda M: **Phosphorylation of Bcl-2 protein by CDC2 kinase during G2/M phases and its role in cell cycle regulation**. *J Biol Chem* 2000, **275**(28):21661-21667.

Futami T, Miyagishi M, Seki M, Taira K: **Induction of apoptosis in HeLa cells with siRNA expression vector targeted against bcl-2**. *Nucleic Acids Res Suppl* 2002(2):251-252.

Galat A: **Peptidylproline cis-trans-isomerases: immunophilins**. *Eur J Biochem* 1993, **216**(3):689-707.

Gao G, Dou QP: **G(1) phase-dependent expression of bcl-2 mRNA and protein correlates with chemoresistance of human cancer cells**. *Mol Pharmacol* 2000, **58**(5):1001-1010.

Gautschi O, Tschopp S, Olie RA, Leech SH, Simoes-Wust AP, Ziegler A, Baumann B, Odermatt B, Hall J, Stahel RA *et al*: **Activity of a novel bcl-2/bcl-xL-bispecific antisense oligonucleotide against tumors of diverse histologic origins**. *J Natl Cancer Inst* 2001, **93**(6):463-471.

Germain M, Shore GC: **Cellular distribution of Bcl-2 family proteins**. *Sci STKE* 2003, **2003**(173):pe10.

Gil-Gomez G, Berns A, Brady HJ: **A link between cell cycle and cell death: Bax and Bcl-2 modulate Cdk2 activation during thymocyte apoptosis**. *Embo J* 1998, **17**(24):7209-7218.

Gold BG: **FK506 and the role of the immunophilin FKBP-52 in nerve regeneration**. *Drug Metab Rev* 1999, **31**(3):649-663.

Gompel A, Sabourin JC, Martin A, Yaneva H, Audouin J, Decroix Y, Poitout P: **Bcl-2 expression in normal endometrium during the menstrual cycle**. *Am J Pathol* 1994, **144**(6):1195-1202.

Gottschalk AR, Boise LH, Thompson CB, Quintans J: **Identification of immunosuppressant-induced apoptosis in a murine B-cell line and its prevention by bcl-x but not bcl-2**. *Proc Natl Acad Sci U S A* 1994, **91**(15):7350-7354.

Green DR, Reed JC: **Mitochondria and apoptosis**. *Science* 1998, **281**(5381):1309-1312.

Greider C, Chattopadhyay A, Parkhurst C, Yang E: **BCL-x(L) and BCL2 delay Myc-induced cell cycle entry through elevation of p27 and inhibition of G1 cyclin-dependent kinases**. *Oncogene* 2002, **21**(51):7765-7775.

Griffiths GJ, Dubrez L, Morgan CP, Jones NA, Whitehouse J, Corfe BM, Dive C, Hickman JA: **Cell damage-induced conformational changes of the pro-apoptotic**

protein Bak in vivo precede the onset of apoptosis. *J Cell Biol* 1999, **144**(5):903-914.

Grigg JM, Savill JS, Sarraf C, Haslett C, Silverman M: **Neutrophil apoptosis and clearance from neonatal lungs**. *Lancet* 1991, **338**(8769):720-722.

Gross A, McDonnell JM, Korsmeyer SJ: **BCL-2 family members and the mitochondria in apoptosis**. *Genes Dev* 1999, **13**(15):1899-1911.

Gschwind M, Huber G: **Apoptotic cell death induced by beta-amyloid 1-42 peptide is cell type dependent**. *J Neurochem* 1995, **65**(1):292-300.

Gu Q, Wang JD, Xia HH, Lin MC, He H, Zou B, Tu SP, Yang Y, Liu XG, Lam SK *et al*: **Activation of the caspase-8/Bid and Bax pathways in aspirin-induced apoptosis in gastric cancer**. *Carcinogenesis* 2005, **26**(3):541-546.

Hacki J, Egger L, Monney L, Conus S, Rosse T, Fellay I, Borner C: **Apoptotic crosstalk between the endoplasmic reticulum and mitochondria controlled by Bcl-2**. *Oncogene* 2000, **19**(19):2286-2295.

Haldar S, Basu A, Croce CM: **Serine-70 is one of the critical sites for drug-induced Bcl2 phosphorylation in cancer cells**. *Cancer Res* 1998, **58**(8):1609-1615.

Halestrap AP: **The mitochondrial permeability transition: its molecular mechanism and role in reperfusion injury**. *Biochem Soc Symp* 1999, **66**:181-203.

Hammond SM, Caudy AA, Hannon GJ: **Post-transcriptional gene silencing by double-stranded RNA**. *Nat Rev Genet* 2001, **2**(2):110-119.

Hannon GJ: **RNA interference**. *Nature* 2002, **418**(6894):244-251.

Harding HP, Zhang Y, Ron D: **Protein translation and folding are coupled by an endoplasmic-reticulum-resident kinase**. *Nature* 1999, **397**(6716):271-274.

Harding MW, Galat A, Uehling DE, Schreiber SL: **A receptor for the immunosuppressant FK506 is a cis-trans peptidyl-prolyl isomerase**. *Nature* 1989, **341**(6244):758-760.

Heimlich G, McKinnon AD, Bernardo K, Brdiczka D, Reed JC, Kain R, Kronke M, Jurgensmeier JM: **Bax-induced cytochrome c release from mitochondria depends on alpha-helices-5 and -6**. *Biochem J* 2004, **378**(Pt 1):247-255.

Hengartner MO: **The biochemistry of apoptosis**. *Nature* 2000, **407**(6805):770-776.

Hockenbery D, Nunez G, Milliman C, Schreiber RD, Korsmeyer SJ: **Bcl-2 is an inner mitochondrial membrane protein that blocks programmed cell death**. *Nature* 1990, **348**(6299):334-336.

Hsu YT, Wolter KG, Youle RJ: **Cytosol-to-membrane redistribution of Bax and Bcl-X(L) during apoptosis**. *Proc Natl Acad Sci U S A* 1997, **94**(8):3668-3672.

Huang DC, O'Reilly LA, Strasser A, Cory S: **The anti-apoptosis function of Bcl-2 can be genetically separated from its inhibitory effect on cell cycle entry**. *Embo J* 1997, **16**(15):4628-4638.

Huang ST, Cidlowski JA: **Phosphorylation status modulates Bcl-2 function during glucocorticoid-induced apoptosis in T lymphocytes**. *Faseb J* 2002, **16**(8):825-832.

Hunter JJ, Bond BL, Parslow TG: **Functional dissection of the human Bc12 protein: sequence requirements for inhibition of apoptosis**. *Mol Cell Biol* 1996, **16**(3):877-883.

Ilmonen S, Hernberg M, Pyrhonen S, Tarkkanen J, Asko-Seljavaara S: **Ki-67, Bcl-2 and p53 expression in primary and metastatic melanoma**. *Melanoma Res* 2005, **15**(5):375-381.

Inoue S, Salah-Eldin AE, Omoteyama K: **Apoptosis and anticancer drug resistance**. *Hum Cell* 2001, **14**(3):211-221.

Ito T, Deng X, Carr B, May WS: **Bcl-2 phosphorylation required for anti-apoptosis function**. *J Biol Chem* 1997, **272**(18):11671-11673.

Jang JH, Surh YJ: **Potentiation of cellular antioxidant capacity by Bcl-2: implications for its antiapoptotic function**. *Biochem Pharmacol* 2003, **66**(8):1371-1379.

Janumyan YM, Sansam CG, Chattopadhyay A, Cheng N, Soucie EL, Penn LZ, Andrews D, Knudson CM, Yang E: **Bcl-xL/Bcl-2 coordinately regulates apoptosis, cell cycle arrest and cell cycle entry**. *Embo J* 2003, **22**(20):5459-5470.

Jin YJ, Albers MW, Lane WS, Bierer BE, Schreiber SL, Burakoff SJ: **Molecular cloning of a membrane-associated human FK506- and rapamycin-binding protein, FKBP-13**. *Proc Natl Acad Sci U S A* 1991, **88**(15):6677-6681.

Jin YJ, Burakoff SJ, Bierer BE: **Molecular cloning of a 25-kDa high affinity rapamycin binding protein, FKBP25**. *J Biol Chem* 1992, **267**(16):10942-10945.

Jin YJ, Burakoff SJ: **The 25-kDa FK506-binding protein is localized in the nucleus and associates with casein kinase II and nucleolin**. *Proc Natl Acad Sci U S A* 1993, **90**(16):7769-7773.

Kang CB, Tai J, Chia J, Yoon HS: **The flexible loop of Bcl-2 is required for molecular interaction with immunosuppressant FK-506 binding protein 38 (FKBP38)**. *FEBS Lett* 2005, **579**(6):1469-1476.

Kannan K, Jain SK: **Oxidative stress and apoptosis**. *Pathophysiology* 2000, **7**(3):153-163.

Karpova TS, Baumann CT, He L, Wu X, Grammer A, Lipsky P, Hager GL, McNally JG: **Fluorescence resonance energy transfer from cyan to yellow fluorescent protein detected by acceptor photobleaching using confocal microscopy and a single laser**. *J Microsc* 2003, **209**(Pt 1):56-70.

Kaufman RJ: **Orchestrating the unfolded protein response in health and disease**. *J Clin Invest* 2002, **110**(10):1389-1398.

Kaufmann SH, Desnoyers S, Ottaviano Y, Davidson NE, Poirier GG: **Specific proteolytic cleavage of poly(ADP-ribose) polymerase: an early marker of chemotherapy-induced apoptosis**. *Cancer Res* 1993, **53**(17):3976-3985.

Keller JN, Guo Q, Holtsberg FW, Bruce-Keller AJ, Mattson MP: **Increased sensitivity to mitochondrial toxin-induced apoptosis in neural cells expressing mutant presenilin-1 is linked to perturbed calcium homeostasis and enhanced oxyradical production**. *J Neurosci* 1998, **18**(12):4439-4450.

Kerr JF, Wyllie AH, Currie AR: **Apoptosis: a basic biological phenomenon with wide-ranging implications in tissue kinetics**. *Br J Cancer* 1972, **26**(4):239-257.

Kim VN: **MicroRNA biogenesis: coordinated cropping and dicing**. *Nat Rev Mol Cell Biol* 2005, **6**(5):376-385.

King KL, Cidlowski JA: **Cell cycle and apoptosis: common pathways to life and death**. *J Cell Biochem* 1995, **58**(2):175-180.

King KL, Cidlowski JA: **Cell cycle regulation and apoptosis**. *Annu Rev Physiol* 1998, **60**:601-617.

Kirsch DG, Doseff A, Chau BN, Lim DS, de Souza-Pinto NC, Hansford R, Kastan MB, Lazebnik YA, Hardwick JM: **Caspase-3-dependent cleavage of Bcl-2 promotes release of cytochrome c**. *J Biol Chem* 1999, **274**(30):21155-21161.

Klee CB, Crouch TH, Krinks MH: **Calcineurin: a calcium- and calmodulin-binding protein of the nervous system**. *Proc Natl Acad Sci U S A* 1979, **76**(12):6270-6273.

Korsmeyer SJ, Wei MC, Saito M, Weiler S, Oh KJ, Schlesinger PH: **Pro-apoptotic cascade activates BID, which oligomerizes BAK or BAX into pores that result in the release of cytochrome c**. *Cell Death Differ* 2000, **7**(12):1166-1173.

Krajewski S, Tanaka S, Takayama S, Schibler MJ, Fenton W, Reed JC: **Investigation of the subcellular distribution of the bcl-2 oncoprotein: residence in the nuclear envelope, endoplasmic reticulum, and outer mitochondrial membranes**. *Cancer Res* 1993, **53**(19):4701-4714.

Kruger K, Grabowski PJ, Zaug AJ, Sands J, Gottschling DE, Cech TR: **Self-splicing RNA: autoexcision and autocyclization of the ribosomal RNA intervening sequence of Tetrahymena**. *Cell* 1982, **31**(1):147-157.

Kuwana T, Mackey MR, Perkins G, Ellisman MH, Latterich M, Schneiter R, Green DR, Newmeyer DD: **Bid, Bax, and lipids cooperate to form supramolecular openings in the outer mitochondrial membrane**. *Cell* 2002, **111**(3):331-342.

Kuwana T, Smith JJ, Muzio M, Dixit V, Newmeyer DD, Kornbluth S: **Apoptosis induction by caspase-8 is amplified through the mitochondrial release of cytochrome c**. *J Biol Chem* 1998, **273**(26):16589-16594.

Lam E, Martin M, Wiederrecht G: **Isolation of a cDNA encoding a novel human FK506-binding protein homolog containing leucine zipper and tetratricopeptide repeat motifs**. *Gene* 1995, **160**(2):297-302.

Lam M, Dubyak G, Chen L, Nunez G, Miesfeld RL, Distelhorst CW: **Evidence that BCL-2 represses apoptosis by regulating endoplasmic reticulum-associated Ca2+ fluxes**. *Proc Natl Acad Sci U S A* 1994, **91**(14):6569-6573.

Lamb JR, Tugendreich S, Hieter P: **Tetratrico peptide repeat interactions: to TPR or not to TPR?** *Trends Biochem Sci* 1995, **20**(7):257-259.

Laudon H, Hansson EM, Melen K, Bergman A, Farmery MR, Winblad B, Lendahl U, von Heijne G, Naslund J: **A nine-transmembrane domain topology for presenilin 1**. *J Biol Chem* 2005, **280**(42):35352-35360.

Lavrik I, Golks A, Krammer PH: **Death receptor signaling**. *J Cell Sci* 2005, **118**(Pt 2):265-267.

Lebeau MC, Myagkikh I, Rouviere-Fourmy N, Baulieu EE, Klee CB: **Rabbit FKBP-59/HBI does not inhibit calcineurin activity in vitro**. *Biochem Biophys Res Commun* 1994, **203**(2):750-755.

Leem JY, Saura CA, Pietrzik C, Christianson J, Wanamaker C, King LT, Veselits ML, Tomita T, Gasparini L, Iwatsubo T *et al*: **A role for presenilin 1 in regulating the delivery of amyloid precursor protein to the cell surface**. *Neurobiol Dis* 2002, **11**(1):64-82.

Leu JI, Dumont P, Hafey M, Murphy ME, George DL: **Mitochondrial p53 activates Bak and causes disruption of a Bak-Mcl1 complex**. *Nat Cell Biol* 2004, **6**(5):443-450.

Levitan D, Greenwald I: **Facilitation of lin-12-mediated signalling by sel-12, a Caenorhabditis elegans S182 Alzheimer's disease gene**. *Nature* 1995, **377**(6547):351-354.

Li H, Kolluri SK, Gu J, Dawson MI, Cao X, Hobbs PD, Lin B, Chen G, Lu J, Lin F *et al*: **Cytochrome c release and apoptosis induced by mitochondrial targeting of nuclear orphan receptor TR3**. *Science* 2000, **289**(5482):1159-1164.

Li LY, Luo X, Wang X: **Endonuclease G is an apoptotic DNase when released from mitochondria**. *Nature* 2001, **412**(6842):95-99.

Lin B, Kolluri SK, Lin F, Liu W, Han YH, Cao X, Dawson MI, Reed JC, Zhang XK: **Conversion of Bcl-2 from protector to killer by interaction with nuclear orphan receptor Nur77/TR3**. *Cell* 2004, **116**(4):527-540.

Linette GP, Li Y, Roth K, Korsmeyer SJ: **Cross talk between cell death and cell cycle progression: BCL-2 regulates NFAT-mediated activation**. *Proc Natl Acad Sci U S A* 1996, **93**(18):9545-9552.

Linjawi A, Kontogiannea M, Halwani F, Edwardes M, Meterissian S: **Prognostic significance of p53, bcl-2, and Bax expression in early breast cancer**. *J Am Coll Surg* 2004, **198**(1):83-90.

Liu J, Farmer JD, Jr., Lane WS, Friedman J, Weissman I, Schreiber SL: **Calcineurin is a common target of cyclophilin-cyclosporin A and FKBP-FK506 complexes**. *Cell* 1991, **66**(4):807-815.

Liu SL, Lin X, Shi DY, Cheng J, Wu CQ, Zhang YD: **Reactive oxygen species stimulated human hepatoma cell proliferation via cross-talk between PI3-K/PKB and JNK signaling pathways**. *Arch Biochem Biophys* 2002, **406**(2):173-182.

Liu X, Kim CN, Yang J, Jemmerson R, Wang X: **Induction of apoptotic program in cell-free extracts: requirement for dATP and cytochrome c**. *Cell* 1996, **86**(1):147-157.

Liu Y, Fiskum G, Schubert D: **Generation of reactive oxygen species by the mitochondrial electron transport chain**. *J Neurochem* 2002, **80**(5):780-787.

Luo D, Cheng SC, Xie Y: **Expression of Bcl-2 family proteins during chemotherapeutic agents-induced apoptosis in the hepatoblastoma HepG2 cell line**. *Br J Biomed Sci* 1999, **56**(2):114-122.

Luo KQ, Chang DC: **The gene-silencing efficiency of siRNA is strongly dependent on the local structure of mRNA at the targeted region**. *Biochem Biophys Res Commun* 2004, **318**(1):303-310.

MacFarlane M, Williams AC: **Apoptosis and disease: a life or death decision**. *EMBO Rep* 2004, **5**(7):674-678.

Manche L, Green SR, Schmedt C, Mathews MB: **Interactions between double-stranded RNA regulators and the protein kinase DAI**. *Mol Cell Biol* 1992, **12**(11):5238-5248.

Mangelsdorf DJ, Thummel C, Beato M, Herrlich P, Schutz G, Umesono K, Blumberg B, Kastner P, Mark M, Chambon P *et al*: **The nuclear receptor superfamily: the second decade**. *Cell* 1995, **83**(6):835-839.

Manser E, Huang HY, Loo TH, Chen XQ, Dong JM, Leung T, Lim L: **Expression of constitutively active alpha-PAK reveals effects of the kinase on actin and focal complexes**. *Mol Cell Biol* 1997, **17**(3):1129-1143.

Marchenko ND, Zaika A, Moll UM: **Death signal-induced localization of p53 protein to mitochondria. A potential role in apoptotic signaling**. *J Biol Chem* 2000, **275**(21):16202-16212.

Marciniak SJ, Yun CY, Oyadomari S, Novoa I, Zhang Y, Jungreis R, Nagata K, Harding HP, Ron D: **CHOP induces death by promoting protein synthesis and oxidation in the stressed endoplasmic reticulum**. *Genes Dev* 2004, **18**(24):3066-3077.

Martinvalet D, Zhu PC, Lieberman J: **Granzyme A induces caspase-independent mitochondrial damage, a required first step for apoptosis**. *Immunity* 2005, **22** (3):355-370.

Masunaga A, Arai T, Yoshitake T, Itoyama S, Sugawara I: **Reduced expression of apoptosis-related antigens in thymuses from patients with myasthenia gravis**. *Immunol Lett* 1994, **39**(2):169-172.

Mazel S, Burtrum D, Petrie HT: **Regulation of cell division cycle progression by bcl-2 expression: a potential mechanism for inhibition of programmed cell death**. *J Exp Med* 1996, **183**(5):2219-2226.

McCullough KD, Martindale JL, Klotz LO, Aw TY, Holbrook NJ: **Gadd153 sensitizes cells to endoplasmic reticulum stress by down-regulating Bcl2 and perturbing the cellular redox state**. *Mol Cell Biol* 2001, **21**(4):1249-1259.

McDonnell TJ, Deane N, Platt FM, Nunez G, Jaeger U, McKearn JP, Korsmeyer SJ: **bcl-2-immunoglobulin transgenic mice demonstrate extended B cell survival and follicular lymphoproliferation**. *Cell* 1989, **57**(1):79-88.

McIlroy D, Sakahira H, Talanian RV, Nagata S: **Involvement of caspase 3-activated DNase in internucleosomal DNA cleavage induced by diverse apoptotic stimuli**. *Oncogene* 1999, **18**(31):4401-4408.

Medema JP, Scaffidi C, Kischkel FC, Shevchenko A, Mann M, Krammer PH, Peter ME: **FLICE is activated by association with the CD95 death-inducing signaling complex (DISC)**. *Embo J* 1997, **16**(10):2794-2804.

Meier P, Finch A, Evan G: **Apoptosis in development**. *Nature* 2000, **407**(6805):796-801.

Meister G, Tuschl T: **Mechanisms of gene silencing by double-stranded RNA**. *Nature* 2004, **431**(7006):343-349.

Meterissian SH, Kontogiannea M, Al-Sowaidi M, Linjawi A, Halwani F, Jamison B, Edwardes M: **Bcl-2 is a useful prognostic marker in Dukes' B colon cancer**. *Ann Surg Oncol* 2001, **8**(6):533-537.

Mikolajczyk M, Nelson MA: **Regulation of stability of cyclin-dependent kinase CDK11p110 and a caspase-processed form, CDK11p46, by Hsp90**. *Biochem J* 2004, **384**(Pt 3):461-467.

Milligan CE, Schwartz LM: **Programmed cell death during animal development**. *Br Med Bull* 1997, **53**(3):570-590.

Minks MA, West DK, Benvin S, Baglioni C: **Structural requirements of double-stranded RNA for the activation of 2',5'-oligo(A) polymerase and protein kinase of interferon-treated HeLa cells**. *J Biol Chem* 1979, **254**(20):10180-10183.

Minn AJ, Velez P, Schendel SL, Liang H, Muchmore SW, Fesik SW, Fill M, Thompson CB: **Bcl-x(L) forms an ion channel in synthetic lipid membranes**. *Nature* 1997, **385**(6614):353-357.

Morgan DO: **Principles of CDK regulation**. *Nature* 1995, **374**(6518):131-134.

Mosmann T: **Rapid colorimetric assay for cellular growth and survival: application to proliferation and cytotoxicity assays**. *J Immunol Methods* 1983, **65**(1-2):55-63.

Muzio M, Salvesen GS, Dixit VM: **FLICE induced apoptosis in a cell-free system. Cleavage of caspase zymogens**. *J Biol Chem* 1997, **272**(5):2952-2956.

Nagata S: **Apoptosis by death factor**. *Cell* 1997, **88**(3):355-365.

Nahta R, Esteva FJ: **Bcl-2 antisense oligonucleotides: a potential novel strategy for the treatment of breast cancer**. *Semin Oncol* 2003, **30**(5 Suppl 16):143-149.

Nakagawa T, Zhu H, Morishima N, Li E, Xu J, Yankner BA, Yuan J: **Caspase-12 mediates endoplasmic-reticulum-specific apoptosis and cytotoxicity by amyloid-beta**. *Nature* 2000, **403**(6765):98-103.

Nechushtan A, Smith CL, Hsu YT, Youle RJ: **Conformation of the Bax C-terminus regulates subcellular location and cell death**. *Embo J* 1999, **18**(9):2330-2341.

Newcomb EW: **P53 gene mutations in lymphoid diseases and their possible relevance to drug resistance**. *Leuk Lymphoma* 1995, **17**(3-4):211-221.

Norbury C, Nurse P: **Animal cell cycles and their control**. *Annu Rev Biochem* 1992, **61**:441-470.

Nykanen A, Haley B, Zamore PD: **ATP requirements and small interfering RNA structure in the RNA interference pathway**. *Cell* 2001, **107**(3):309-321.

Oliver FJ, Menissier-de Murcia J, de Murcia G: **Poly(ADP-ribose) polymerase in the cellular response to DNA damage, apoptosis, and disease**. *Am J Hum Genet* 1999, **64**(5):1282-1288.

Oltvai ZN, Milliman CL, Korsmeyer SJ: **Bcl-2 heterodimerizes in vivo with a conserved homolog, Bax, that accelerates programmed cell death**. *Cell* 1993, **74**(4):609-619.

Omi K, Tokunaga K, Hohjoh H: **Long-lasting RNAi activity in mammalian neurons**. *FEBS Lett* 2004, **558**(1-3):89-95.

Papadopoulos MC, Koumenis IL, Xu L, Giffard RG: **Potentiation of murine astrocyte antioxidant defence by bcl-2: protection in part reflects elevated glutathione levels**. *Eur J Neurosci* 1998, **10**(4):1252-1260.

Pedersen KM, Finsen B, Celis JE, Jensen NA: **muFKBP38: a novel murine immunophilin homolog differentially expressed in Schwannoma cells and central nervous system neurons in vivo**. *Electrophoresis* 1999, **20**(2):249-255.

Pellicer A, Wigler M, Axel R, Silverstein S: **The transfer and stable integration of the HSV thymidine kinase gene into mouse cells**. *Cell* 1978, **14**: 131-141

Persengiev SP, Zhu X, Green MR: **Nonspecific, concentration-dependent stimulation and repression of mammalian gene expression by small interfering RNAs (siRNAs)**. *Rna* 2004, **10**(1):12-18.

Peter ME, Krammer PH: **The CD95(APO-1/Fas) DISC and beyond**. *Cell Death Differ* 2003, **10**(1):26-35.

Peterson CL, Cote J: **Cellular machineries for chromosomal DNA repair**. *Genes Dev* 2004, **18**(6):602-616.

Petros AM, Medek A, Nettesheim DG, Kim DH, Yoon HS, Swift K, Matayoshi ED, Oltersdorf T, Fesik SW: **Solution structure of the antiapoptotic protein bcl-2**. *Proc Natl Acad Sci U S A* 2001, **98**(6):3012-3017.

Pisha E, Chai H, Lee IS, Chagwedera TE, Farnsworth NR, Cordell GA, Beecher CW, Fong HH, Kinghorn AD, Brown DM *et al*: **Discovery of betulinic acid as a selective inhibitor of human melanoma that functions by induction of apoptosis**. *Nat Med* 1995, **1**(10):1046-1051.

Portier BP, Taglialatela G: **Bcl-2 localizaed at the nuclear compartment induces apoptosis after transient overexpression.** *J Biol Chem* 2006, **281**(52):40493-40502.

Pratt WB: **The role of heat shock proteins in regulating the function, folding, and trafficking of the glucocorticoid receptor**. *J Biol Chem* 1993, **268**(29):21455-21458.

Radanyi C, Chambraud B, Baulieu EE: **The ability of the immunophilin FKBP59-HBI to interact with the 90-kDa heat shock protein is encoded by its tetratricopeptide repeat domain**. *Proc Natl Acad Sci U S A* 1994, **91**(23):11197-11201.

Raha S, Robinson BH: **Mitochondria, oxygen free radicals, and apoptosis**. *Am J Med Genet* 2001, **106**(1):62-70.

Rand TA, Petersen S, Du F, Wang X: **Argonaute2 cleaves the anti-guide strand of siRNA during RISC activation**. *Cell* 2005, **123**(4):621-629.

Ratajczak T, Carrello A, Mark PJ, Warner BJ, Simpson RJ, Moritz RL, House AK: **The cyclophilin component of the unactivated estrogen receptor contains a tetratricopeptide repeat domain and shares identity with p59 (FKBP59)**. *J Biol Chem* 1993, **268**(18):13187-13192.

Reed JC, Tsujimoto Y, Alpers JD, Croce CM, Nowell PC: **Regulation of bcl-2 proto-oncogene expression during normal human lymphocyte proliferation**. *Science* 1987, **236**(4806):1295-1299.

Reed JC: **Bcl-2 family proteins: regulators of apoptosis and chemoresistance in hematologic malignancies**. *Semin Hematol* 1997, **34**(4 Suppl 5):9-19.

Reed JC: **Bcl-2: prevention of apoptosis as a mechanism of drug resistance**. *Hematol Oncol Clin North Am* 1995, **9**(2):451-473.

Reers M, Smiley ST, Mottola-Hartsborn C, Chen A, Lin M, Chen LB: **Mitochondrial membrane potential monitored by JC-1 dye**. Methods Enzymol 1995, **260**: 406-417.

Reutelingsperger CP: **Annexins: key regulators of haemostasis, thrombosis, and apoptosis**. *Thromb Haemost* 2001, **86**(1):413-419.

Ribbeck K, Gorlich D. **Kinetic analysis of translocation through nuclear pore complexes**. *EMBO J* 2001, **20**: 1320–1330.

Riggs DL, Roberts PJ, Chirillo SC, Cheung-Flynn J, Prapapanich V, Ratajczak T, Gaber R, Picard D, Smith DF: **The Hsp90-binding peptidylprolyl isomerase FKBP52 potentiates glucocorticoid signaling in vivo**. *Embo J* 2003, **22**(5):1158-1167.

Riviere S, Menez A, Galat A: **On the localization of FKBP25 in T-lymphocytes**. *FEBS Lett* 1993, **315**(3):247-251.

Rosner M, Hofer K, Kubista M, Hengstschlager M: **Cell size regulation by the human TSC tumor suppressor proteins depends on PI3K and FKBP38**. *Oncogene* 2003, **22**(31):4786-4798.

Roucou X, Montessuit S, Antonsson B, Martinou JC: **Bax oligomerization in mitochondrial membranes requires tBid (caspase-8-cleaved Bid) and a mitochondrial protein**. *Biochem J* 2002, **368**(Pt 3):915-921.

Rubin LL, Philpott KL, Brooks SF: **Apoptosis: the cell cycle and cell death**. *Curr Biol* 1993, **3**(6):391-394.

Rudel T, Bokoch GM: **Membrane and morphological changes in apoptotic cells regulated by caspase-mediated activation of PAK2**. *Science* 1997, **276**(5318):1571-1574.

Ruff VA, Yem AW, Munns PL, Adams LD, Reardon IM, Deibel MR, Jr., Leach KL: **Tissue distribution and cellular localization of hsp56, an FK506-binding protein. Characterization using a highly specific polyclonal antibody**. *J Biol Chem* 1992, **267**(30):21285-21288.

Ruvolo PP, Deng X, May WS: **Phosphorylation of Bcl2 and regulation of apoptosis**. *Leukemia* 2001, **15**(4):515-522.

Ruvolo PP, Deng X, May WS: **Phosphorylation of Bcl2 and regulation of apoptosis**. *Leukemia* 2001, **15**(4):515-522.

Sakahira H, Enari M, Nagata S: **Cleavage of CAD inhibitor in CAD activation and DNA degradation during apoptosis**. *Nature* 1998, **391**(6662):96-99.

Sartorius UA, Krammer PH: **Upregulation of Bcl-2 is involved in the mediation of chemotherapy resistance in human small cell lung cancer cell lines**. *Int J Cancer* 2002, **97**(5):584-592.

Sattler M, Liang H, Nettesheim D, Meadows RP, Harlan JE, Eberstadt M, Yoon HS, Shuker SB, Chang BS, Minn AJ *et al*: **Structure of Bcl-xL-Bak peptide complex: recognition between regulators of apoptosis**. *Science* 1997, **275**(5302):983-986.

Schendel SL, Xie Z, Montal MO, Matsuyama S, Montal M, Reed JC: **Channel formation by antiapoptotic protein Bcl-2**. *Proc Natl Acad Sci U S A* 1997, **94**(10):5113-5118.

Schiene-Fischer C, Yu C: **Receptor accessory folding helper enzymes: the functional role of peptidyl prolyl cis/trans isomerases**. *FEBS Lett* 2001, **495**(1-2):1-6.

Schlesinger PH, Gross A, Yin XM, Yamamoto K, Saito M, Waksman G, Korsmeyer SJ: **Comparison of the ion channel characteristics of proapoptotic BAX and antiapoptotic BCL-2**. *Proc Natl Acad Sci U S A* 1997, **94**(21):11357-11362.

Schreiber SL: **Chemistry and biology of the immunophilins and their immunosuppressive ligands**. *Science* 1991, **251**(4991):283-287.

Schroder M, Kaufman RJ: **ER stress and the unfolded protein response**. *Mutat Res* 2005, **569**(1-2):29-63.

Schwartz SM: **Cell death and the caspase cascade**. *Circulation* 1998, **97**(3):227-229.

Scorrano L, Oakes SA, Opferman JT, Cheng EH, Sorcinelli MD, Pozzan T, Korsmeyer SJ: **BAX and BAK regulation of endoplasmic reticulum Ca2+: a control point for apoptosis**. *Science* 2003, **300**(5616):135-139.

Shaw P, Bovey R, Tardy S, Sahli R, Sordat B, Costa J: **Induction of apoptosis by wild-type p53 in a human colon tumor-derived cell line**. *Proc Natl Acad Sci U S A* 1992, **89**(10):4495-4499.

Shen WG: **RNA interference and its current application in mammals**. *Chin Med J (Engl)* 2004, **117**(7):1084-1091.

Shibasaki F, Kondo E, Akagi T, McKeon F: **Suppression of signalling through transcription factor NF-AT by interactions between calcineurin and Bcl-2**. *Nature* 1997, **386**(6626):728-731.

Shimizu S, Eguchi Y, Kamiike W, Funahashi Y, Mignon A, Lacronique V, Matsuda H, Tsujimoto Y: **Bcl-2 prevents apoptotic mitochondrial dysfunction by regulating proton flux**. *Proc Natl Acad Sci U S A* 1998, **95**(4):1455-1459.

Shirane M, Nakayama KI: **Inherent calcineurin inhibitor FKBP38 targets Bcl-2 to mitochondria and inhibits apoptosis**. *Nat Cell Biol* 2003, **5**(1):28-37.

Siekierka JJ, Hung SH, Poe M, Lin CS, Sigal NH: **A cytosolic binding protein for the immunosuppressant FK506 has peptidyl-prolyl isomerase activity but is distinct from cyclophilin**. *Nature* 1989, **341**(6244):755-757.

Silverstein AM, Galigniana MD, Chen MS, Owens-Grillo JK, Chinkers M, Pratt WB: **Protein phosphatase 5 is a major component of glucocorticoid receptor.hsp90 complexes with properties of an FK506-binding immunophilin**. *J Biol Chem* 1997, **272**(26):16224-16230.

Simon HU, Haj-Yehia A, Levi-Schaffer F: **Role of reactive oxygen species (ROS) in apoptosis induction**. *Apoptosis* 2000, **5**(5):415-418.

Smith DF, Baggenstoss BA, Marion TN, Rimerman RA: **Two FKBP-related proteins are associated with progesterone receptor complexes**. *J Biol Chem* 1993, **268**(24):18365-18371.

Srinivasula SM, Ahmad M, Fernandes-Alnemri T, Litwack G, Alnemri ES: **Molecular ordering of the Fas-apoptotic pathway: the Fas/APO-1 protease Mch5 is a CrmA-inhibitable protease that activates multiple Ced-3/ICE-like cysteine proteases**. *Proc Natl Acad Sci U S A* 1996, **93**(25):14486-14491.

Srivastava RK, Mi QS, Hardwick JM, Longo DL: **Deletion of the loop region of Bcl-2 completely blocks paclitaxel-induced apoptosis**. *Proc Natl Acad Sci U S A* 1999, **96**(7):3775-3780.

Standaert RF, Galat A, Verdine GL, Schreiber SL: **Molecular cloning and overexpression of the human FK506-binding protein FKBP**. *Nature* 1990, **346**(6285):671-674.

Stark GR, Kerr IM, Williams BR, Silverman RH, Schreiber RD: **How cells respond to interferons**. *Annu Rev Biochem* 1998, **67**:227-264.

Susin SA, Lorenzo HK, Zamzami N, Marzo I, Snow BE, Brothers GM, Mangion J, Jacotot E, Costantini P, Loeffler M *et al*: **Molecular characterization of mitochondrial apoptosis-inducing factor**. *Nature* 1999, **397**(6718):441-446.

Susin SA, Zamzami N, Castedo M, Hirsch T, Marchetti P, Macho A, Daugas E, Geuskens M, Kroemer G: **Bcl-2 inhibits the mitochondrial release of an apoptogenic protease**. *J Exp Med* 1996, **184**(4):1331-1341.

Suzuki M, Youle RJ, Tjandra N: **Structure of Bax: coregulation of dimer formation and intracellular localization**. *Cell* 2000, **103**(4):645-654.

Suzuki YJ, Forman HJ, Sevanian A: **Oxidants as stimulators of signal transduction**. *Free Radic Biol Med* 1997, **22**(1-2):269-285.

Takahashi Y, Ogra Y, Suzuki KT: **Synchronized generation of reactive oxygen species with the cell cycle**. *Life Sci* 2004, **75**(3):301-311.

Tang G: **siRNA and miRNA: an insight into RISCs**. *Trends Biochem Sci* 2005, **30**(2):106-114.

Tenson T, Mankin A: **Antibiotics and the ribosome**. *Mol Microbiol* 2006, **59**(6):1664-1677.

Thomas A, Giesler T, White E: **p53 mediates bcl-2 phosphorylation and apoptosis via activation of the Cdc42/JNK1 pathway**. *Oncogene* 2000, **19**(46):5259-5269.

Thompson CB: **Apoptosis in the pathogenesis and treatment of disease**. *Science* 1995, **267**(5203):1456-1462.

Tsujimoto Y, Cossman J, Jaffe E, Croce CM: **Involvement of the bcl-2 gene in human follicular lymphoma**. *Science* 1985, **228**(4706):1440-1443.

Tsujimoto Y, Finger LR, Yunis J, Nowell PC, Croce CM: **Cloning of the chromosome breakpoint of neoplastic B cells with the t(14;18) chromosome translocation**. *Science* 1984, **226**(4678):1097-1099.

Tsuruta F, Sunayama J, Mori Y, Hattori S, Shimizu S, Tsujimoto Y, Yoshioka K, Masuyama N, Gotoh Y: **JNK promotes Bax translocation to mitochondria through phosphorylation of 14-3-3 proteins**. *Embo J* 2004, **23**(8):1889-1899.

Urano F, Wang X, Bertolotti A, Zhang Y, Chung P, Harding HP, Ron D: **Coupling of stress in the ER to activation of JNK protein kinases by transmembrane protein kinase IRE1**. *Science* 2000, **287**(5453):664-666.

Vairo G, Soos TJ, Upton TM, Zalvide J, DeCaprio JA, Ewen ME, Koff A, Adams JM: **Bcl-2 retards cell cycle entry through p27(Kip1), pRB relative p130, and altered E2F regulation**. *Mol Cell Biol* 2000, **20**(13):4745-4753.

Vander Heiden MG, Chandel NS, Williamson EK, Schumacker PT, Thompson CB: **Bcl-xL regulates the membrane potential and volume homeostasis of mitochondria**. *Cell* 1997, **91**(5):627-637.

Veis DJ, Sorenson CM, Shutter JR, Korsmeyer SJ: **Bcl-2-deficient mice demonstrate fulminant lymphoid apoptosis, polycystic kidneys, and hypopigmented hair**. *Cell* 1993, **75**(2):229-240.

Vermes I, Haanen C, Steffens-Nakken H, Reutelingsperger C: **A novel assay for apoptosis. Flow cytometric detection of phosphatidylserine expression on early apoptotic cells using fluorescein labelled Annexin V**. *J Immunol Methods* 1995, **184**(1):39-51.

Violette S, Poulain L, Dussaulx E, Pepin D, Faussat AM, Chambaz J, Lacorte JM, Staedel C, Lesuffleur T: **Resistance of colon cancer cells to long-term 5-fluorouracil exposure is correlated to the relative level of Bcl-2 and Bcl-X(L) in addition to Bax and p53 status**. *Int J Cancer* 2002, **98**(4):498-504.

Voehringer DW, McConkey DJ, McDonnell TJ, Brisbay S, Meyn RE: **Bcl-2 expression causes redistribution of glutathione to the nucleus**. *Proc Natl Acad Sci U S A* 1998, **95**(6):2956-2960.

Voinnet O, Vain P, Angell S, Baulcombe DC: **Systemic spread of sequence-specific transgene RNA degradation in plants is initiated by localized introduction of ectopic promoterless DNA**. *Cell* 1998, **95**(2):177-187.

Wang HQ, Nakaya Y, Du Z, Yamane T, Shirane M, Kudo T, Takeda M, Takebayashi K, Noda Y, Nakayama KI *et al*: **Interaction of presenilins with FKBP38 promotes apoptosis by reducing mitochondrial Bcl-2**. *Hum Mol Genet* 2005, **14**(13):1889-1902.

Wang K, Yin XM, Chao DT, Milliman CL, Korsmeyer SJ: **BID: a novel BH3 domain-only death agonist**. *Genes Dev* 1996, **10**(22):2859-2869.

Wang X: **The expanding role of mitochondria in apoptosis**. *Genes Dev* 2001, **15**(22):2922-2933.

Watson AJ: **Necrosis and apoptosis in the gastrointestinal tract**. *Gut* 1995, **37**(2):165-167.

Webb A, Cunningham D, Cotter F, Clarke PA, di Stefano F, Ross P, Corbo M, Dziewanowska Z: **BCL-2 antisense therapy in patients with non-Hodgkin lymphoma**. *Lancet* 1997, **349**(9059):1137-1141.

Wei MC, Lindsten T, Mootha VK, Weiler S, Gross A, Ashiya M, Thompson CB, Korsmeyer SJ: **tBID, a membrane-targeted death ligand, oligomerizes BAK to release cytochrome c**. *Genes Dev* 2000, **14**(16):2060-2071.

Weiwad M, Edlich F, Erdmann F, Jarczowski F, Kilka S, Dorn M, Pechstein A, Fischer G: **A reassessment of the inhibitory capacity of human FKBP38 on calcineurin**. *FEBS Lett* 2005, **579**(7):1591-1596.

Wolter KG, Hsu YT, Smith CL, Nechushtan A, Xi XG, Youle RJ: **Movement of Bax from the cytosol to mitochondria during apoptosis**. *J Cell Biol* 1997, **139**(5):1281-1292.

Wong GH, Goeddel DV: **Induction of manganous superoxide dismutase by tumor necrosis factor: possible protective mechanism**. *Science* 1988, **242**(4880):941-944.

Woolley KL, Gibson PG, Carty K, Wilson AJ, Twaddell SH, Woolley MJ: **Eosinophil apoptosis and the resolution of airway inflammation in asthma**. *Am J Respir Crit Care Med* 1996, **154**(1):237-243.

Wu P, Brand L: **Resonance energy transfer: methods and applications**. *Anal Biochem* 1994, **218**(1):1-13.

Yaglom JA, Goldberg AL, Finley D, Sherman MY: **The molecular chaperone Ydj1 is required for the p34CDC28-dependent phosphorylation of the cyclin Cln3 that signals its degradation**. *Mol Cell Biol* 1996, **16**(7):3679-3684.

Yang E, Zha J, Jockel J, Boise LH, Thompson CB, Korsmeyer SJ: **Bad, a heterodimeric partner for Bcl-XL and Bcl-2, displaces Bax and promotes cell death**. *Cell* 1995, **80**(2):285-291.

Yem AW, Tomasselli AG, Heinrikson RL, Zurcher-Neely H, Ruff VA, Johnson RA, Deibel MR, Jr.: **The Hsp56 component of steroid receptor complexes binds to immobilized FK506 and shows homology to FKBP-12 and FKBP-13**. *J Biol Chem* 1992, **267**(5):2868-2871.

Yin XM, Oltvai ZN, Korsmeyer SJ: **BH1 and BH2 domains of Bcl-2 are required for inhibition of apoptosis and heterodimerization with Bax**. *Nature* 1994, **369**(6478):321-323.

Yoneda T, Imaizumi K, Oono K, Yui D, Gomi F, Katayama T, Tohyama M: **Activation of caspase-12, an endoplastic reticulum (ER) resident caspase, through tumor necrosis factor receptor-associated factor 2-dependent mechanism in response to the ER stress**. *J Biol Chem* 2001, **276**(17):13935-13940.

Yonish-Rouach E, Resnitzky D, Lotem J, Sachs L, Kimchi A, Oren M: **Wild-type p53 induces apoptosis of myeloid leukaemic cells that is inhibited by interleukin-6**. *Nature* 1991, **352**(6333):345-347.

Youn CK, Cho HJ, Kim SH, Kim HB, Kim MH, Chang IY, Lee JS, Chung MH, Hahm KS, You HJ: **Bcl-2 expression suppresses mismatch repair activity through inhibition of E2F transcriptional activity**. *Nat Cell Biol* 2005, **7**(2):137-147.

Zamble DB, Lippard SJ: **Cisplatin and DNA repair in cancer chemotherapy**. *Trends Biochem Sci* 1995, **20**(10):435-439.

Zamzami N, Marchetti P, Castedo M, Decaudin D, Macho A, Hirsch T, Susin SA, Petit PX, Mignotte B, Kroemer G: **Sequential reduction of mitochondrial transmembrane potential and generation of reactive oxygen species in early programmed cell death**. *J Exp Med* 1995, **182**(2):367-377.

Zha J, Harada H, Osipov K, Jockel J, Waksman G, Korsmeyer SJ: **BH3 domain of BAD is required for heterodimerization with BCL-XL and pro-apoptotic activity**. *J Biol Chem* 1997, **272**(39):24101-24104.

Zhang XM, Lin H, Chen C, Chen BD: **Inhibition of ubiquitin-proteasome pathway activates a caspase-3-like protease and induces Bcl-2 cleavage in human M-07e leukaemic cells**. *Biochem J* 1999, **340 (Pt 1)**:127-133.

Zou H, Henzel WJ, Liu X, Lutschg A, Wang X: **Apaf-1, a human protein homologous to C. elegans CED-4, participates in cytochrome c-dependent activation of caspase-3**. *Cell* 1997, **90**(3):405-413.

Zou H, Li Y, Liu X, Wang X: **An APAF-1.cytochrome c multimeric complex is a functional apoptosome that activates procaspase-9**. *J Biol Chem* 1999, **274**(17):11549-11556.

Conferences and publications

- **Feng L**, Ye W, Yu K and Yoon HS. RNA interference of Bcl-2 enhances sensitivities of cancer cells to therapeutic drugs, but their effects appear to be cancer cell-dependent. The 4th Annual Congress of International Drug Discovery Science and Technology, May 2006.
- Kang CB, **Feng L**, Chia J and Yoon HS (2005). The molecular characterization of FK-506 binding protein 38 (FKBP38) and its potential regulatory role on the anti-apoptotic protein Bcl-2. Biochem. Biophys. Res. Commun. 337, 30-38.
- **Feng L**, Yoon HS (2007). FKBP38 works as a novel link between cell cycle and cell death through the ROS-mediated damages on the mitochondrial membrane potential. (submitted)